

UCSF

UC San Francisco Electronic Theses and Dissertations

Title

Function and regulation of the human NAD⁺-dependent protein deacetylase SIRT2

Permalink

<https://escholarship.org/uc/item/08n521zc>

Author

North, Brian Joseph

Publication Date

2005

Peer reviewed|Thesis/dissertation

Function and Regulation of the Human NAD⁺-dependent Protein Deacetylase SIRT2

By

Brian Joseph North

DISSERTATION

Submitted in partial satisfaction of the requirements for the degree of

DOCTOR OF PHILOSOPHY

in

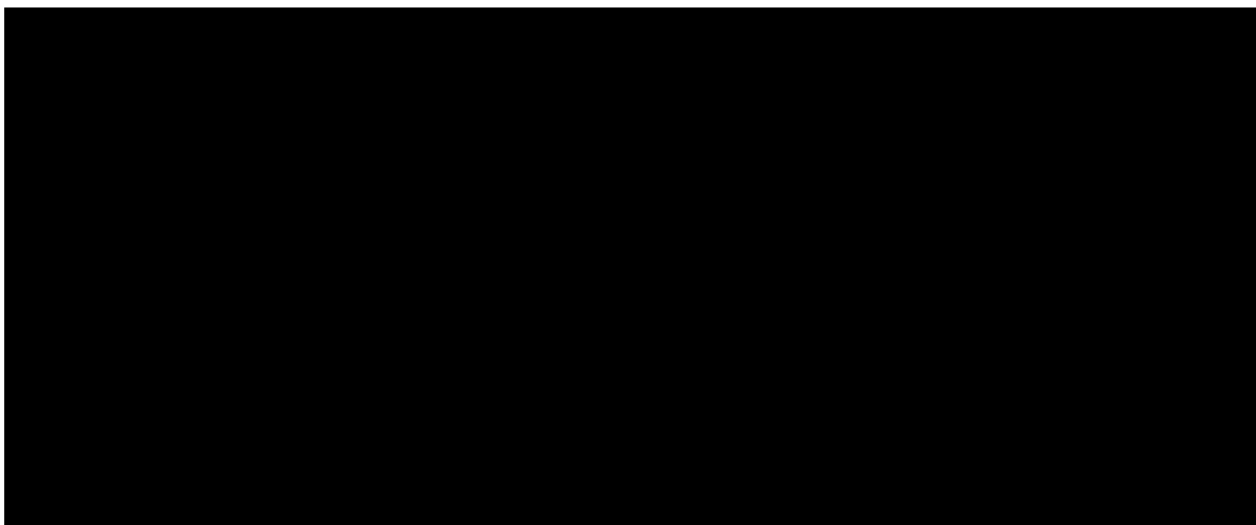
BIOMEDICAL SCIENCES

in the

GRADUATE DIVISION

of the

UNIVERSITY OF CALIFORNIA, SAN FRANCISCO



Date

University Librarian

Degree Conferred: _____

Copyright 2005

By

Brian Joseph North

Acknowledgments

Many people have been instrumental in my training as a scientist even before the starting of this Ph.D. thesis. The Department of Biology at Gustavus Adolphus College shaped the base of my scientific knowledge during my undergraduate education. Specifically, I am grateful to my first mentor, Dr. Colleen Jacks, for her guidance and patience. Colleen instilled in me confidence to be able to function independently in a research lab as she gave me tremendous freedom when I carried out my research project in her lab. In addition, she had a passion for both science and teaching, and her enthusiasm influenced greatly my decision to pursue a Ph.D. and a career in research. Colleen was not only an extraordinary mentor, but also a friend that I have great respect for.

I owe a remarkable amount of gratitude to my Ph.D advisor, Dr. Eric Verdin, for this thesis would not have been possible without his support and guidance. Eric provided important insight and direction in my work as well as teaching me the value of thinking creatively about my research projects. The most considerable aspect of Eric's mentorship has been his willingness to allow my own scientific passion to develop in his lab. Although I joined his lab to study the molecular virology of HIV, my studies quickly transitioned down a different course. Eric permitted me to follow these new directions even as they took my work outside the more general interest of the lab. I am indebted to this aspect of Eric's mentorship, as my scientific career interest were breed out of these studies and would not have been possible without Eric's guidance, open mind, and generosity.

In addition to allowing my scientific interest to be reared in his lab, Eric also assembled a group of students and postdoctoral fellows that would contribute

significantly to my scientific development. In no particular order, these colleagues were Wolfgang Fischle, Frank Dequiedt, Veronique Kiermer, Christian Callebaut, Albert Jordan, Melanie Ott, Dwayne Bisgrove, Herbert Kasler, Laura Saunders, Prerana Jayakumar, Brett Marshall, Bjoern Schwer, Tokameh Mahmoudi, Maribel Parra-Bola, and Steven Kauder. My graduate research experience would not have been the same without these colleagues, as they were open to discussions about projects, results, and the daily life of working in the lab. I was fortunate to be surrounded by such a extensive number of individuals who would not only become great colleagues, but also turned out to become good friends.

My scientific experience at UCSF would not have been complete without the members of my thesis committee, Drs. Elizabeth Blackburn, David Agard and Ron Vale. I was always astonished by my growth as a scientist during each of our committee meetings. I am appreciative of the candid approach each of my committee members took with discussions of my experimental design, data interpretation, and progress of my projects during the course of my training. One of the only regrets I had was not taking the advantage of meeting with each of them on a more frequent basis.

The Gladstone Institutes also had a number of individuals who contributed to my progress over the course of my graduate studies. In particular, Dr. Warner C. Greene was a second mentor in many regards. Both in informal discussions as well as in joint lab meetings, Warner and his lab were always willing to give their honest interpretation of my data and conclusions. In addition, H. Ewa Witkowska, Steven C. Hall, and Scott E. Dixon of the Biomolecular Research Center Mass Spectrometry Facility at UCSF, made important scientific contributions in experimental design, and the acquisition and analysis

of mass spectrometry data presented in chapter 4. Funding for my research was provided by the J. David Gladstone Institutes through their institutional support program to Dr. Eric Verdin.

My family has always been supportive of my educational ambitions through their unconditional love and guidance. My great-aunt and uncle Georgianne and Don Houser always welcomed me in their home whenever I needed a break from my studies. After my mother's passing during my first year in graduate school, Georgianne, probably unbeknownst to her, became my surrogate mother, and was always someone I could go to whenever I needed maternal advice. My brothers Chris and John North, my father Wayne North, and Jeannie North, who became a welcomed addition to our family, were always supportive in making sure that I had everything available to me that I needed to be successful in my education. In addition, they continue to be supportive of my present and future endeavors. I realize more every day how similar I am to my father. Both his heredity and nurturing have been instrumental in my success far beyond what I am able to comprehend. And finally, none of this would have been possible without the influence of my mother Georgiana North. In her struggle with Lou Gehrig's disease, she taught me that no matter how difficult life may become, every upcoming day always brings about something new to look forward to. It is from her that I acquired my desire to constantly question doctrine, and seek to understand the unknown. Her love, courage and strength continue to guide me each and every day of my life.

Contributions of Co-Authors to the Presented Work

Chapter 1 of this dissertation is based on a review published, in part, in *Genome Biology* (2004) 5:224, titled, “Sirtuins: Sir2-related NAD-dependent protein deacetylases.” In accordance with *Genome Biology* policy, no permission is required for the reproduction of work published by the same author. This review was co-authored by Eric Verdin.

Chapter 2 is based, in part, on previously published material. Reprinted from *Molecular Cell*, volume 11, North, B.J., *et al.*, The human Sir2 ortholog, SIRT2, is an NAD⁺-dependent tubulin deacetylase, pages 437–44, copyright (2003), with permission from Elsevier. Contributing author Brett L. Marshall supplied helpful advice and reagents to this work. Contributing authors Margie T. Borra and John M. Denu collaborated on the generation and analysis of enzymology experiments shown in figure 2.5. This work was supervised by Eric Verdin.

Chapter 3 is based on data prepared in a manuscript titled “Cell Cycle-dependent Localization of SIRT2,” by Brian J. North and Eric Verdin, and is to be submitted to a peer-reviewed scientific journal. This work was supervised by Eric Verdin.

Chapter 4 is based on data prepared in a manuscript titled “Mitotic regulation of SIRT2 by Cdk1-dependent phosphorylation,” by Brian J. North and Eric Verdin, and is to be submitted to a peer-reviewed scientific journal. This work was supervised by Eric Verdin.

Function and Regulation of the Human NAD⁺-dependent Protein Deacetylase SIRT2


Brian Joseph North

Silent information regulator 2 (Sir2) proteins, or sirtuins, are NAD⁺-dependent protein deacetylases present in organisms ranging from bacteria to humans. In eukaryotes, sirtuins function in regulation of transcriptional repression, recombination, cell cycle division, DNA damage repair, and the molecular mechanisms governing aging. In addition to a conserved catalytic domain, sirtuins contain variable amino- and carboxy-terminal extensions that are suspected to regulate their subcellular localization and catalytic activity.

We identify human sirtuin type 2 (SIRT2) as a predominantly cytoplasmic protein colocalizing with the microtubule network. SIRT2 deacetylates lysine-40 of α -tubulin and knockdown of SIRT2 by siRNA results in α -tubulin hyperacetylation. α -Tubulin deacetylation by SIRT2 results in cytoplasmic sequestration of the transcription factor MIZ-1 by regulating its interaction with the microtubule network. During interphase, SIRT2 shuttles between the nucleus and cytoplasm, and maintains a predominantly cytoplasmic localization via active nuclear export in a Crm1-dependent manner. We have identified a functional Leptomycin B-sensitive nuclear export signal sequence within the amino-terminal extension of SIRT2. During mitotic entry, SIRT2 accumulates in the nucleus prior to nuclear envelope breakdown and during mitosis is enriched on microtubule-derived structures, beginning with the centrosome during prophase, the mitotic spindle during metaphase, and the midbody during cytokinesis. Cells overexpressing either wild-type or catalytically inactive SIRT2 have a greater

susceptibility for cytokinesis defects in which cells become multinucleated. During mitosis, we find that SIRT2 is phosphorylated on serine-368, which can be regulated by the opposing activities of the Cdk1 kinase and the CDC14A and CDC14B phosphatases. Overexpression of SIRT2 mediates a delay in cellular proliferation that is dependent on the presence of serine-368.

Within this thesis, we have characterized SIRT2 as a regulator of α -tubulin acetylation and define a novel role for α -tubulin acetylation as a reversible signal mediating protein: microtubule interaction. Furthermore, SIRT2 is found on mitotic structures containing acetylated microtubules, suggesting the potential for a finely tuned mechanism regulating SIRT2 activity during mitosis. Finally, SIRT2 delays cellular proliferation dependent on its phosphorylation by Cdk1. These results demonstrate that SIRT2 may perhaps be a novel protein to target for cancer therapy.



Eric Verdin, M.D.
Advisor

Table of Contents

Chapter 1: Introduction to Acetylation and the Sir2 Family of Deacetylases	1
Reversible Acetylation	2
Sirtuin Function from Bacteria to Humans	5
<i>Bacteria</i>	5
<i>Saccharomyces cerevisiae</i>	7
<i>Caenorhabditis elegans</i>	11
<i>Drosophila melanogaster</i>	12
Mammals	13
SIRT1	13
SIRT2	14
SIRT3	15
SIRT4–7	16
Sirtuins and Aging	17
Characteristic Structural Features	20
Enzymology	23
Chapter 2: Deacetylation of α-Tubulin by SIRT2 Regulates Microtubule Interaction and Subcellular Localization of MIZ-1	27
Introduction	28
Results	30
<i>SIRT2 is a Cytoplasmic Protein that Colocalizes with the Microtubule Network</i>	30
<i>α-Tubulin Deacetylation by Human SIRT2 in vivo</i>	32
<i>Human SIRT2 Deacetylates α-Tubulin in vitro</i>	34
<i>Enzymatic Kinetics of Human SIRT2 and Yeast Hst2p</i>	38
<i>Knockdown of SIRT2 and HDAC6 Expression Leads to α-Tubulin Hyperacetylation</i>	41
<i>SIRT2 and HDAC6 Colocalize and Coimmunoprecipitate</i>	43
<i>Regulation of MIZ-1 Microtubule Interaction by α-Tubulin Acetylation</i>	47
Discussion	51
<i>SIRT2 is a bona fide α-Tubulin Deacetylase</i>	51
<i>Binding of MIZ-1 to Acetylated Microtubules</i>	52
Experimental Procedures	54
Chapter 3: Cell Cycle-dependent Localization of SIRT2	63
Introduction	64
Results	66
<i>Nucleocytoplasmic Shuttling of SIRT2</i>	66
<i>Identification of a Nuclear Export Signal in SIRT2</i>	69
<i>Nuclear Entry of SIRT2 Prior to Mitosis</i>	73
<i>Localization of SIRT2 During Mitosis</i>	75
<i>Defined Enzymatic Activity of SIRT2 Controls Efficient Cytokinesis</i>	79

Discussion	83
<i>Identification of a Nuclear Export Signal Sequence in SIRT2</i>	83
<i>Nuclear Import of SIRT2 During Mitotic Entry</i>	85
<i>Enrichment of SIRT2 on Microtubule Structures During Mitosis</i>	85
Experimental Procedures	87
Chapter 4: Mitotic Regulation of SIRT2 by Cdk1-dependent Phosphorylation	91
Introduction	92
Results	94
<i>Generation of Multiple Isoforms of SIRT2 by Alternative Translational Start Sites</i>	94
<i>SIRT2 is Targeted for Phosphorylation</i>	96
<i>Mapping of Primary Phosphorylation Site in SIRT2 to Serine-368</i>	97
<i>Cdk1 Regulates SIRT2 Phosphorylation in vitro on Serine-368</i>	101
<i>Modulation of SIRT2 Phosphorylation by Cdk1-Cyclin B1</i>	103
<i>Colocalization and Interaction of SIRT2 and Cdk1-Cyclin B1</i>	108
<i>Dephosphorylation of SIRT2 by the Human CDC14 Phosphatases</i>	110
<i>SIRT2-mediated Reduction in Cellular Proliferation is Dependent on Serine-368</i>	113
Discussion	116
<i>Alternative Translational Start Sites in SIRT2</i>	116
<i>Phosphorylation of SIRT2 by Cdk1</i>	116
<i>Phosphorylation Dependent Regulation of Cellular Proliferation by SIRT2</i>	118
Experimental Procedures	120
Chapter 5: Concluding Remarks and Perspectives	128
<i>Sirtuin Activity</i>	129
<i>SIRT2 is a α-Tubulin Deacetylase</i>	131
<i>Two α-Tubulin Deacetylases in One Complex</i>	133
<i>Acetylation-dependent Association of Factors with the Microtubule Network</i>	136
<i>A Tubulin Code for Microtubule Posttranslational Modifications?</i>	138
<i>SIRT2 is exported from the nucleus</i>	138
<i>Mitotic Localization of SIRT2</i>	140
<i>Regulation of SIRT2 Function by Phosphorylation</i>	141
<i>SIRT2, Aging and Human Disease</i>	146
References	148

List of Figures and Illustrations

Figure	Title	Page
Figure 1.1	Schematic depiction of reversible lysine acetylation.	3
Figure 1.2	Phylogenetic analysis of sirtuin proteins.	6
Figure 1.3	Three-dimensional high-resolution crystal structures of four sirtuin proteins.	22
Figure 1.4	The enzymatic activity of sirtuins.	25
Figure 2.1	SIRT2 is predominantly cytoplasmic and colocalizes with the microtubule network.	31
Figure 2.2	<i>In vivo</i> α -tubulin deacetylation by GFP-SIRT2.	33
Figure 2.3	Catalytic mutants of SIRT2 lack deacetylase activity <i>in vitro</i> and <i>in vivo</i> .	35
Figure 2.4	SIRT2 deacetylates α -tubulin <i>in vitro</i> .	37
Figure 2.5	α -Tubulin is a preferred substrate for SIRT2 in comparison to Hst2p.	39
Figure 2.6	Knockdown of SIRT2 and HDAC6 with siRNA.	42
Figure 2.7	Coimmunoprecipitation and colocalization of SIRT2 and HDAC6.	44
Figure 2.8	Deacetylation of various α -tubulin substrates by SIRT2 and HDAC6.	46
Figure 2.9	Regulation of MIZ-1 nuclear cytoplasmic distribution by acetylated α -tubulin.	48
Figure 2.10	Induced microtubule colocalization of MIZ-1 by α -tubulin acetylation.	49
Figure 3.1	Cytoplasmic localization of SIRT2 is dependent on constitutive nuclear export.	67
Figure 3.2	Nuclear import of SIRT2 is not dependent on transit through mitosis.	68
Figure 3.3	A Crm1-dependent NES is in the amino-terminus of SIRT2.	70
Figure 3.4	Mutational analysis of Crm1-dependnet NES sequence in SIRT2.	72
Figure 3.5	SIRT2 is excluded from nucleoli when maintained in the nucleus.	74
Figure 3.6	Nuclear import of SIRT2 prior to nuclear envelope breakdown during mitotic entry.	76
Figure 3.7	Colocalization and coimmunoprecipitation of SIRT2 and Aurora A on the centrosome and spindle fibers.	78
Figure 3.8	Colocalization and coimmunoprecipitation of SIRT2 and Aurora B at the midbody.	80
Figure 3.9	Compromised cytokinesis by overexpression of SIRT2.	81
Figure 4.1	Exogenous SIRT2 migrates as multiple species on SDS-PAGE.	95
Figure 4.2	SIRT2 is targeted for phosphorylation <i>in vivo</i> .	97
Figure 4.3	Phosphorylation of SIRT2 occurs on serine-368.	99
Figure 4.4	Phosphorylation of SIRT2 is enhanced during mitosis.	100

Figure 4.5	<i>In vitro</i> phosphorylation of SIRT2 by Cdk1 occurs on serine-368.	102
Figure 4.6	Reduction of SIRT2 phosphorylation by pharmacological inhibition of Cdk1 or expression of Cdk1-Cyclin B1 factors.	104
Figure 4.7	Interaction and colocalization of SIRT2 and the Cdk1-Cyclin B1 complex.	107
Figure 4.8	Colocalization of SIRT2 and Cyclin B1 during centrosome separation.	109
Figure 4.9	Dephosphorylation of SIRT2 by coexpression with CDC14A and CDC14B.	111
Figure 4.10	Serine-368 is not required for SIRT2 enzymatic activity <i>in vitro</i> .	112
Figure 4.11	Regulation of cellular proliferation by SIRT2 is dependent on Serine-368 phosphorylation.	114
Figure 5.1	Schematic diagram of α -tubulin deacetylation by HDAC6 and SIRT2	134
Figure 5.2	Regulation of SIRT2 by phosphorylation	142

Reversible Acetylation

Controlling protein function occurs at multiple levels within the eukaryotic cell. Regulation of transcription, translation, and degradation, all contribute to controlling protein function through abundance. However, controlling the function of a protein is not solely directed by its expression level, but also includes a complex network of posttranslational modifications occurring on amino acid side chains. There are over 200 posttranslational modifications that can occur on eukaryotic proteins. Common modifications include, but are not limited to: glycosylation of serine and threonine residues; phosphorylation of serine, threonine, and tyrosine residues; methylation of arginine and lysine residues; and the ubiquitylation, sumoylation, and acetylation of lysine residues (1, 2). For many of these modifications, the enzymes catalyzing the addition and removal of these molecules have been identified, and the literature discussing the functional consequences of these posttranslational modifications in the proteome is growing extensively.

Reversible protein acetylation, occurring on the ϵ -amino groups of lysine residues, results in the conversion of a lysine residue to a more acidic, hydrophilic side chain (3). Lysine acetylation is controlled by the opposing enzymatic activities of histone deacetylases (HDACs) and histone acetyltransferases (HATs) (figure 1.1). As their name suggest, HATs and HDACs were initially identified and studied for their role in regulating histone acetylation (4). Histone H2A, H2B, H3 and H4 proteins form a multimeric complex, termed the nucleosome, that serve as a scaffold for packaging DNA into higher ordered structures. Highly basic amino-terminal extensions (or “tails”) of histone proteins protrude out from the nucleosome and are subjected to a variety of

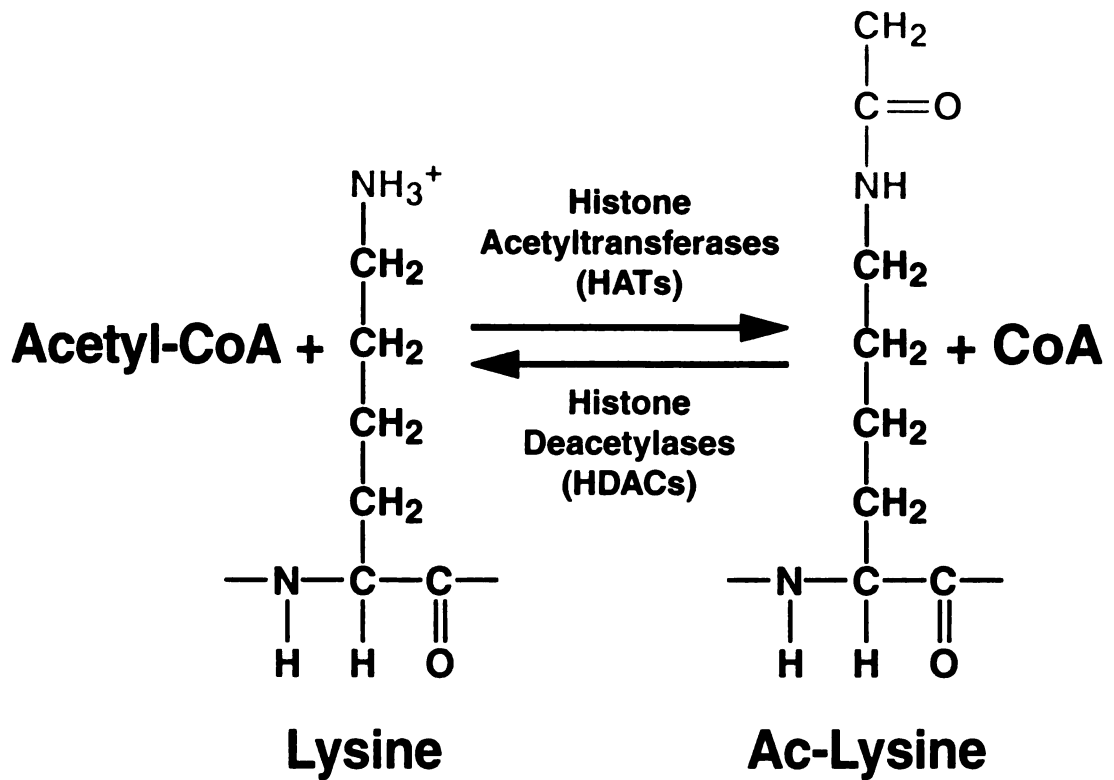


Figure 1.1. Schematic depiction of reversible lysine acetylation. Addition and removal of the acetyl group is mediated by histone acetyltransferases (HATs) and histone deacetylases (HDACs).

posttranslational modifications, including acetylation. Functionally, hyperacetylation of histone tails is associated with transcriptional activation of nearby promoters, while hypoacetylation of histone tails is associated with transcriptional repression. Although HATs and HDACs were initially characterized by their ability to regulate acetylation of histones, a rapidly growing number of non-histone proteins are also targeted for reversible acetylation by these enzymes (reviewed in (2)). Acetylation of histone and non-histone proteins has been associated with a wide variety of cellular processes through the regulation of various protein functions including DNA recognition, protein-protein interactions and protein stability (reviewed in (5)).

Over 20 HAT enzymes have been characterized to date including the prominent acetyltransferases p300, CREB-binding protein (CBP) and p300/CBP-associated factor (PCAF) (2). Likewise, there are 18 mammalian HDAC enzymes that are separated into three distinct classes based on their homology to yeast transcriptional repressors. Class I and II HDACs, which share significant homology within their catalytic cores, are homologues of Rpd3p and Hda1p, respectively (reviewed in (6, 7)). The class III HDACs are homologous to the yeast transcriptional repressor Sir2p, and share no homology in protein structure or catalytic mechanism with class I and II HDACs (reviewed in (8, 9)).

Silent information regulator (Sir) genes were identified in the yeast *Saccharomyces cerevisiae*, where a mutation in Sir1, *sir1-1*, suppressed mating and sporulation defects of mutations present in the mating-type loci (10). In further studies, four individual genes termed *SIR1*, *SIR2*, *SIR3*, and *SIR4* were isolated that complemented Sir mutations *in vivo* (11-13). Subsequently, the protein products of these genes were demonstrated to function in transcriptional repression, yet the mechanism

remained elusive. Two decades following their initial identification, an enzymatic activity was discovered for Sir2p. Sir2p was characterized as an NAD⁺-dependent histone deacetylase, an activity required for the silencing observed at Sir2p controlled loci (14-16).

Sirtuin Function from Bacteria to Humans

Sir2 proteins, or sirtuins, exist in organisms ranging from bacteria to eukaryotes (17, 18). The hallmark of this protein family is a highly conserved ~260 amino acid domain. Sirtuins are divided into 5 classes (I–IV, and U) based on phylogenetic analysis of 60 sirtuins from a wide array of organisms (figure 1.2) (17). Eukaryotic genomes encode sirtuins with representatives from four classes (I–IV), whereas the U class sirtuins are found specifically in gram-positive bacteria (17).

Bacteria

In prokaryotes, the bacterial sirtuin CobB, controls the activity of both acetyl- and propionyl-coenzyme A synthetase. CobB regulates the acetylation of Lys-609 in acetyl-coenzyme A synthetase and Lys-592 in propionyl-coenzyme A synthetase and deacetylation of these enzymes by CobB induces their activity in an NAD⁺-dependent manner (19, 20). Furthermore, *CobB*-deficient strains of *Salmonella enterica* undergo growth arrest when grown in the presence of acetate (19).

The crenarchaeon *Sulfolobus solfataricus* P2 genome encodes a sirtuin homologue, ssSir2, which functions both as an NAD⁺-dependent deacetylase and a mono-ADP-ribosyltransferase (21). The acetylated archaeal chromatin protein Alba

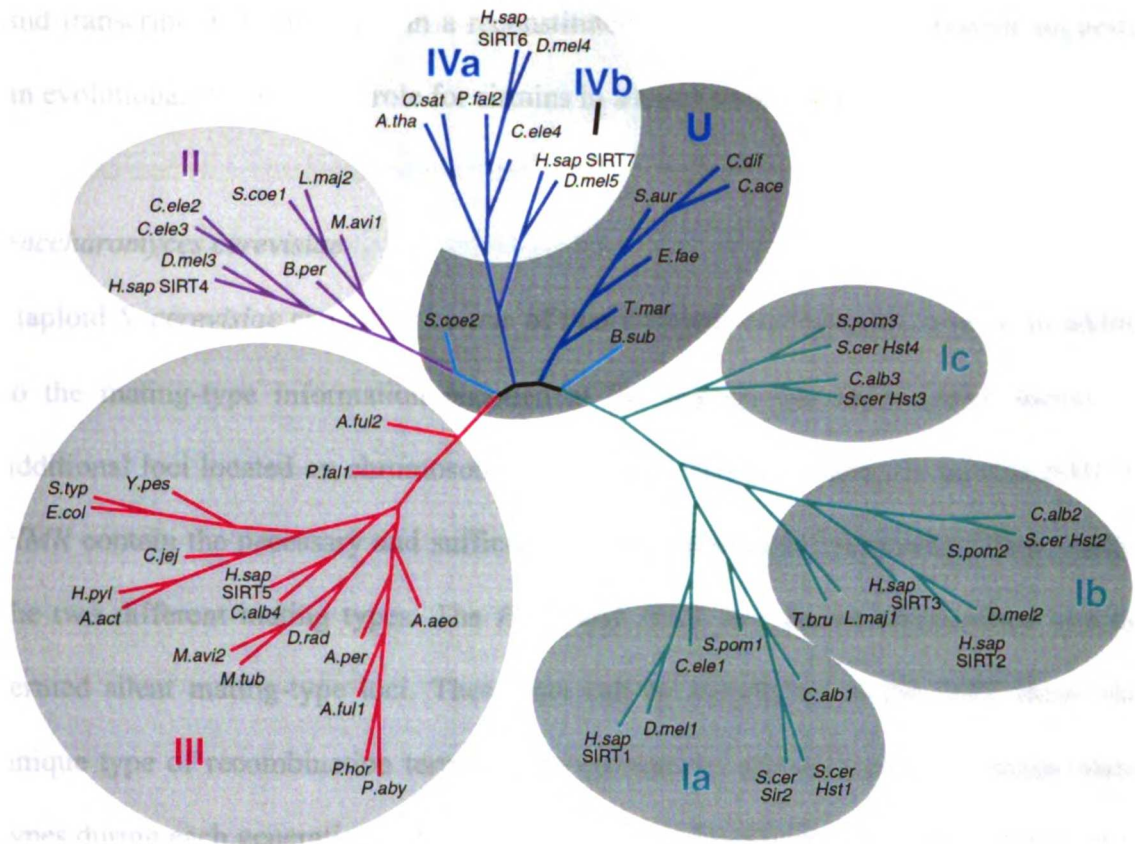


Figure 1.2. Phylogenetic analysis of sirtuin proteins. An unrooted tree diagram derived from phylogenetic analysis of the conserved domains of 60 sirtuin sequences separates sirtuins into five classes. Classes I, II, III, IV, and U and subdivisions of classes I and IV are indicated. Organism abbreviations: A. act, *Actinobacillus actinomycetemcomitans*; A. aeo, *Aquifex aeolicus*; A. ful, *Archaeoglobus fulgidus*; A. per, *Aeropyrum pernix*; A. tha, *Arabidopsis thaliana*; B. per, *Bordetella pertussis*; B. sub, *Bacillus subtilis*; C. ace, *Clostridium acetabutylicum*; C. alb, *Candida albicans*; C. dif, *Clostridium difficile*; C. ele, *Caenorhabditis elegans*; C. jej, *Campylobacter jejuni*; D. mel, *Drosophila melanogaster*; D. rad, *Deinococcus radiodurans*; E. col, *Escherichia coli*; E. fae, *Enterococcus faecalis*; H. sap, *Homo sapiens*; H. pyl, *Helicobacter pylori*; L. maj, *Leishmania major*; M. avi, *Mycobacterium avium*; M. tub, *Mycobacterium tuberculosis*; O. sat, *Oryza sativa*; P. aby, *Pyrococcus abyssi*; P. fal, *Plasmodium falciparum*; P. hor, *Pyrococcus horikoshii*; S. aur, *Staphylococcus aureus*; S. coe, *Streptomyces coelicolor*; S. pom, *Schizosaccharomyces pombe*; S. typ, *Salmonella typhimurium*; S. cer, *Saccharomyces cerevisiae*; T. bru, *Trypanosoma brucei*; T. mar, *Thermotoga maritima*; Y. pes, *Yersinia pestis*. Adapted with modification from (17).

interacts with and is deacetylated by ssSir2 resulting in increased DNA binding-activity and transcriptional repression in a reconstituted *in vitro* transcription system suggesting an evolutionarily conserved role for sirtuins in transcriptional regulation (21).

Saccharomyces cerevisiae

Haploid *S. cerevisiae* can either be one of two different mating types, **a** or **α** . In addition to the mating-type information encoded at the mating-type locus (*MAT* locus), two additional loci located on chromosome III of the *S. cerevisiae* genome termed *HML* and *HMR* contain the necessary and sufficient genetic information required to direct each of the two different mating types. The *HML* and *HMR* loci are non-transcribed and thus termed silent mating-type loci. These loci can be transferred to the *MAT* locus via a unique type of recombination termed gene conversion, allowing cells to change mating types during each generation (22). Sir2p activity regulates heterochromatin formation and transcriptional repression at the silent mating-type loci. A multimeric protein complex containing Sir2p, Sir3p and Sir4p is recruited to the silent mating-type loci via interaction with Sir1p and a complex of DNA-binding proteins comprised of Rap1, Orc and Abf1 (23-25). Recruitment of the Sir complex mediates histone hypoacetylation and the formation of a heterochromatic region responsible for maintaining these loci in a transcriptionally silent state.

Similar to the silent mating-type loci, telomeric silencing requires Sir2p, Sir3p and Sir4p, but does not require Sir1p (26). Telomeres are protein-DNA complexes formed at the ends of chromosomes that are important for chromosomal end stability and promote the organization of chromosomes within the nucleus (27, 28). In *S. cerevisiae*,

telomeric DNA consists of C₁₋₃A/TG₁₋₃ repeats that are ~300 bp in length, and are organized into a non-nucleosomal chromatin structure termed the telosome (29). At the yeast telomeres a transient form of silencing termed telomere position-effect is observed, characterized as a stochastic alternation between transcriptional silencing and activation in a telomere distal distance-dependent manner (26). Sir proteins are components of the telosome and may be recruited either by the interaction between Sir4p and telomeric repeats, interaction of the Sir2/3/4p complex with the telomere-repeat binding protein Rap1p, or a yet undefined mechanism (25, 30-32).

Sir2p-dependent silencing is capable of extending over considerable lengths of chromatin. A model has been proposed for the mechanism of nucleation and spreading of the Sir2/3/4p complex along targeted regions of the genome. Nucleation of the Sir2/3/4p complex is established by interaction with sequence specific DNA binding factors. Following recruitment of the initial Sir2/3/4p complex, Sir2p will deacetylate histones within the neighboring nucleosome, allowing for recruitment of a new Sir2/3/4p complex via interactions between Sir3p/Sir4p and the newly hypoacetylated histones (33-37). This cycle of deacetylation followed by recruitment continues across the loci, until a boundary element is encountered (38, 39). Consistent with this hypothesis, loci silenced in a Sir2p-dependent manner are associated with histone hypoacetylation and display features of a heterochromatin-like structure (36, 40, 41).

The nucleolus, the site of ribosomal RNA (rRNA) transcription and ribosome assembly, is the third characterized site of Sir2p function in yeast (42, 43). The *rDNA* array consists of a 9-kb unit tandemly repeated 100–200 times on chromosome 12. This repetitive array encodes both the 35S and 5S rRNA species. Sir2p-mediated alterations in

chromatin structure at the *rDNA* array suppress homologous recombination among the repetitive *rDNA* copies. In addition, Sir2p silences transcription of RNA polymerase II-dependent marker genes inserted within the *rDNA* array (42-45). However, unlike the mating-type loci or the telomeres, Sir2p functions independently of Sir3p and Sir4p at the *rDNA* array, and is recruited to the nucleolus via its interaction with the RENT (*regulator of nucleolar silencing and telophase*) complex, containing Net1p, and a telophase-regulating phosphatase, Cdc14p (46, 47).

Sir2p is implicated in repair of double-strand DNA breaks, cell cycle progression, and chromosomal stability in yeast (48-50). Telomeric silencing also requires the Ku70 and Ku80 proteins, DNA-binding proteins involved in the non-homologous end-joining (NHEJ) pathway of double-strand DNA break repair (51). In yeast, Ku70/80 heterodimers are localized primarily at telomeres and are targeted transiently to sites of DNA damage. Ku-deficient strains are defective in telomere silencing possibly due to mislocalization of the Sir complex (49-52). In addition, upon DNA damage, the Sir proteins relocate to sites of DNA breaks in a Ku70/80-dependent manner (49, 50). In mammals, the Ku proteins are a component of the DNA-dependent protein kinase complex that is involved in NHEJ. The potential role of Sir protein-mediated histone deacetylation during NHEJ, and a role of mammalian sirtuins in this process, remain unclear. The establishment of a heterochromatic environment surrounding DNA breaks mediated by Sir proteins may enhance the efficiency of the repair process. Further studies in both yeast and higher organisms are necessary to define the importance of the Ku70/80 and Sir complex interaction, and its role in telomere silencing and DNA break repair.

By its association with the RENT complex, Sir2p may function in regulating mitotic exit. The Cdc14p phosphatase is a critical regulator of mitotic exit by opposing cyclin-dependent kinase activity, but is held in an inactive state in the nucleolus by association with the RENT complex. During anaphase, Cdc14p dissociates from the RENT complex, disperses throughout the cell and is involved in triggering mitotic exit (47). Nucleolar sequestration may play a primary role in the negative regulation of Cdc14p during interphase and mitotic entry, and a role for Sir2 in this regulatory mechanism of Cdc14p activity remains to be elucidated.

In addition to Sir2p, *S. cerevisiae* has four homologues of Sir2 (*HST1-4*), which are also NAD⁺-dependent deacetylases. Members of this gene family share between 26% and 63% identity within their open reading frames, and contain a central core domain of ~155 amino acids where identity is as high as 89% (48). Hst1p is the most closely related Hst protein to Sir2p, and like Sir2p, it localizes predominantly in the nucleus. *HST1* overexpression restores transcriptional silencing in a *sir2* deletion strain, suggesting sufficient homology exist between Hst1p and Sir2p allowing Hst1p to be incorporated into Sir2p complexes (48). However, a unique function of Hst1p is repressing expression of genes involved in NAD⁺ biosynthesis, a group of genes that does not appear to be targeted for silencing by Sir2p. A decrease in cellular NAD⁺ levels lowers Hst1p enzymatic activity, allowing the derepression of genes involved in NAD⁺ biosynthesis. Expression of these genes results in a restoration of cellular NAD⁺ levels (53). Therefore, a mechanism for controlling cellular NAD⁺ levels is directly coupled to the NAD⁺ dependency of Hst1p enzymatic activity.

Hst2p, which also possesses NAD⁺-dependent deacetylase activity, exhibits a predominantly cytoplasmic localization (54). Although Hst2p is found in the cytoplasm, it has the potential to regulate transcriptional silencing at Sir2p-dependent loci (54). However, in contrast to Hst1p, Hst2p does not restore silencing in a *sir2*-deletion mutant. Overexpression of Hst2p leads to derepression of telomere silencing while increasing silencing at the *rDNA* locus. The ability of Hst2p to regulate rDNA silencing has been demonstrated to be the mechanism for the ability of Hst2p to regulate yeast longevity in a *sir2* deletion strain (54, 55). One proposed mechanism is Hst2p and Sir2p could compete for a substrate, or ligand, that is required for Sir2p to perform silencing functions at the telomere but not the rDNA array (54). However, the targeting of a fraction of cellular Hst2p protein to the nucleus is a possibility that has not been completely explored yet.

Hst3p and Hst4p are more distantly related to Sir2p and no homologs have been identified in mammals. *HST3/HST4* double mutants are defective in telomere silencing (48), and Hst4p from *Schizosaccharomyces pombe* functions in centromere silencing in addition to its role in regulating telomeric silencing (56). In addition, Hst3p and Hst4p together contribute to proper cell cycle progression, radiation resistance, and genomic stability, thereby establishing new connections between genomic silencing and these fundamental cellular processes (48). However the mechanism by which Hst3p and Hst4p mediate these functions remains elusive.

Caenorhabditis elegans

There are four homologous genes of Sir2p in the nematode *C. elegans*. Genetic studies have implicated *Sir-2.1*, the closest homolog to yeast Sir2p, in the insulin/insulin-like

growth factor 1 (IGF-1) endocrine system and regulation of aging and dauer formation. Interestingly, the ability of *Sir-2.1* to regulate aging in *C. elegans* requires a functional DAF-16 protein (a forkhead transcription factor). However, the molecular interplay between *Sir-2.1* and the DAF pathway remains elusive, and understanding how the Sir2.1 protein regulates the DAF pathway will shed light on the potential role mammalian homologues might function to regulate this pathway (57).

Drosophila melanogaster

The *Drosophila* genome encodes five homologues of Sir2p. dSir2 is the closest homologue to yeast Sir2p and functions as a histone deacetylase towards all four acetylable lysine residues of histone H4 (58). dSir2 is required for heterochromatic silencing and interacts genetically and physically with members of the Hairy/Deadpan/E(Spl) family of bHLH repressor proteins, which are key regulators of *Drosophila* development (59). Furthermore, dSir2 is involved in epigenetic inheritance of silent chromatin states mediated by the *Drosophila* polycomb group proteins and consistent with this function, dSir2 physically associates with a complex containing the E(Z) histone methyltransferase (60). Contradictory reports have been published on the role of dSir2 in various physiological processes such as genomic silencing, segmentation, sex determination, and aging. Further studies will need to be conducted to fully understand the role of dSir2 in these processes, as well as to uncover the functions of the additional four *Drosophila* Sir2 homologues (59, 61, 62).

Mammals

The mammalian genome encodes seven sirtuin proteins, which contain significant homology within the catalytic core, but vary considerably in their amino- and carboxy-terminal extensions.

SIRT1

The most extensively characterized mammalian sirtuin is SIRT1, also referred to Sir2 α in mice. Expression profiling of SIRT1 by a number of groups indicate that SIRT1 is expressed in all tissues examined, with the highest expression in lung and testis, and moderate expression in skeletal muscle, ovary, spleen, thymus, and heart as well as in the embryonic heart and brain (18, 63-67). SIRT1 targets a number of factors for deacetylation, including TAF₁₆₈, PGC-1 α , PCAF, Ku70, MyoD, MEF2, p300, p53, NF- κ B, Forkhead transcription factors, and the HIV-1 tat protein (68-82). In addition to these non-histone substrates, SIRT1 is also recruited to promoters and directly regulates histone acetylation via interaction with sequence-specific DNA binding factors such as BCL11A, PPAR- γ , COUP-TF-interacting proteins 1 and 2 (CTIP1 and CTIP2), the MyoD/PCAF complex, and the bHLH repressor proteins hHES1 and hHEY2 (homologues of the *Drosophila* Hairy and Deadpan proteins described above) (59, 78, 83-85). Therefore, SIRT1 regulates transcription through a number of histone and non-histone mechanisms, resulting in the regulation of development, and cell fate decisions between apoptosis and cell survival following DNA damage. Consistent with the role of Sir-2.1 regulating DAF-16 (a forkhead transcription factor) in *C. elegans*, SIRT1 deacetylates mammalian forkhead transcription factors FOXO3 and FOXO4, attenuating FOXO-induced apoptosis

and potentiating FOXO-induced cell cycle arrest (74-76). A role for SIRT1 in these physiological processes have been substantiated by knockout-mouse studies, in which animals homozygous for the null allele of SIRT1 are born at only half the expected frequency, due to a prenatal or early postnatal loss of half the animals with the knockout genotype. Both embryos and pups of homozygous null animals are smaller than their wild-type and heterozygous littermates and have various developmental defects of the heart, eyes, lungs and pancreas (64, 65). In addition, thymocytes from SIRT1-deficient cells demonstrate ionizing radiation-induced increase in p53 hyperacetylation followed by apoptosis confirming a role for SIRT1 in regulation of p53 activity (64).

SIRT2

The human SIRT2 protein shares sequence similarity as well as cytoplasmic localization with the *S. cerevisiae* Hst2p (54, 86, 87). Expression profiling of SIRT2 indicates a prominent expression in adult heart, brain, skeletal muscle, kidney, liver and testis and in fetal brain and liver (18, 67, 88). A potential role for SIRT2 in tumorigenesis was recently described with studies using a proteomics-based approach (89). *SIRT2*, which is located on chromosome 19q13.2, is within a chromosome region frequently deleted in human gliomas and SIRT2 expression (both mRNA and protein levels) is reduced in a high percentage of human glioma cell lines. Ectopic expression of *SIRT2* in these cell lines suppressed colony formation and modified the microtubule network. These results indicate that SIRT2 may act as a tumor suppressor, however the mechanism underlying this activity remains unclear (89). One possible mechanism is through negative regulation of mitotic exit by SIRT2 (90). However a direct link has not been clearly demonstrated.

In addition, SIRT2 interacts with the homeobox protein, HOX10A (91). Initially identified in *Drosophila*, homeobox (HOX) proteins are evolutionarily conserved transcription factors that are important in developmental regulation through pattern formation by activating and repressing genes required for cell-type determination (92). The HOX family of proteins contains a common domain called the homeodomain that is responsible for binding DNA in a sequence-specific manner (93). Depending on cofactor binding to HOX proteins they can alternate between functioning as coactivators and corepressors (94). Human HOX10A, located at the 5' end of the HOX-A gene cluster, plays a key role in myeloid and B-lymphoid progenitor cell differentiation (95) and knockout mice exhibit defects in reproductive organs (96). Interaction between SIRT2 and HOX10A suggest a role for SIRT2 in transcriptional regulation in a HOX10A-dependent manner, although a direct effect of SIRT2 activity on regulation of gene expression has not been studied extensively.

SIRT3

Human SIRT3 is primarily localized in the mitochondrial matrix (97, 98), and is expressed in all tissues tested with prominent expression in brown adipose tissue, testis, brain, skeletal muscle, liver, kidney, and heart (18, 66, 67, 88, 97). Mitochondrial import is mediated by an amphipathic α -helix located within the amino-terminal extension of SIRT3. In addition to mediating mitochondrial targeting of SIRT3, this amino-terminal extension negatively regulates SIRT3 enzymatic activity. The amino-terminus of both endogenous and overexpressed SIRT3 is proteolytically processed *in vivo* resulting in the removal of the first 100 amino acids. This proteolytic processing can be recapitulated *in*

in vitro using purified mitochondrial matrix processing peptidase (MPP) (98). Unprocessed *in vitro*-translated protein is enzymatically inactive and becomes active after proteolytic processing by MPP, suggesting that SIRT3 is maintained in an inactive state until imported into the mitochondrial matrix. Although SIRT3 exhibits robust deacetylase activity on a histone H4 peptide *in vitro*, the absence of histones in the mitochondria suggest the presence of a set of novel mitochondrial proteins regulated by acetylation (97, 98). Upon overexpression of SIRT3-GFP a small fraction of cells have nuclear staining in addition to the mitochondrial localization (B. North, unpublished observation). The relevance of this observation is unclear but could indicate selective targeting of SIRT3 to different compartments under a variety of physiological conditions.

SIRT4–7

Similar to SIRT3, SIRT4 has also targeted to the mitochondrial matrix (N. Ahuja, B. North and E. Verdin, unpublished observation). In addition, SIRT5 has been characterized with a mitochondrial-like localization pattern, however import of SIRT5 into this organelle has not been fully characterized (67). SIRT6 is localized to the nucleus where it appears to be associated with chromatin during interphase and the chromosomes during mitosis (67). Like SIRT1 and SIRT6, SIRT7 is targeted to the nucleus, but with a nucleolar localization pattern (67). SIRT4 is prominently expressed in the heart, liver, kidney, spleen, testis, as well as most fetal tissues. SIRT5 appears ubiquitously expressed where SIRT6 is strongly expressed in fetal brain, as well as the adult heart, brain, lung, liver and kidney. SIRT7 is expressed in nearly all tissues with strong expression in the fetal and adult brain, fetal and adult liver, testis, kidney and heart (18, 67, 99).

Enzymatically, SIRT5 has weak deacetylase activity, whereas SIRT4 and SIRT6 both possess ADP-ribosyltransferase activity as their primary enzymatic function (N. Ahuja and E. Verdin, unpublished observation and (99)). And no enzymatic activity has been demonstrated for SIRT7.

Sirtuins and Aging

One of the most intriguing functions of sirtuins is their role in the regulation of aging in a wide variety of organisms including *S. cerevisiae*, *Drosophila*, and *C. elegans* (57, 100-102). Increasing Sir2 dosage in *S. cerevisiae* results in lifespan extension, whereas a reduction of Sir2 dosage results in reduced lifespan. Aging in *S. cerevisiae* occurs, at least in part, as a result of recombination between *rDNA* repeats, which can lead to the excision of extrachromosomal rDNA circles (ERC). An autonomous replicating sequence within the *rDNA* array allows for extrachromosomal rDNA circles to replicate during the DNA synthesis phase of the cell cycle. ERCs are preferentially segregated to mother cells during cell division, and can accumulate in old cells to a DNA content greater than that of the entire yeast genome. This extensive DNA accumulation is thought to be the cause of cell death, potentially by titrating essential transcription and/or replication factors (103). As described earlier, Sir2p functions in *S. cerevisiae* in transcriptional repression at the telomeres, silent mating-type loci, and both repression of transcription and recombination at the *rDNA* array. Deletion of *Sir2* eliminates *rDNA* silencing and increases the frequency that a marker gene is recombined out of the *rDNA* (103, 104). This latter activity, suppression of recombination at the *rDNA* array, underlies the mechanism of Sir2p regulation of yeast aging (44, 45). The laboratory of Leonard Guarente screened for

long-lived yeast cells and identified a long-lived mutant form of Sir4, termed *Sir4-42*. This mutant caused a relocalization of the Sir2/3/4p complex from the telomeres and silent mating-type loci to the *rDNA* array, in effect locally increasing the dosage of Sir2p at the *rDNA* array (105). Relocalization of the Sir2/3/4p complex to the nucleolus occurs naturally in aging wild-type cells, however the *Sir4-42* allele caused a premature relocalization of the Sir complex in young yeast cells, extending their lifespan (105). Furthermore, the Sir2/3/4p complex at the mating-type loci suppresses aging by regulating the formation of extrachromosomal rDNA circles via transcriptional repression of the genetic programs for **a** and α mating-types. Deletion of *Sir3* or *Sir4* causes derepression of both the silent mating-type loci resulting in coexpression of genes responsible for the **a** and α mating types. Activation of both mating type pathways results in an increase in *RAD52*-mediated recombination of the *rDNA* array (104). These data suggest that both nucleolar Sir2p, associated with the RENT complex, as well as the Sir2/3/4p complex at the mating-type loci function to increase lifespan by regulation of rDNA recombination and extrachromosomal rDNA circle formation.

A link between aging and Sir2 is not only observed in *S. cerevisiae*, but has been demonstrated in multiple model organisms. However the role Sir2 proteins in these different organisms regulate aging is by diverse mechanisms. In *C. elegans*, Sir-2.1 functions within the Insulin/IGF-1 pathway, which has been demonstrated through mutational analysis to function in regulation of aging and dauer formation (57). Mutations in components of the IGF-1 pathway, such as DAF-2 (the IGF-1 receptor), leading to reduced signal transduction through the pathway, extend lifespan in *C. elegans* (106, 107). An extra copy of *Sir2.1* in *C. elegans* significantly extends lifespan, which

requires a functional DAF-16 molecule, a forkhead transcription factor that is a downstream effector of activation of the insulin signaling pathway (57). By regulating the Insulin/IGF-1 signaling pathway, *Sir-2.1* also enhances dauer formation a specialized survival form of the worm (57). However, the molecular mechanisms by which *Sir-2.1* control the Insulin/IGF-1 pathway and dauer formation leading to regulation of *C. elegans* longevity, and whether these mechanisms are conserved in higher organisms such as mammals remains to be elucidated.

For more than sixty years, reduction of caloric intake has been known to extend lifespan in a wide variety of organisms. “Calorie restriction” is a dietary regimen in which organisms are fed 30–50% less calories than a normal *ad libitum* diet. The mechanism underlying the increase in lifespan in response to calorie restriction remains elusive. However, the observed lifespan extension mediated by low glucose levels (i.e. caloric restriction) in yeast has been demonstrated to be dependent on Sir2p (55, 100). Furthermore, lifespan extension mediated by caloric restriction also requires NAD⁺, as strains lacking NPT1 or other components of the NAD⁺ synthesis pathway, do not display lifespan extension in response to caloric restriction (100). The connection between the “caloric restriction” phenotype and Sir2 has not been limited to yeast cells, as increased lifespan mediated by caloric restriction has been observed in nearly all organisms tested including yeast, worms, and flies, and evidence suggest the effect is mediated through Sir2 proteins (101, 108, 109). The laboratory of David Sinclair has observed that mice fed a calorically restricted diet, or mammalian cells cultured in the presence of serum from calorically restricted mice, induce expression of the Sir2p homologue in humans,

SIRT1 (69). These results suggest SIRT1 may function in mediating the caloric restriction effect in mammals.

Characteristic Structural Features

Compared to class I and II HDACs, the class III HDACs have a unique catalytic domain illustrated by their requirement for the cofactor NAD⁺ (110). The structure of four sirtuins, *Archaeoglobus fulgidus* Sir2-Af1 and Sir2-Af2, human SIRT2 and *S. cerevisiae* Hst2p, have been obtained at atomic resolution and a number of common features are emerging (111-114). All proteins are organized in two bi-lobed globular domains, a small domain with two distinct modules and a large domain (figure 1.3).

The large domain (figure 1.3, shown in green) contains an inverted classical open α/β Rossmann fold structure, which is a common structural fold found in NAD(H)/NADP(H) binding proteins (111-113). This domain consists of eight α helices (α 1, 2, 6, 7, 9–12) that pack against six parallel β strands forming a central β sheet (β 1–3 and 7–9) (figure 1.3). SIRT2 and Hst2p each have an additional crystallized α helix, α 13, that packs against the outside of the large domain, but is not found in Sir2-Af1 or Af2. The most significant difference within the large domains of these structures is an insertion in the region of the α 11 helix within SIRT2 that is absent in Sir2-Af1 and Sir-Af2. This helix is located outside the catalytic pocket, but along the same face, and could possibly be involved in substrate recognition or macromolecular complex formation (111).

Two structural modules comprising the small domain result from two insertions in the Rossmann fold of the large domain (111-113). The first insertion consists of three α -

helices (α_3 , α_4 and α_5) that fold to form the helical module (figure 1.3, shown in yellow). This module has a pocket lined with hydrophobic residues that may be a class-specific protein-protein interaction domain, possibly recognizing substrate specific residues. Based on sequence alignments, all class I sirtuins have the α_3 , α_3 , α_4 and α_5 helices that form the hydrophobic pocket. However, classes II, III and IV sirtuins contain deletions in this module, suggesting class specific differences in this region, which might contribute to the observed differences in enzymatic activity or substrate specificity. The second insertion forms a zinc-binding module (figure 1.3, shown in blue), composed of antiparallel β strands containing two Cys-X-X-Cys motifs, separated by 15–20 amino acids, involved in zinc coordination (111-114). Replacing the cysteine residues with alanines abolishes Sir2 enzymatic activity (113, 115). Likewise, the presence of zinc is required for enzymatic activity, as the zinc chelator *o*-phenanthroline inhibits enzymatic activity (113). The localization of zinc away from the catalytic pocket suggests that the zinc ion does not participate directly in catalysis, however is likely to be involved in protein stability. This is in contrast with class I and II HDACs where zinc ions are part of the active site and catalytic mechanism (113, 116).

A large groove is formed at the interface between the large and small domains and runs perpendicular to the long axis formed by the two domains (figure 1.3). Based on mutagenesis studies, a role in substrate recognition and catalysis has been proposed for this region (112, 113). Crystal structure analysis of Sir2-Af2 from *A. fulgidus* complexed with an acetylated p53 peptide, demonstrates that the peptide substrate lies in the large groove (111). The binding of an acetylated peptide, such as p53, is suggested to occur via

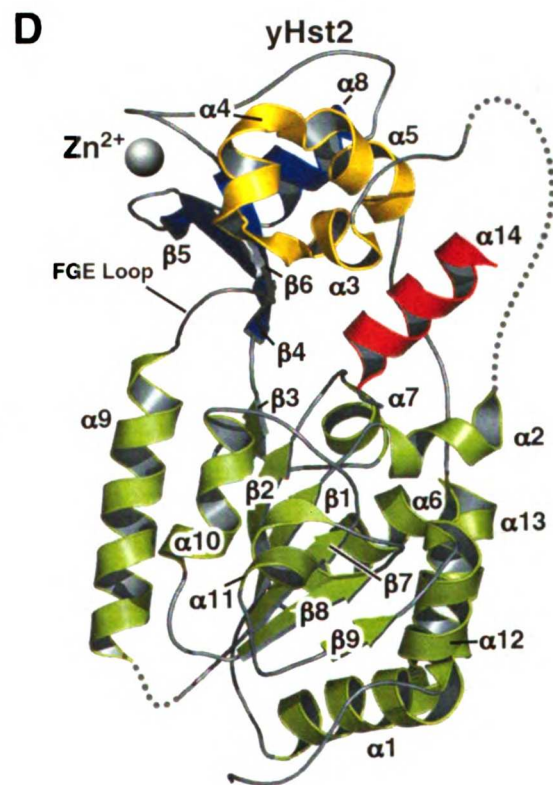
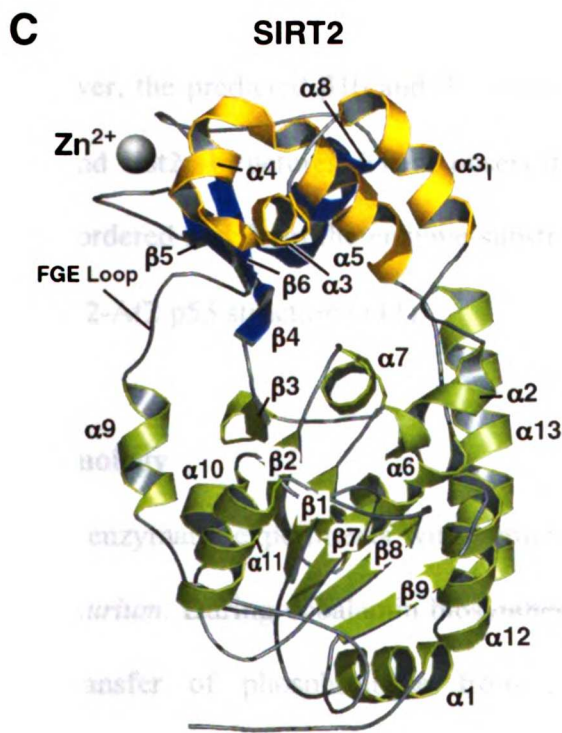
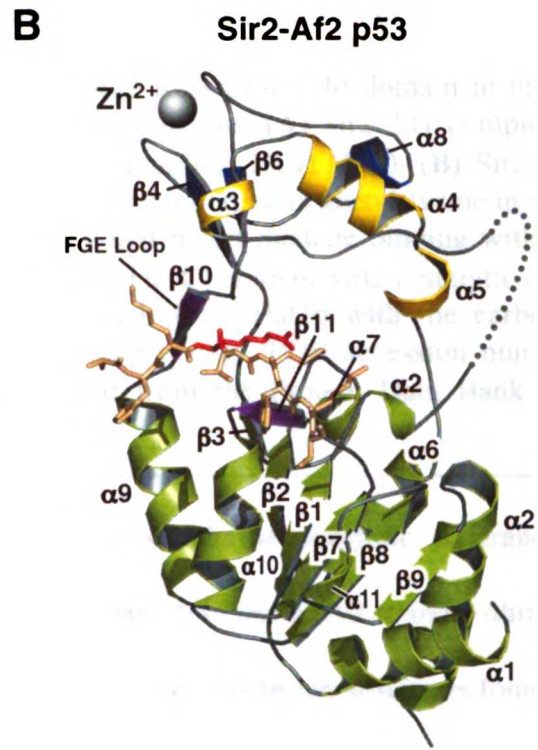
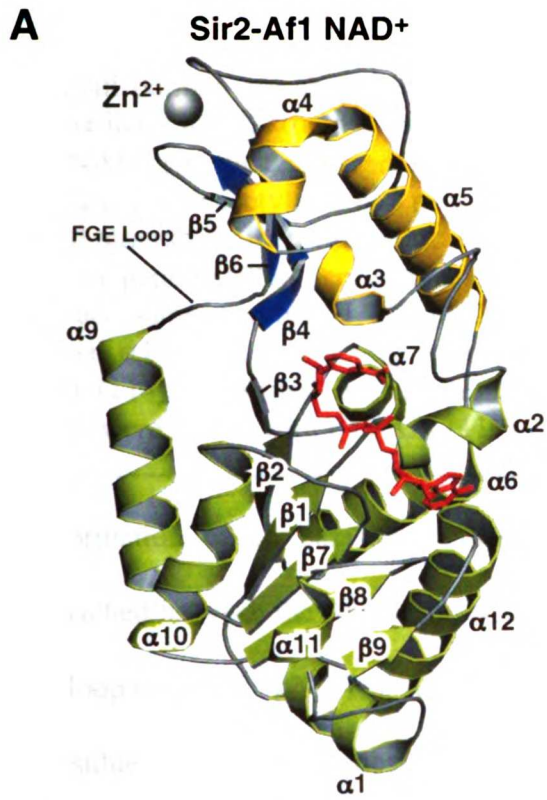


Figure 1.3. Three-dimensional high-resolution crystal structures of four sirtuin proteins. The zinc-binding module is shown in blue in each panel, the helical modules of the small domain are shown in yellow, and the large Rossmann-fold domain in green. Each α -helix and β -strand is labeled to facilitate comparisons. (A) Sir2-Af1 complexed with NAD⁺ (in stick representation; PDB accession number: 1ICI) (113). (B) Sir2-Af2 complexed with acetylated p53 peptide (in stick representation, with acetyl-lysine in red). Two β -strands (β 10 and β 11) are shown in purple that might mediate binding with the substrate peptide (PDB accession number: IMA3) (111). (C) Human Sirt2 (catalytic core; PDB accession number: 1J8F) (112). (D) Full-length yeast Hst2p with the carboxy-terminal α 14 helix interacting with the NAD-binding pocket (PDB accession number: 1Q14) (114). Structural coordinates were obtained from the Protein Data Bank and models were drawn with PYMOL (117).

the formation of an enzyme-substrate β sheet, in which the substrate β strand is sandwiched between the β 11 strand within the Rossmann fold and a β 10 strand within the FGE loop (figure 1.3A) (111). A high degree of conservation between sirtuins is found in the residues implicated in substrate peptide binding, specifically in the region of the FGE loop, named for the highly conserved FGExL motif found in sirtuins (figure 1.3B) (111). However, the predicted β 10 and β 11 strands of Sir2-Af2 are absent in the SIRT2, Sir2-Af1 and Hst2p structures. These observations suggests that these two regions become more ordered and form the enzyme-substrate β sheet upon substrate binding, as seen in the Sir2-Af2 p53 structure (111).

Enzymology

Initial enzymatic experiments with sirtuins were carried out in the bacteria *Salmonella typhimurium*. During cobalamin biosynthesis, the CobT enzyme in *Salmonella* catalyzes the transfer of phosphoribose from nicotinic acid mononucleotide (NaMN) to dimethylbenzimidazole (DMB) to form DMB-5'-ribosyl-phosphate (118, 119). In the absence of CobT, the Sir2-like protein CobB could partially compensate in the catalysis

of this reaction (120). Later, recombinant Sir2 proteins from both bacteria and humans demonstrated NAD⁺-dependent ADP-ribosyltransferase activity *in vitro* (18, 121). Although the initial enzymatic activity associated with sirtuins was an ADP-ribosyltransferase activity, protein deacetylase activity was subsequently shown to represent the primary enzymatic function of Sir2p as well as other sirtuins (14-16). The deacetylation reaction generates three products: the deacetylated peptide substrate, nicotinamide, and the unique metabolite 2'-*o*-acetyl-ADP-ribose (figure 1.4) (122). The ratio of these products is 1:1:1, consistent with the model that hydrolysis of one NAD⁺ to 2'-*o*-acetyl-ADP-ribose and nicotinamide occurs for each acetyl group removed and that deacetylation requires an enzyme-ADP-ribose intermediate (figure 1.4) (110, 122). Nicotinamide, as a byproduct of the NAD⁺-dependent deacetylation reaction, can function both *in vitro* and *in vivo* as a sirtuin inhibitor when present in excessive concentrations with respect to NAD⁺ (73, 110, 123). In addition, the recent observation that *o*-acetyl-ADP-ribose delays oocyte maturation and embryo cell division in blastomeres suggest that it might represent a *bona fide* secondary messenger linked to the enzymatic activity of sirtuins (124-126). The demonstration that the ribosyltransferase and NAD⁺ cleavage are dependent on the presence of an acetylated substrate confirms the fundamental link between these two activities (16, 110, 121, 125, 126).

A physiological role of ADP-ribosyltransferase activity remains likely for many sirtuins. A recently identified *Trypanosoma brucei* class Ib sirtuin, called TbSIR2RP1, exhibits robust histone deacetylase and ADP-ribosyltransferase activities towards histones H2A and H2B (128). A correlation between the activity of TbSIR2RP1, the

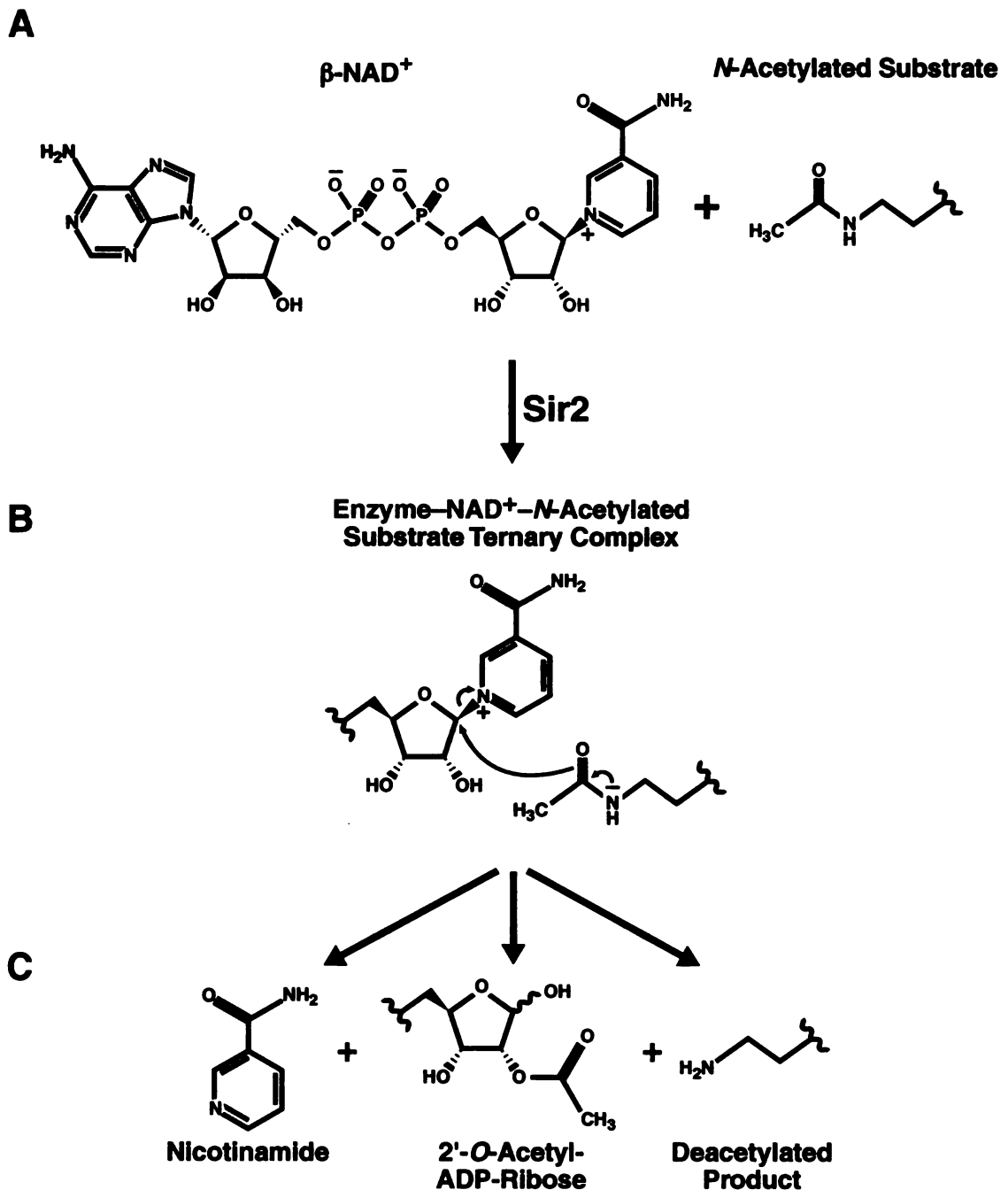


Figure 1.4. The enzymatic activity of sirtuins. (A) The components necessary for sirtuin-mediated deacetylase activity are the sirtuin enzyme, $\beta\text{-NAD}^+$, and the *N*-acetylated substrate. (B) The components form a tertiary complex and, during the enzymatic reaction, the nicotinamide is expelled from bound NAD^+ to generate an oxocarbenium-like transition state in which the carbonyl oxygen of the acetyl group attacks the C1 carbon of ADP. After alkylamidate and cyclic intermediates and possibly protonation of the amine leaving group (not shown), the products, (C) the deacetylated protein, 2'-*o*-acetyl-ADP-ribose, and nicotinamide are formed (127).

extent of chromatin ADP-ribosylation, and the sensitivity of trypanosomes to DNA damaging agents has been observed (128). In addition, human SIRT4 and SIRT6 might possess ADP-ribosyltransferase activity as their primary function (N. Ahuja and E. Verdin, unpublished observation and (99)), however, biologically relevant targets for the activity of these proteins remain unknown.

Since the identification that sirtuins are NAD^+ -dependent protein deacetylases, involved in molecular pathways regulating transcriptional silencing, DNA damage repair, development, and aging in lower organisms, the identification of substrates and functions attributed to mammalian sirtuins has been of considerable interest. The focus of this thesis has been on the function and mechanisms regulating the human SIRT2 protein. We have found that SIRT2 is localized primarily in the cytoplasm on the microtubule network where SIRT2 functions to deacetylate lysine-40 of α -tubulin. During mitosis, SIRT2 is localized to microtubule derived mitotic structures including the centrosome, spindle, and midbody. Finally, we demonstrate that SIRT2 regulates cellular proliferation in a manner that is dependent on its phosphorylation by the mitotic regulator Cdk1.

Chapter 2:

Deacetylation of α -Tubulin by SIRT2 Regulates Microtubule Interaction and Subcellular Localization of MIZ-1

Introduction

In addition to histones, a rapidly growing number of non-histone proteins are acetylated on lysine residues (reviewed in (2)). The human SIRT2 protein shows a cytoplasmic distribution (54, 86). Both SIRT2 and Hst2p may regulate rDNA and telomeric silencing indirectly from their cytoplasmic location (54), but this does not exclude the possibility that these enzymes have cytoplasmic targets as well. One possible target for deacetylation in the cytoplasmic compartment is α -tubulin within the microtubule network.

The microtubule network is formed by the polymerization of α - and β -tubulin heterodimers and plays an important role in the regulation of cell shape, intracellular transport, cell motility, and cell division (129). α - and β -tubulin subunits are subject to numerous posttranslational modifications, including tyrosination, phosphorylation, polyglutamylation, polyglycylation, and acetylation (130). Tubulin acetylation occurs on lysine-40 of the α -tubulin subunit (131, 132). A variety of drug treatments and physiological signals have been reported to modulate the level of α -tubulin acetylation, including the anticancer drug paclitaxel (Taxol) (131), Trichostatin A (TSA) (133), Ras activation (134), as well as microtubule interaction of MAP1, MAP2C, tau, and the herpes simplex virus encoded protein VP22 (135). Similarly, microtubules associated with stable structures, such as cilia, contain relatively hyperacetylated α -tubulin (136, 137). However, a lack of knowledge on the enzymes responsible for the reversible acetylation and deacetylation of α -tubulin has precluded a thorough analysis of the biological role of α -tubulin acetylation in microtubule functions.

In this chapter we identify human SIRT2 as a α -tubulin deacetylase. We also show that deacetylation of α -tubulin is involved in regulating the interaction of the

Results

SIRT2 is a Cytoplasmic Protein that Colocalizes with the Microtubule Network

We determined the subcellular localization of endogenous SIRT2 in a human fibroblast cell line using indirect immunofluorescence and a specific antiserum against SIRT2. Endogenous SIRT2 was predominantly cytoplasmic with a distinct localization pattern reminiscent of the microtubule network (figure 2.1A). Merging of the pictures obtained with the SIRT2 antiserum and with an antiserum specific for α -tubulin showed strong colocalization between SIRT2 and tubulin (figure 2.1A). Cytoplasmic localization of SIRT2 was verified by fractionation of 293T cells into nuclear and cytoplasmic fractions. Western blotting analysis with a SIRT2 antiserum showed that SIRT2 was localized predominantly in the cytoplasm but was also present to a lesser degree in the nucleus (figure 2.1B). Probing the same fractions for a known cytoplasmic protein, p65, and for a known nuclear protein, lamin A, confirmed the purity of our cytoplasmic and nuclear fractions (figure 2.1B). Biochemical fractionation of cells overexpressing SIRT2 tagged at the carboxy-terminus with the FLAG peptide (SIRT2-FLAG) or SIRT2 tagged at the amino-terminus with GFP (GFP-SIRT2) was performed that recapitulated the observations with the endogenous protein (figure 2.1C). However, GFP-SIRT2 demonstrated a more strict regulation of subcellular distribution with a greater level in the cytoplasm, suggesting that the tagging of SIRT2 with GFP might influence the regulation of SIRT2 nuclear localization.

These observations are in agreement with previously published results showing that SIRT2 is predominantly cytoplasmic (86, 88). In addition, the colocalization with the microtubule network also suggested a possible role for SIRT2 in microtubule function.

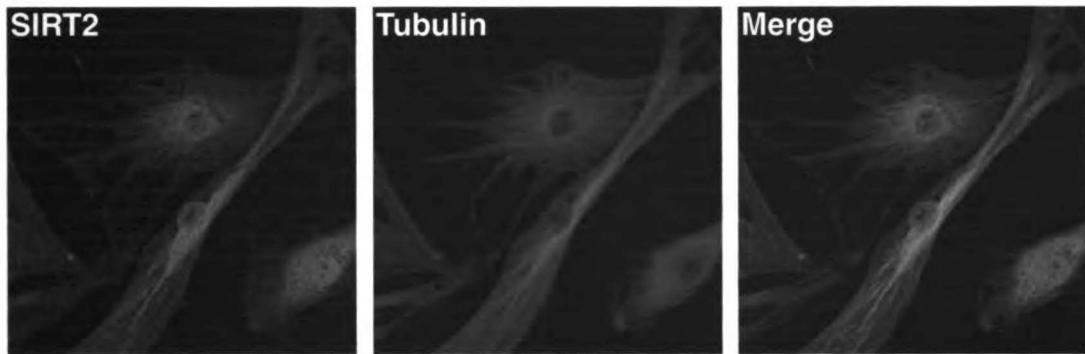
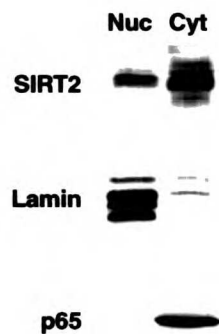
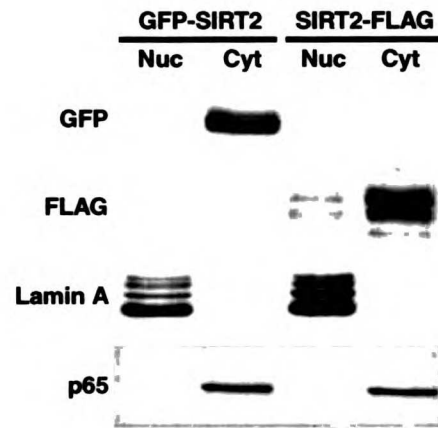
A**B****C**

Figure 2.1. SIRT2 is predominantly cytoplasmic and colocalizes with the microtubule network. (A) Confocal microscopy analysis of SIRT2 and tubulin in human fibroblast. Cells were stained for SIRT2 (green) and tubulin (red) to visualize the microtubule network. (B) Nuclear and cytoplasmic extracts from 293T cells were analyzed by western blotting with specific antisera for SIRT2, lamin A and p65. (C) Nuclear and cytoplasmic extracts from 293T cells transfected with GFP-SIRT2 or SIRT2-FLAG were analyzed by western blotting with specific antisera for GFP, FLAG, lamin A and p65.

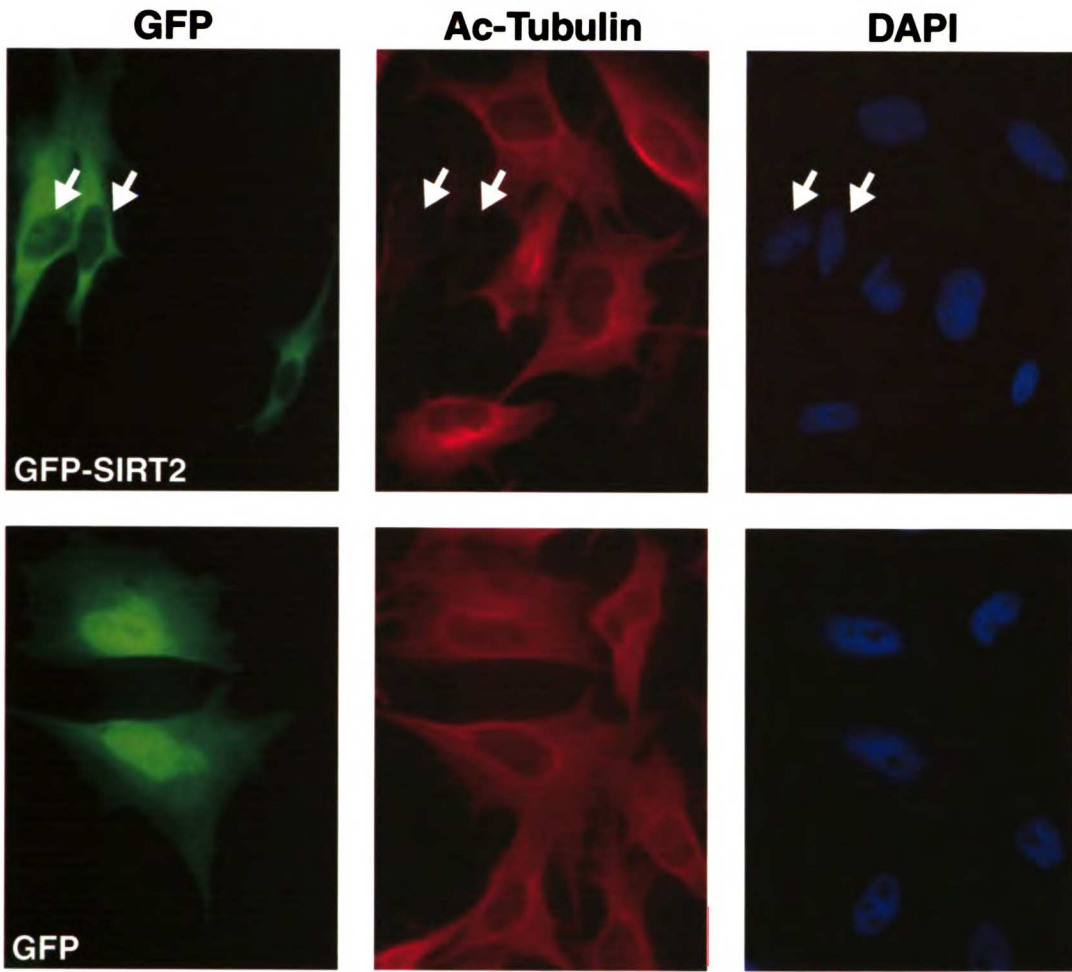
α-Tubulin Deacetylation by Human SIRT2 in vivo

The localization of SIRT2 along the microtubule network and the previous observation that α -tubulin is acetylated, enticed us to test whether SIRT2 can deacetylate α -tubulin. HeLa cells were transfected with GFP-SIRT2, which remains catalytically active as a deacetylase on a histone substrate (figure 2.3B), and were stained with an antiserum specific for α -tubulin acetylated at lysine-40 (131). Cells expressing GFP-SIRT2 had markedly less acetylated α -tubulin than neighboring untransfected cells (figure 2.2A). As a control, cells transfected with an expression vector for GFP alone exhibited no alteration in the level of acetylated α -tubulin (figure 2.2A). Importantly, staining with another α -tubulin antiserum that recognizes α -tubulin independently of its acetylation state showed no significant change in α -tubulin levels or the microtubule network, quantitatively or qualitatively, in response to GFP-SIRT2 expression (figure 2.2B). These observations indicate that SIRT2 functions to regulate α -tubulin acetylation *in vivo*, directly or indirectly.

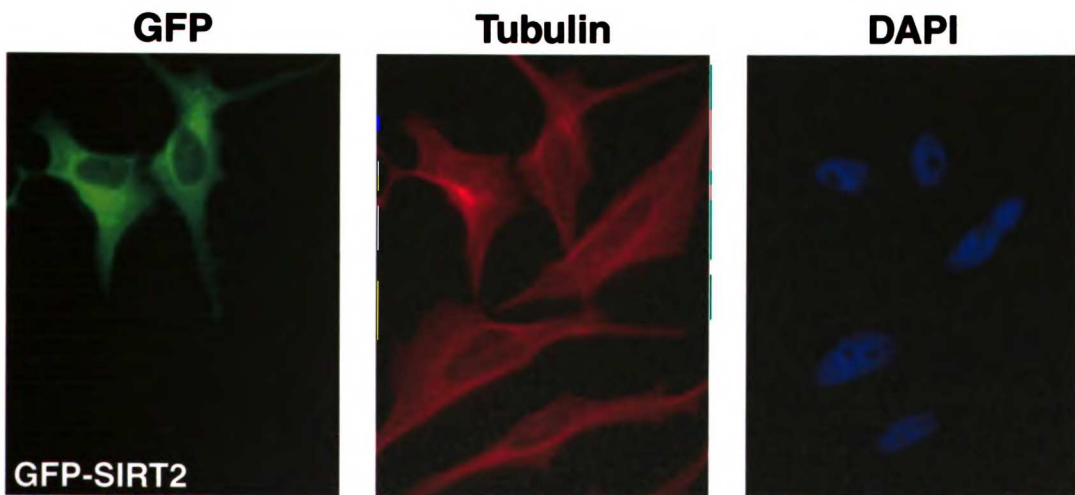
The Sir2 proteins contain a highly conserved domain, associated with enzymatic activity. A number of highly conserved residues within this domain are necessary for deacetylase activity (figure 2.3A) (112). We replaced asparagine-168 with alanine (N168A) or histidine-187 with tyrosine (H187Y) in GFP-SIRT2. Fusion proteins with these substitutions were inactive on a histone substrate whereas the wild-type GFP-SIRT2 showed robust activity after immunoprecipitation with antiserum for GFP (figure 2.3B). To verify that the deacetylase activity of SIRT2 was necessary for α -tubulin deacetylation, we transfected GFP-SIRT2 expression vectors containing catalytically inactive mutations into HeLa cells. The catalytically inactive mutants N168A or H187Y

11007 11007 11007

A



B



1100F (1000ADW)

Figure 2.2. *In vivo* α -tubulin deacetylation by GFP-SIRT2. (A) HeLa cells transfected with GFP-SIRT2 or GFP alone were treated with 400 nM TSA for 12 hours and subsequently stained for acetylated α -tubulin. DNA was stained with DAPI. Each frame was visualized for GFP (green), acetylated α -tubulin (red), and DNA (blue). White arrows identify cells transfected with GFP-SIRT2. (B) HeLa cells transfected with GFP-SIRT2 and treated as in (A) were stained for total α -tubulin (red) to examine the microtubule network.

did not modify the level of α -tubulin acetylation (figure 2.3C). These results indicate that expression of wild-type SIRT2 *in vivo* leads to the deacetylation of lysine-40 on α -tubulin, mediated by the deacetylase activity of SIRT2.

Human SIRT2 Deacetylates α -Tubulin in vitro

To directly test the ability of SIRT2 to deacetylate α -tubulin, we developed an *in vitro* tubulin deacetylation assay (figure 2.4A). We transfected 293T cells with SIRT2-FLAG and immunoprecipitated the FLAG-tagged protein. The immunoprecipitated material was separated into two fractions. The first fraction was used to measure HDAC activity using a peptide corresponding to the amino-terminal tail of histone H4 (amino acids 1–23) acetylated *in vitro*. The second fraction was used for a tubulin deacetylation activity assay using total cellular lysates from untransfected 293T cells. The extent of α -tubulin deacetylation was determined by western blotting with an antiserum specific for acetylated α -tubulin or for total α -tubulin. Material immunoprecipitated after transfection of 293T cells with an empty FLAG vector had no effect on α -tubulin acetylation (figure 2.4B, lane 1). Thus, neither the lysate utilized as acetylated α -tubulin substrate nor the immunoprecipitation procedure contributed any significant levels of α -tubulin deacetylase activity. However, incubation of cellular lysate with the immunoprecipitated

1102110001

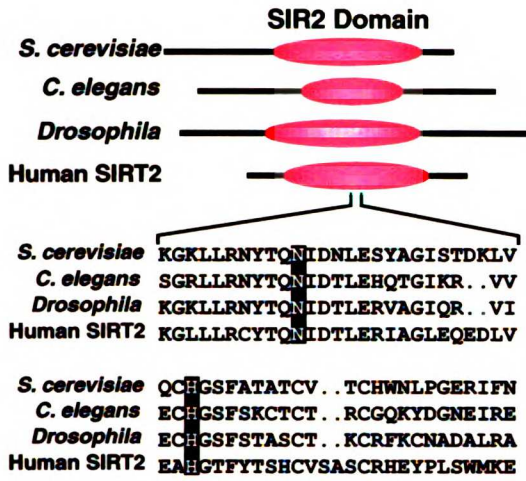
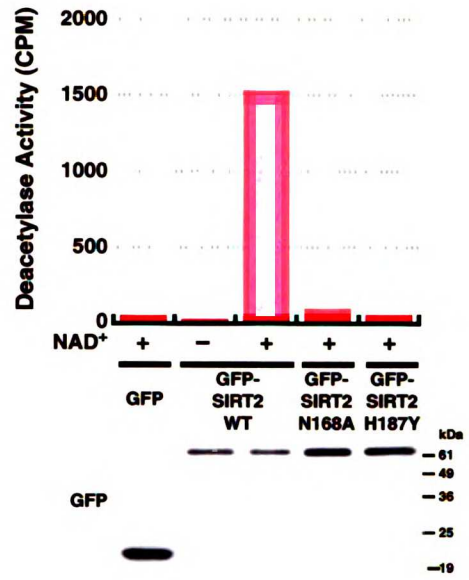
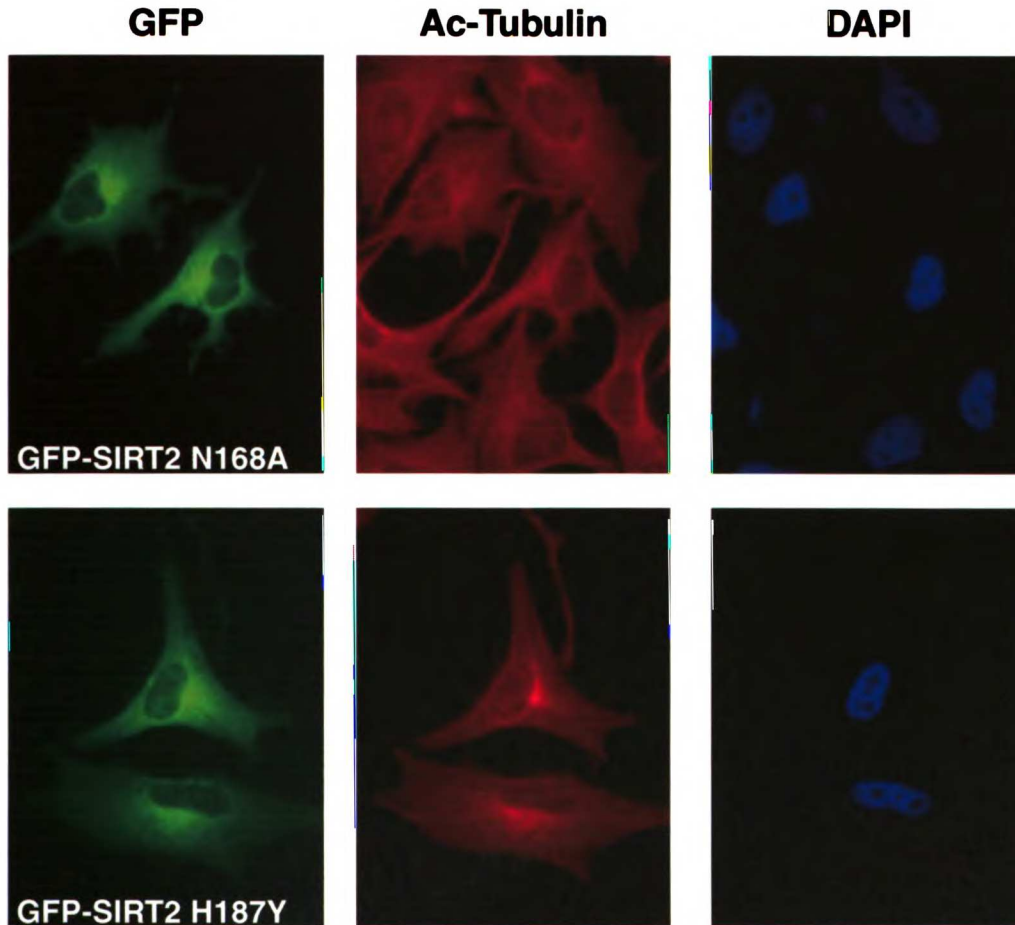
A**B****C**

Figure 2.3. Catalytic mutants of SIRT2 lack deacetylase activity *in vitro* and *in vivo*. (A) Schematic diagram of the highly conserved catalytic pocket within the Sir2 domain of SIRT2 homologues from four species. (B) Immunoprecipitated GFP-SIRT2 wild-type, N168A, or H187Y proteins were subjected to HDAC activity assay with an [³H] acetylated histone H4 peptide with or without 1 mM NAD⁺ *in vitro*. The immunoprecipitated GFP proteins were separated by SDS-PAGE and visualized by western blotting with specific antisera for GFP. (C) HeLa cells transfected with the N168A or H187Y point mutants of GFP-SIRT2 and treated, stained, and visualized, as in figure 2.2A.

SIRT2-FLAG protein deacetylated α -tubulin in a NAD⁺-dependent manner (figure 2.4B, lanes 2 and 3). In addition, the catalytically inactive mutant N168A did not deacetylate α -tubulin (figure 2.4B, lane 4). The same immunoprecipitated material was tested for HDAC activity using an acetylated histone H4 peptide (figure 2.4B, deacetylase activity (CPM) row). These data suggest that SIRT2 has intrinsic NAD⁺-dependent α -tubulin deacetylase activity.

Humans have seven highly conserved proteins with homology to *S. cerevisiae* Sir2p (17, 18). To determine whether α -tubulin deacetylase activity is restricted to SIRT2, we expressed all seven human SIRT proteins each with a carboxy-terminal FLAG tag in 293T cells. Only SIRT2 deacetylated α -tubulin *in vitro*, whereas the remaining SIRT proteins contained no significant tubulin deacetylase activity (figure 2.4C). This is in contrast with the activity of the same immunoprecipitated proteins on a histone H4 peptide; where SIRT1, 2, 3 and 5 showed significant deacetylase activity, and SIRT4, 6, and 7 had low to undetectable deacetylase activity on the histone H4 peptide (figure 2.4C). These results demonstrate that SIRT2 is the only class III HDAC capable of deacetylating α -tubulin.

Purification of a SET3 complex from *S. cerevisiae* has identified both class I and class III HDACs present in the same multi-protein complex (138). Although our *in vitro*

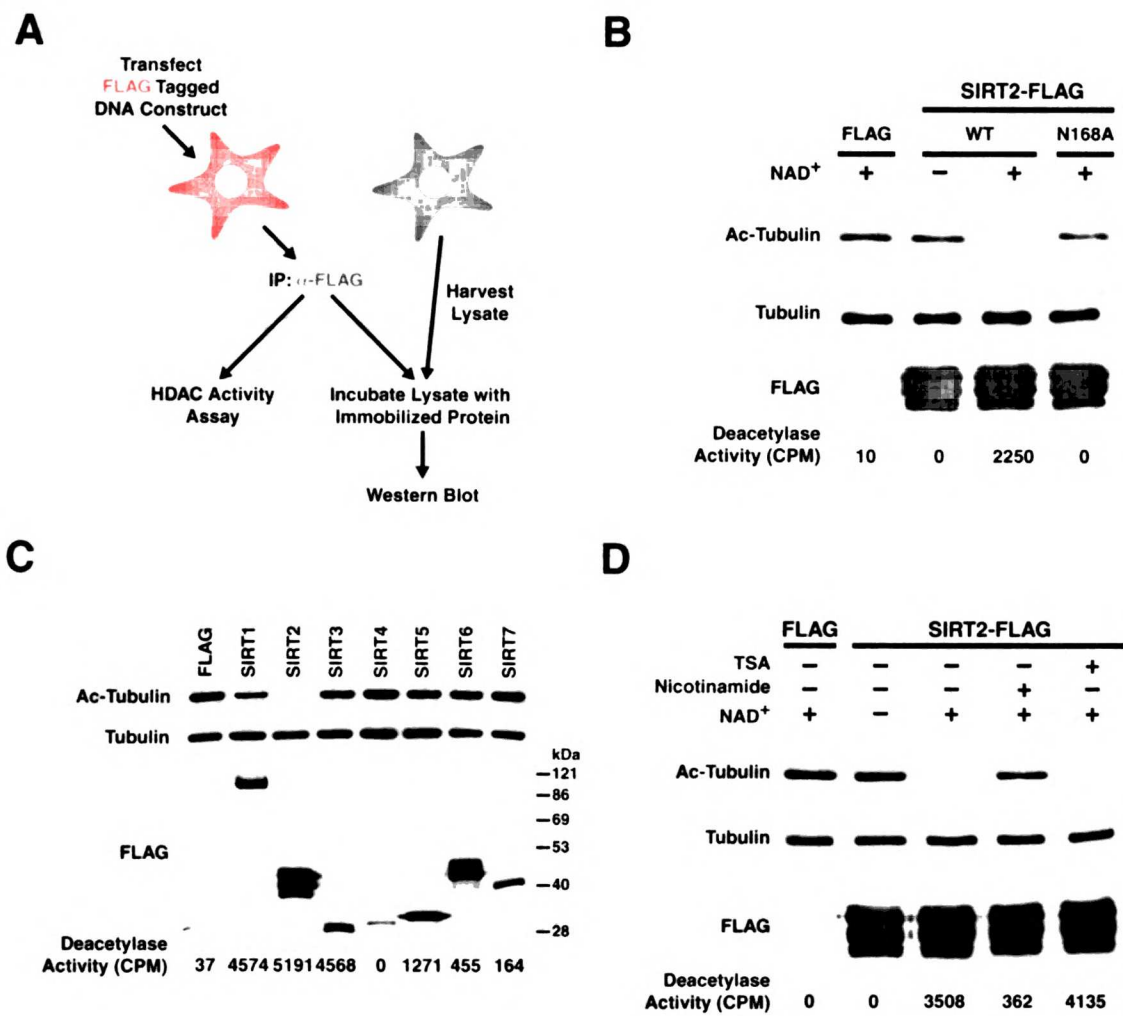


Figure 2.4. SIRT2 deacetylates α -tubulin *in vitro*. (A) Schematic diagram of *in vitro* α -tubulin deacetylation assay. (B) One-half of the immunoprecipitated protein corresponding to SIRT2-FLAG wild-type, or N168A, was incubated with cellular lysate with or without 1 mM NAD⁺ *in vitro*. The reaction products were separated by SDS-PAGE and visualized by western blotting with specific antisera for acetylated α -tubulin, α -tubulin, and FLAG. The second half of the immunoprecipitated material was subjected to HDAC activity assay with an [³H] acetylated histone H4 peptide. (C) The same assays as in (B) were conducted using the seven class III HDACs, SIRT1-7-FLAG. (D) Inhibition of SIRT2 α -tubulin deacetylation was tested using the assay described in (B). Reactions were incubated with or without 1 mM NAD⁺, and specified reactions were incubated with either 5 mM nicotinamide or 400 nM TSA.

tubulin deacetylation assay data suggest that SIRT2 functions as an NAD^+ -dependent α -tubulin deacetylase, we wanted to exclude the possibility that the immunoprecipitated material contained a class I or class II HDAC mediating to the observed α -tubulin deacetylation. This was tested by using specific inhibitors for class III HDACs (nicotinamide) or for class I–II HDACs (TSA) on the α -tubulin deacetylase activity associated with SIRT2. In contrast to class I and class II HDACs, class III HDACs are reported to be insensitive to TSA (16, 139). Nicotinamide, the resulting product from the hydrolysis of the pyridinium-*N*-glycosidic bond of NAD^+ (14), effectively inhibits SIRT1, a class III HDAC (71). We transfected 293T cells with SIRT2-FLAG or the empty FLAG vector as a control, followed by immunoprecipitation with anti-FLAG. As shown above, we observed an NAD^+ -dependent deacetylation of α -tubulin by SIRT2 (figure 2.4D, lanes 2 and 3). This reaction was completely inhibited by 5 mM nicotinamide (figure 2.4D, lanes 4). TSA at 400 nM had no effect on tubulin deacetylation by SIRT2 (figure 2.4D, lane 5). Utilizing the same immunoprecipitated material in an HDAC activity assay on a histone H4 peptide, we observed a reduction in SIRT2 activity in the presence of 5 mM nicotinamide (figure 2.4D, lanes 3 and 4), and no effect on SIRT2 activity in the presence of 400 nM TSA (figure 2.4D, lane 5). These results confirm that the sole α -tubulin deacetylase within the immunoprecipitated SIRT2 material after overexpression can be attributed to SIRT2.

Enzymatic Kinetics of Human SIRT2 and Yeast Hst2p

To test whether recombinant human SIRT2 has NAD^+ -dependent deacetylase activity, we incubated recombinant human SIRT2 purified from *Escherichia coli* with increasing

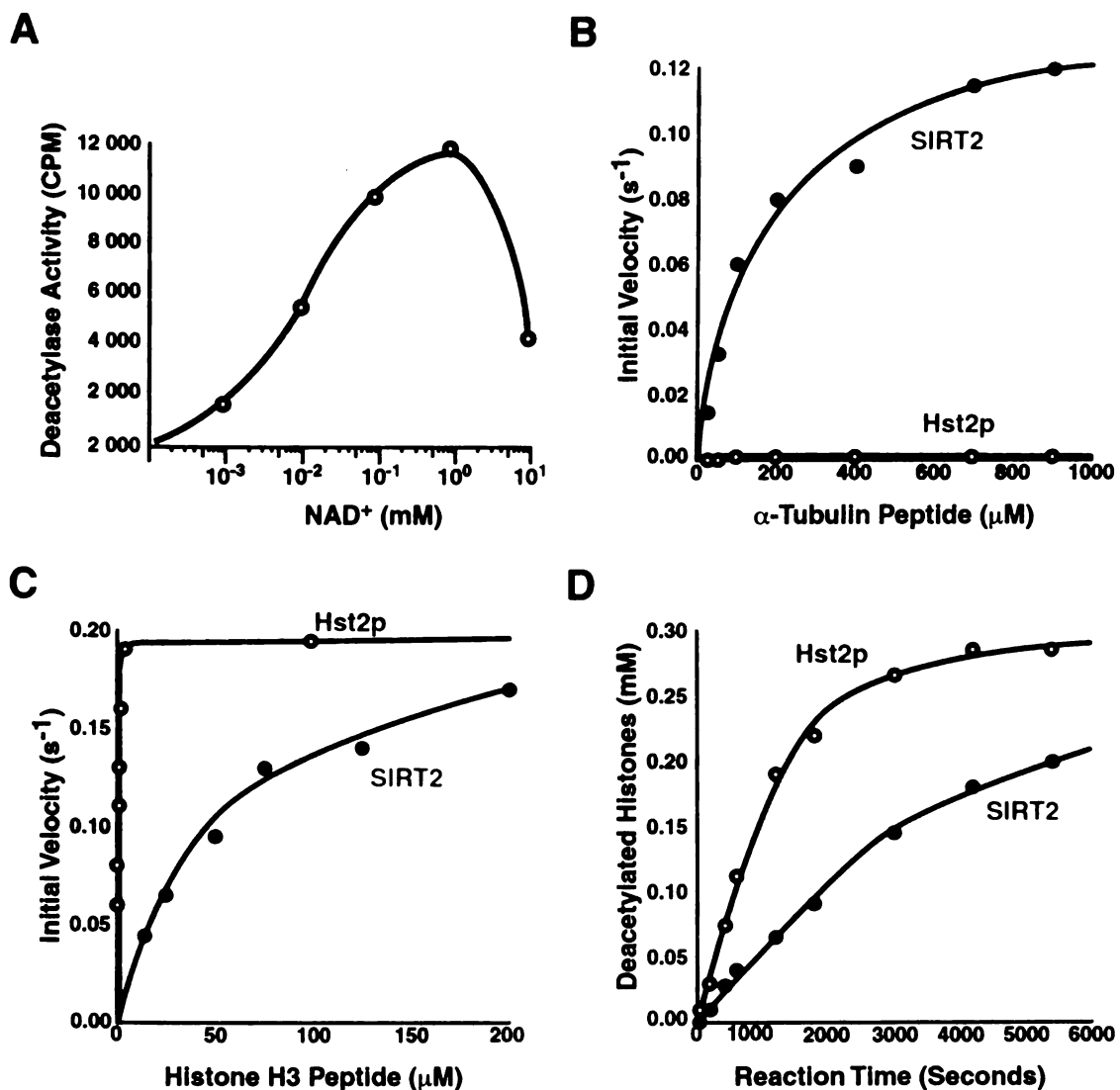


Figure 2.5. α -Tubulin is a preferred substrate for SIRT2 in comparison to Hst2p. (A) The enzymatic activity of recombinant 6-His-SIRT2 on a [³H] acetylated histone H4 peptide was measured in the presence of increasing concentrations of NAD⁺ (0, 0.001, 0.01, 0.1, 1.0, and 10 mM). (B) Initial velocities measured at varying concentrations of an acetylated α -tubulin peptide for SIRT2 (closed circles) and for Hst2p (open circles) with concentrations and conditions described in materials and methods. The curve with SIRT2 represents the average rates from three different experiments. The Hst2p curve is a representative data set from one of three separate experiments. (C) Initial velocities for each enzyme measured at varying concentrations of acetylated H3 peptide for SIRT2 and for Hst2p with concentrations and conditions described in materials and methods. (D) Kinetic progress curves of histone deacetylation by SIRT2 and Hst2p. Either SIRT2 (50 nM) or Hst2p (20 nM) were incubated with ~ 1.2 μ M PCAF-acetylated calf thymus core histones.

concentrations of NAD^+ and an acetylated histone H4 peptide. A dose-dependent increase in HDAC activity was observed with increasing concentrations of NAD^+ up to 1 mM (figure 2.5A). A further increase in NAD^+ concentration to 10 mM resulted in a reduction in deacetylase activity.

To further analyze the deacetylation of α -tubulin by SIRT2, a detailed enzymatic analysis was performed. For comparison, the highly active yeast histone deacetylase Hst2p was analyzed alongside the human enzyme. Hst2p exhibits strong selectivity for peptides corresponding to histone H3 acetylated at lysine-14 (14, 125). We utilized a 9-amino acid synthetic acetylated α -tubulin peptide (corresponding to amino acids 36–44) acetylated at lysine-40 and a 20-amino acid synthetic histone H3 peptide (corresponding to amino acids 1–20) acetylated at lysine-14 to measure initial velocities of Hst2p and SIRT2 at various acetylated α -tubulin or histone H3 concentrations. The resulting saturation curves were fitted to the Michaelis-Menten equation, yielding the kinetic parameters k_{cat} , K_m , and V/K . K_{cat} is the maximal rate of enzyme turnover when substrates are at saturating concentrations. K_m is the concentration of substrate needed to reach half the maximal velocity. The most physiologically relevant constant is V/K , as this second-order constant defines the rate of the reaction when substrate concentrations are not at saturating levels and reflects both substrate binding and catalysis. Because cellular enzymatic reactions rarely occur under maximal velocity conditions (i.e., saturating substrate levels), dramatic differences in the V/K value of the enzyme will likely reflect the most relevant *in vivo* consequences.

SIRT2 exhibited a striking preference for acetylated α -tubulin peptide as a substrate relative to yeast Hst2p (figure 2.5B). This difference was ~60-fold and was

reflected in both the k_{cat} and V/K values, which were $0.144 \pm 0.005 \text{ s}^{-1}$ and $894 \pm 100 \text{ M}^{-1}\text{s}^{-1}$ for SIRT2 and $0.00254 \pm 0.0003 \text{ s}^{-1}$ and $14.9 \pm 5.4 \text{ M}^{-1}\text{s}^{-1}$ for Hst2p, respectively. In contrast, with acetylated H3 peptide as the substrate, Hst2p demonstrated a ~200-fold stronger preference for H3 peptide relative to SIRT2 (figure 2.5C). These differences were reflected in the V/K and K_m values, which were $3930 \pm 261 \text{ M}^{-1}\text{s}^{-1}$ and $54.2 \pm 3.6 \text{ }\mu\text{M}$ for SIRT2, and $717,900 \pm 35,900 \text{ M}^{-1}\text{s}^{-1}$ and $0.280 \pm 0.014 \text{ }\mu\text{M}$ for Hst2p, respectively. The k_m values ($\sim 0.2 \text{ s}^{-1}$) were similar between the two enzymes.

These results indicate that the Sir2-family of NAD^+ -dependent deacetylases display remarkable differences in substrate specificity and that human SIRT2 has a marked preference for the acetylated α -tubulin peptide relative to the yeast enzyme Hst2p (figures 2.5B and C). To provide further evidence that SIRT2 has reduced capacity to deacetylate histones in comparison to Hst2p, we examined the ability of SIRT2 and Hst2p to deacetylate core histone proteins. Purified histones acetylated *in vitro* by PCAF were incubated with catalytic amounts of either SIRT2 or Hst2p, and deacetylation was quantified (figure 2.5D). Consistent with the peptide results, Hst2p exhibited a 7-fold higher V/K value than SIRT2.

Knockdown of SIRT2 and HDAC6 Expression Leads to α -Tubulin Hyperacetylation

A recent report has indicated that HDAC6, a class II HDAC, functions as a microtubule-associated deacetylase (140). To evaluate the relative role of both HDAC6 and SIRT2 in the deacetylation of α -tubulin *in vivo*, we used specific siRNAs to knockdown the expression of either gene. An siRNA specific for SIRT2 was transfected into 293T cells leading to a marked inhibition of SIRT2 expression (figure 2.6). Treatment of cells with

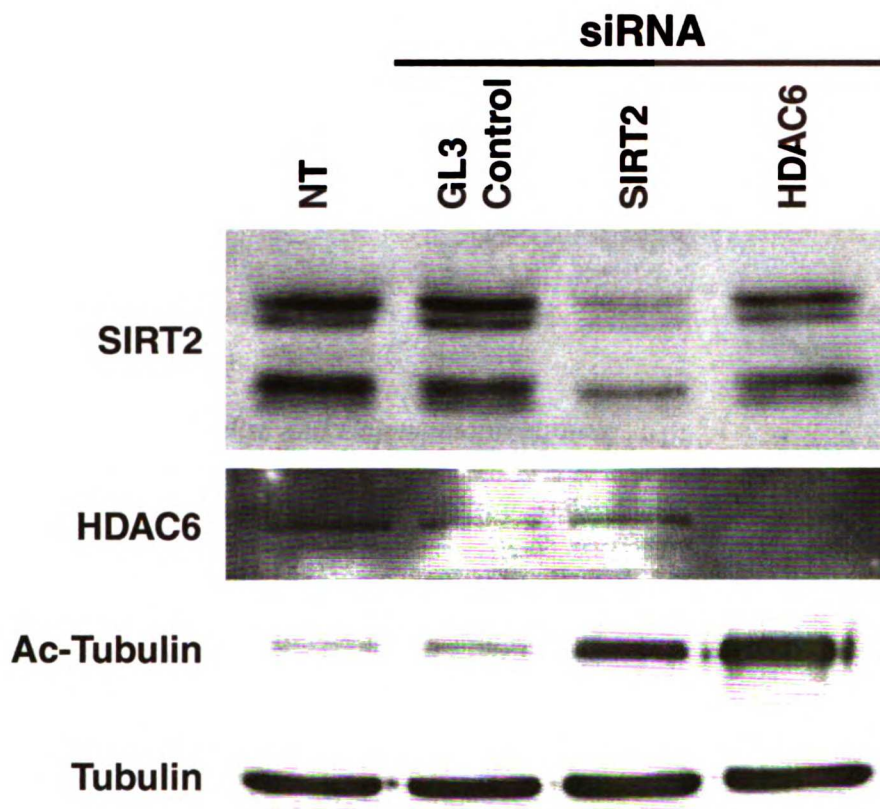


Figure 2.6. Knockdown of SIRT2 and HDAC6 with siRNA. 293T cells were either mock transfected or transfected with siRNA duplexes for GL3 luciferase (control), SIRT2 (260-278) and HDAC6 (211-229) three times over 5 days and collected 48 hours post final transfection. Cellular lysates were probed by western blotting with specific antisera for acetylated α -tubulin, tubulin, SIRT2 and HDAC6.

this siRNA led to an increase in the level of acetylated α -tubulin when compared to mock transfected cells or to cells transfected with an unrelated siRNA (figure 2.6, lane 1, 2 and 3). Likewise, knockdown of HDAC6 by siRNA resulted in an increase in acetylated α -tubulin (figure 2.6, lane 4). Transfection of siRNAs for both SIRT2 and HDAC6 led to the same degree of α -tubulin hyperacetylation, suggesting that the function of both proteins might be redundant under these experimental conditions (data not shown). These results demonstrate that both SIRT2 and HDAC6 function in the regulation of α -tubulin acetylation.

SIRT2 and HDAC6 Colocalize and Coimmunoprecipitate

Considering that both SIRT2 and HDAC6 appear to colocalize with microtubules (figure 1B, data not shown, and (140-142)), we wanted to determine whether both proteins might interact. First, we transiently cotransfected 293T cells with a FLAG epitope-tagged HDAC6 (HDAC6-FLAG) and an HA epitope-tagged SIRT2 (SIRT2-HA) and immunoprecipitated the HDAC6-FLAG protein. We observed that when both SIRT2-HA and HDAC6-FLAG were coexpressed, SIRT2-HA coimmunoprecipitated with HDAC6-FLAG (figure 2.7A, lane 4). As a control, transfection of SIRT2-HA alone followed by anti-FLAG immunoprecipitation did not immunoprecipitate SIRT2-HA (figure 2.7A, Lane 3). In a similar reverse experiment, immunoprecipitation of SIRT2-HA with an anti-HA antiserum led to the coimmunoprecipitation of HDAC6-FLAG (data not shown). Second, we used indirect immunofluorescence and antisera specific for endogenous SIRT2 and HDAC6 in a fibroblast cell line and visualized that both proteins colocalized on a cytoplasmic network reminiscent of the microtubule network (figure 2.7B). The

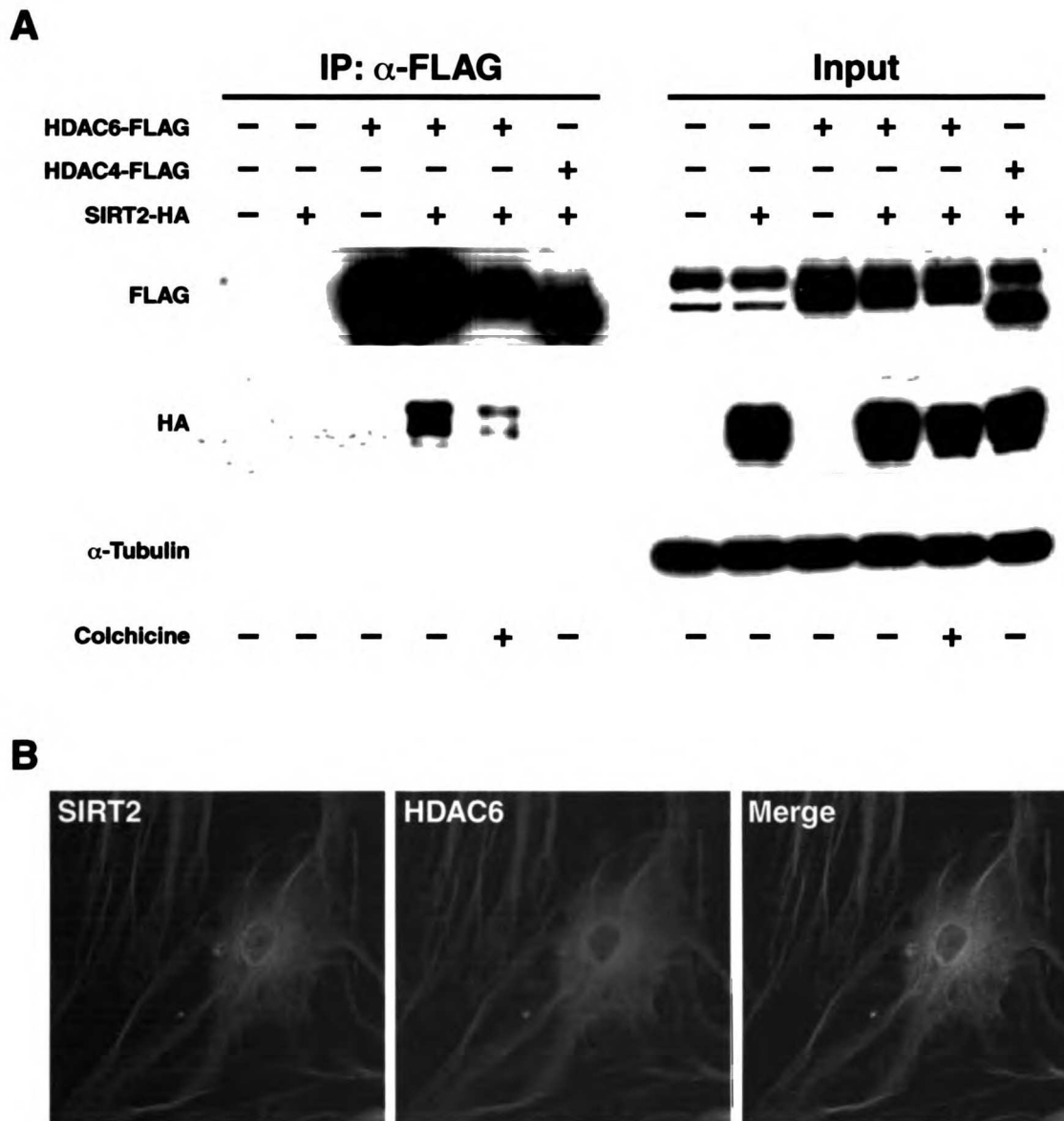


Figure 2.7. Coimmunoprecipitation and colocalization of SIRT2 and HDAC6. (A) 293T cells were either mock transfected or transfected with SIRT2-HA, HDAC6-FLAG or both. Cellular lysates were immunoprecipitated with anti-FLAG and probed by western blotting with antisera specific for FLAG and HA. 10% of protein input was analyzed by western blotting with antisera for FLAG or HA. (B) Confocal microscopy analysis of SIRT2 localization with HDAC6 in human fibroblast. Cells were stained for SIRT2 (green) and HDAC6 (red).

colocalization of endogenous SIRT2 and HDAC6 and their ability to coimmunoprecipitate suggest that SIRT2 and HDAC6 interact either directly or indirectly within a multiprotein complex.

Our deacetylation experiments indicate that SIRT2 can directly deacetylate α -tubulin in the context of a free heterodimer with β -tubulin (figure 2.4B) or in the context of a polymerized microtubule *in vivo* (figure 2.2A). However, characterization of the α -tubulin deacetylase activity associated with HDAC6 suggests that only polymerized α -tubulin found within microtubules can serve as a substrate (140). To better characterize the substrate specificities of SIRT2 and HDAC6, we compared the deacetylase activities of immunoprecipitated SIRT2-FLAG with HDAC6-FLAG on a variety of α -tubulin substrates. When using purified tubulin heterodimers (figure 2.8A, purified tubulin dimers), or microtubules polymerized from purified tubulin heterodimers by addition of Taxol and GTP as substrates (figure 2.8A, Taxol stabilized microtubules), both SIRT2 and HDAC6 deacetylated α -tubulin efficiently. The SIRT2 activity was NAD^+ -dependent, whereas the HDAC6 activity was constitutive, as predicted. When MAP-stabilized microtubules were used as substrate, we also observed deacetylation by both SIRT2 and HDAC6 (figure 2.8A, MAP-stabilized microtubules), however, the level of deacetylation was markedly lower than with purified heterodimers or microtubules. Finally, we analyzed the deacetylation of tubulin heterodimers or microtubules induced with Taxol and GTP from 293T lysates (figure 2.8B, lysate tubulin dimers and lysate taxol stabilized). SIRT2 deacetylated both substrates equally either as tubulin heterodimers or as microtubules while the activity of HDAC6 on these substrates was barely detectable. These data suggest that, while SIRT2 can deacetylate α -tubulin in the

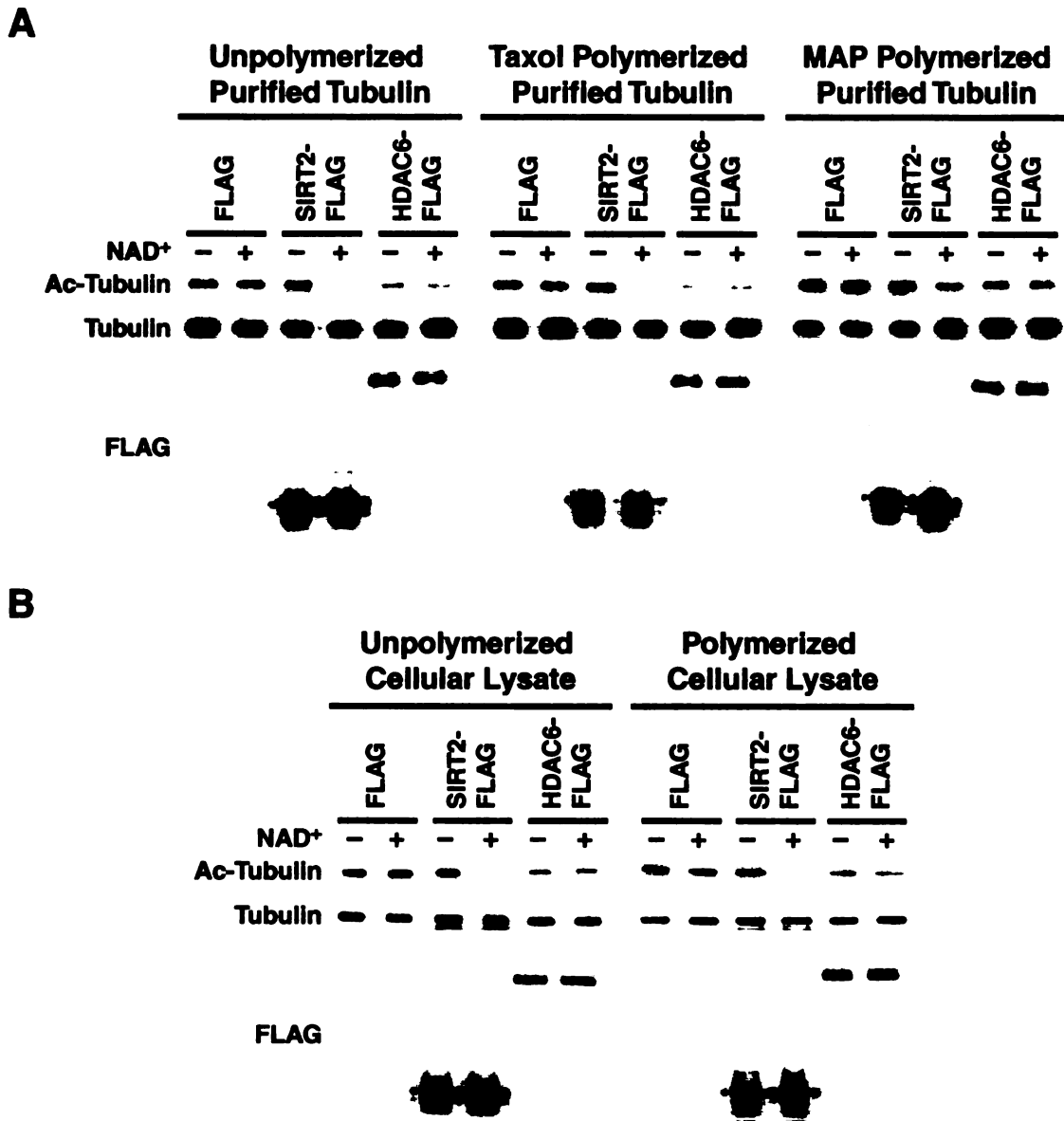


Figure 2.8. Deacetylation of various α -tubulin substrates by SIRT2 and HDAC6. (A) 293T cells were transfected with FLAG, SIRT2-FLAG, or HDAC6-FLAG. Cellular lysates were harvested and immunoprecipitated with antiserum for FLAG. The immunoprecipitated protein corresponding to FLAG, SIRT2-FLAG, or HDAC6-FLAG was incubated with purified tubulin substrates with or without 1 mM NAD⁺ *in vitro*. The reaction products were analyzed by western blotting with specific antisera for acetylated α -tubulin, α -tubulin, and FLAG. (B) Same as in (A) except that tubulin from whole cell lysates was used, either as dimers or as taxol-stabilized microtubules.

context of most substrates, tubulin or microtubules reconstituted from whole cell lysates are relatively resistant to the deacetylase activity of HDAC6.

Regulation of MIZ-1 Microtubule Interaction by α -Tubulin Acetylation

The transcription factor MIZ-1 is sequestered in the cytoplasm by binding to polymerized microtubules. MIZ-1 is released from microtubules and translocates to the nucleus after depolymerization of the microtubule network induced by Colchicine (143). We observed that α -tubulin becomes deacetylated in response to Colchicine treatment in a variety of cell lines (figure 2.9A). This observation suggested that the reported interaction of MIZ-1 with the microtubule network could be regulated by the acetylation state of α -tubulin. In preliminary experiments, we noted that MIZ-1 was predominantly, but not exclusively, nuclear in some cell lines (in HeLa cells, for example) and reasoned that this inconsistent subcellular distribution in different cell lines might be attributed to differences in α -tubulin acetylation levels. To test this possibility, we transfected a GFP-tagged MIZ-1 (GFP-MIZ-1) construct into HeLa cells, followed by incubation with or without TSA to induce α -tubulin hyperacetylation. In untreated cells, MIZ-1 was predominantly nuclear (figure 2.9B). Treatment of these cells with TSA resulted in a marked hyperacetylation of α -tubulin by immunofluorescence (figure 2.9B) and western blotting analysis (figure 2.9C). In agreement with our prediction, GFP-MIZ-1 became cytoplasmically localized in response to TSA treatment (figures 2.9B). To test whether TSA-induced cytoplasmic relocation of MIZ-1 was solely dependent on α -tubulin acetylation, we coexpressed GFP-MIZ-1 with FLAG, SIRT2-FLAG or the catalytically inactive mutant, SIRT2-FLAG N168A, in HeLa cells (figure 2.9D). In the absence of TSA, GFP-MIZ-1 localized

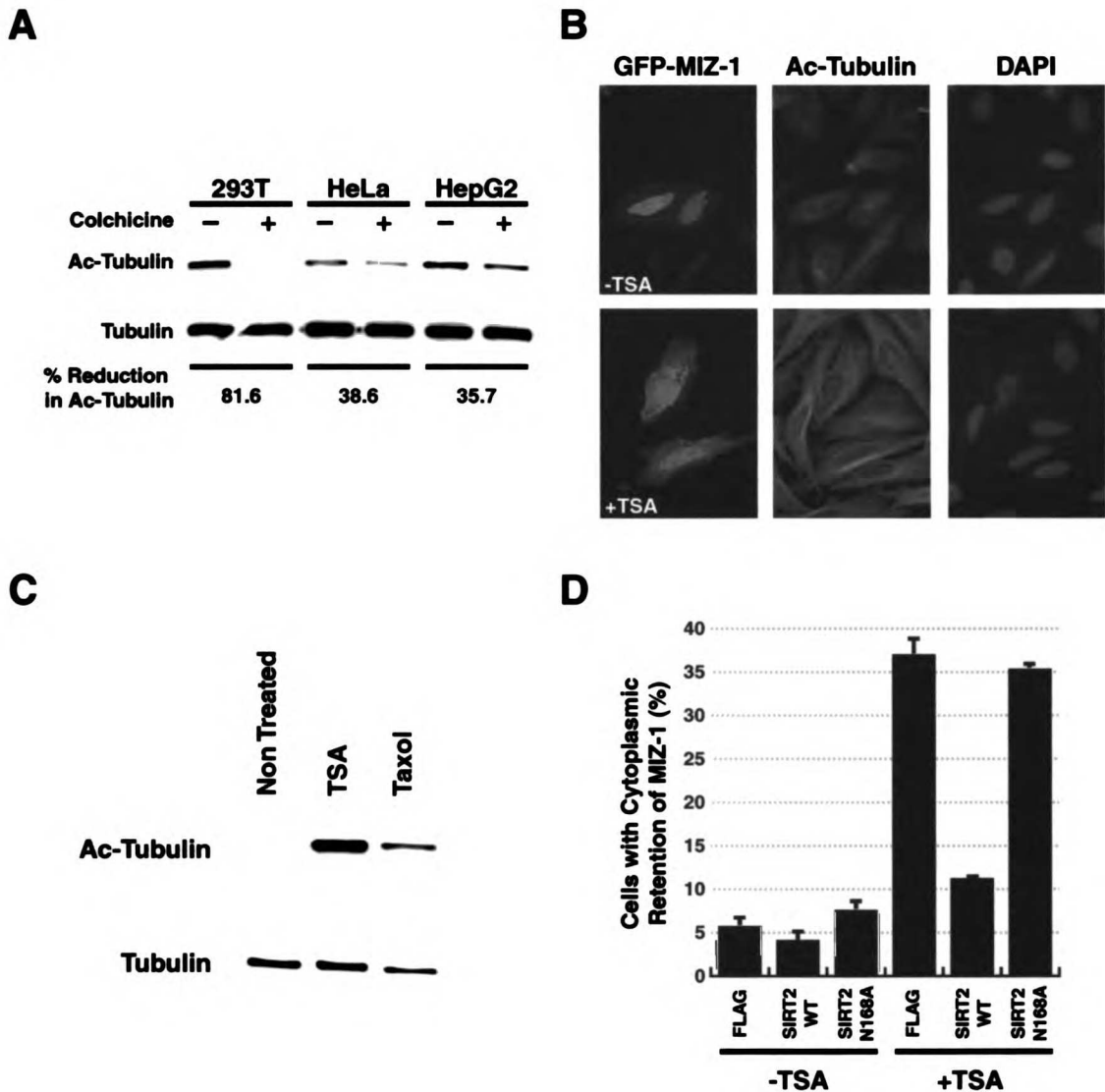


Figure 2.9. Regulation of MIZ-1 nuclear cytoplasmic distribution by acetylated α -tubulin. (A) HeLa, 293T and HepG2 cells were treated with 25 μ M colchicine for 6 hours. Cell lysates were analyzed by western blotting using specific antisera for acetylated α -tubulin and for total α -tubulin. (B) HeLa cells cotransfected with GFP-MIZ-1 were incubated with or without 400 nM TSA for 12 hours and examined for both GFP localization and for acetylated α -tubulin. (C) HeLa cells were treated with or without either 400 nM TSA or 20 μ M Taxol for 6 hours. Cellular lysates were analyzed by western blotting with specific antisera for acetylated α -tubulin and total α -tubulin. (D) Transfected cells were scored for the subcellular localization of GFP-MIZ-1. Cells with detectable cytoplasmic staining for GFP-MIZ-1 were counted as cytoplasmic while cells containing exclusively nuclear GFP-MIZ-1 were scored as nuclear. Cell counts were derived from inspection of at least 150 transfected cells from six microscopic fields. Results represent the average of three separate transfections with error bars representing standard deviation. Data set is representative of three independent experiments.

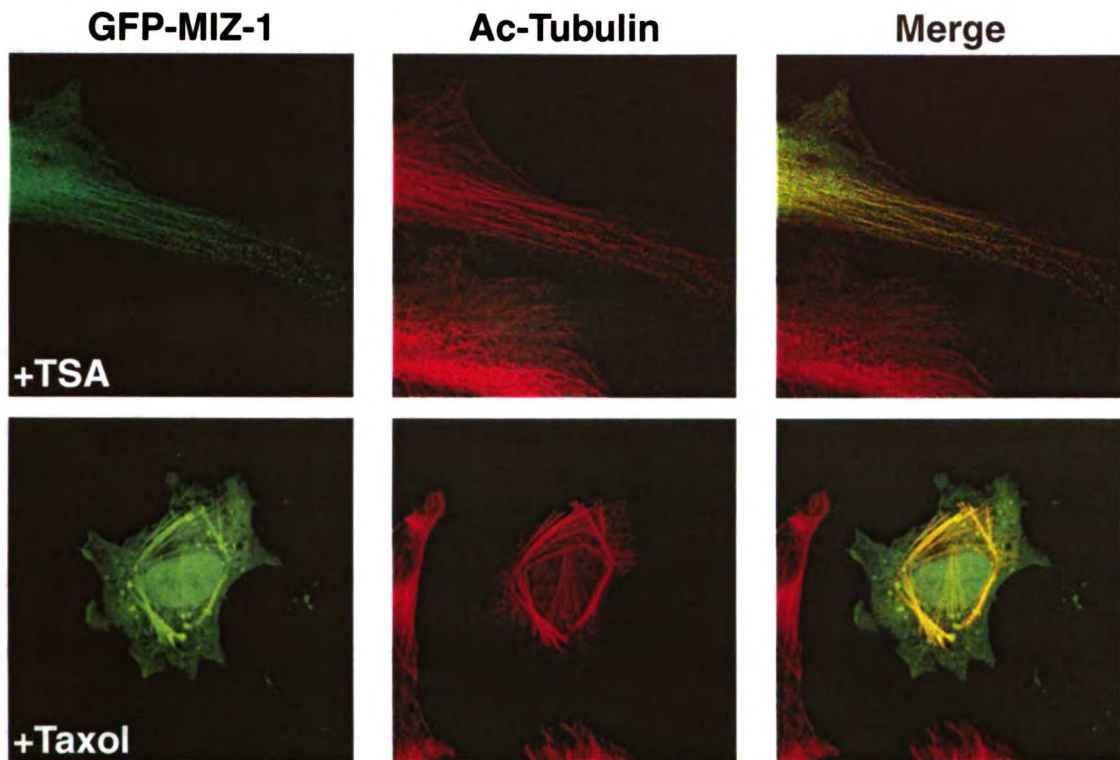


Figure 2.10. Induced microtubule colocalization of GFP-MIZ-1 by α -tubulin acetylation. HeLa cells transfected with GFP-MIZ-1 were incubated with or without either 400 nM TSA or 20 μ M Taxol for 12 hours and stained for acetylated α -tubulin. Cells were visualized and images acquired by confocal microscopy.

predominantly to the nucleus. After TSA treatment, GFP-MIZ-1 was sequestered in the cytoplasm in 37% of cells cotransfected with the control empty FLAG vector. When GFP-MIZ-1 was coexpressed with SIRT2-FLAG, TSA-induced relocalization of GFP-MIZ-1 to the cytoplasm was suppressed to 11%. This suppression was dependent on the deacetylase activity of SIRT2 since a catalytically inactive SIRT2 (N168A) had no effect on the TSA-induced cytoplasmic localization of GFP-MIZ-1. These data indicate that expression of the α -tubulin deacetylase SIRT2 can reverse the relocalization of MIZ-1 to the cytoplasm induced by TSA treatment.

To further test the model that the interaction between MIZ-1 and microtubules is acetylation-dependent, we examined the localization of GFP-MIZ-1 in cells containing hyperacetylated microtubules. Treatment of HeLa cells with 400 nM TSA or 20 μ M Taxol for 12 hours led to hyperacetylation of α -tubulin (figure 2.9C). Using confocal microscopy, we observed that GFP-MIZ-1 colocalized in the cytoplasm with acetylated α -tubulin after TSA treatment (figure 2.10, TSA). The same strong colocalization of MIZ-1 and hyperacetylated microtubules was observed in response to Taxol treatment (figure 2.10, Taxol). These data support the notion that the subcellular distribution of MIZ-1 is primarily regulated by the acetylation state of α -tubulin within the microtubule network.

Discussion

Despite its identification more than 20 years ago, the role of α -tubulin acetylation in eukaryotic cells has remained elusive. The lack of data on the nature of the enzymes involved in α -tubulin acetylation has represented a major obstacle to the identification of a physiological function for this posttranslational modification of the microtubule network. By analogy with histone proteins, we can anticipate that the level of α -tubulin acetylation reflects the competing influences of α -tubulin acetyltransferase(s) and α -tubulin deacetylase(s). In this chapter we report the identification of a human α -tubulin deacetylase, the class III deacetylase SIRT2.

SIRT2 is a bona fide α -Tubulin Deacetylase

The microtubule localization of SIRT2 suggested that it could function as a α -tubulin deacetylase. We demonstrate that GFP-SIRT2 deacetylates α -tubulin *in vivo*, a phenotype that requires its catalytic deacetylase activity. Furthermore, knockdown of endogenous SIRT2 by siRNA resulted in α -tubulin hyperacetylation. Humans have seven SIR2-like proteins, which all contain a highly conserved Sir2 domain (17, 18). We demonstrate that α -tubulin deacetylation is a unique activity for SIRT2; as none of the six remaining human SIRT proteins catalyzed this reaction *in vitro*.

The fact that SIRT2 may be part of a multiprotein complex containing HDAC6 raises the possibility that HDAC6 might represent the exclusive α -tubulin deacetylase. However, three observations indicate that SIRT2 is a *bona fide* α -tubulin deacetylase in addition to HDAC6. First, the α -tubulin deacetylase activity of SIRT2 is not modified by TSA, confirming that a class I or II HDAC is not responsible for the α -tubulin

deacetylase activity associated with SIRT2-FLAG immunoprecipitated material. Second, the enzymatic activity associated with the SIRT2 immunoprecipitates was inhibited by nicotinamide, a SIR2-like deacetylase inhibitor (71). Third, we observed specific α -tubulin deacetylase activity associated with a recombinant form of SIRT2 purified after expression in *E. Coli*.

The Sir2 family in *S. cerevisiae* is comprised of five proteins, Sir2p and Hst1–4p. Human SIRT2 is most closely related to yeast Hst2p, which is also localized to the cytoplasm (54). The substrate specificities of these two closely related proteins have diverged significantly. Although our results suggest that SIRT2 has maintained an ability to deacetylate histone H3 peptide acetylated on lysine-14 (figure 4C), Hst2p cannot efficiently deacetylate an acetylated α -tubulin peptide (figure 4B). Our results are consistent with the notion that SIRT2 has evolved away from its close relatives, Hst2p and the other human SIRT proteins, to specifically deacetylate α -tubulin.

Binding of MIZ-1 to Acetylated Microtubules

The subcellular distribution and thus the transcriptional activity of the transcription factor MIZ-1 is regulated through binding to the polymerized microtubule network (143). Depolymerization of the microtubule network by Colchicine leads to translocation of MIZ-1 into the nucleus, suggesting that the integrity of the microtubule network is essential to ensure cytoplasmic retention of MIZ-1. Depolymerization of the microtubule network also leads to deacetylation of lysine-40 of α -tubulin. In contrast to HepG2 cells, where MIZ-1 is mostly cytoplasmic (143), MIZ-1 is localized primarily in the nucleus of HeLa cells, which still maintain an extensively polymerized microtubule network. These

observations suggested that the subcellular distribution of MIZ-1 is not only regulated by the polymerization state of the microtubule network, rather α -tubulin acetylation might be essential for the cytoplasmic retention of MIZ-1. In agreement with this model, TSA treatment of HeLa cells leads to relative α -tubulin hyperacetylation and to the relocalization of MIZ-1 into the cytoplasm. Transfection of these cells with wild-type SIRT2-FLAG, which deacetylates lysine-40 of α -tubulin, leads to the nuclear localization of GFP-MIZ-1. Furthermore, GFP-MIZ-1 colocalizes with acetylated microtubule structures upon hyperacetylation of α -tubulin by either TSA or Taxol treatment. In conclusion, our data indicates that the ability of MIZ-1 to bind to the microtubule network is primarily regulated by the acetylation state of α -tubulin.

In this chapter we demonstrate that SIRT2 is a α -tubulin deacetylase localized on the microtubule network. Deacetylation of α -tubulin by SIRT2 can regulate the interaction of microtubule-associated proteins with the microtubule network.

Experimental Procedures

Tissue Culture

293T and HeLa cells were obtained from American Type Culture Collection (ATCC, Manassas, VA), grown in Dulbecco's modified Eagle's medium (DMEM, Mediatech, Inc., Herndon, VA) supplemented with 10% fetal bovine serum (Gemini Bio-products, Woodland, CA) in the presence of penicillin, streptomycin and 2 mM L-Glutamine (Gibco Invitrogen Corp., Carlsbad, CA). HepG2 was obtained from ATCC and grown in medium as described above supplemented with 0.1 mM MEM non-essential amino acids (Gibco Invitrogen Corp). The human fibroblast cell line (GM03318) was obtained from NIGMS Human Genetic Mutant Cell Repository and grown in Minimum Essential Media (MEM, Gibco Invitrogen Corp.) supplemented with 10% fetal bovine serum in the presence of penicillin, streptomycin and 2 mM L-Glutamine.

Plasmids and Mutagenesis

Human SIRT1, SIRT2 and SIRT3 constructs were a kind gift from Roy A. Frye. Human SIRT4–7 were cloned from testis and spleen cDNA libraries (Clontech, Mountain View, CA) into pcDNA3.1(+) vector (Invitrogen, Carlsbad, CA) by standard PCR-based strategies and confirmed by sequencing. All SIRT and HDAC6 cDNAs were sub-cloned to generate carboxy-terminal FLAG-tagged fusions in a derivative of the pcDNA3.1(+) vector containing the FLAG peptide sequence (FLAG vector) and wild-type human SIRT2 was cloned into pEGFP-C1 vector (Clontech), and in a derivative of the pcDNA3.1(+) vector containing the HA peptide sequence (HA vector) to generate carboxy-terminal HA-tagged fusion by standard PCR-based strategies. pEGFP-MIZ-1

was a kind gift from John E. Wilson (144). Site-directed mutagenesis for SIRT2 constructs were performed with QuikChange Site-Directed Mutagenesis Kit (Stratagene, La Jolla, CA) as recommended by the manufacturer.

Purification of Recombinant SIRT2

DH5 α F'IQ bacteria (Gibco InVitrogen Corp.) were transformed with pHEX vector containing the human SIRT2 cDNA and induced with 0.1 mM IPTG (isopropyl- β -D-thiogalactopyranoside) at 37°C for 2 hours. The resulting 6x His-tagged protein was purified under native conditions at 4°C by Ni-NTA (Qiagen, Valencia, CA), HiPrep 26/10 Desalting and Sepharose Q chromatographies (Amersham Pharmacia Biotech, Inc., Piscataway, NJ). Recombinant protein was aliquoted and stored at -20°C.

Generation of Human SIRT2 Antiserum

SIRT2 antiserum used in western blotting and microscopy experiments was generated by injection of purified recombinant SIRT2 into chickens (Aves Labs, Inc., Tigard, OR) and affinity purified using recombinant full-length SIRT2 coupled to Affy-gel (Bio-Rad, Hercules, California).

Transient Transfections and Immunoprecipitations

293T cells were transfected by the calcium phosphate DNA precipitation method and lysed 48 hours after transfection in low-stringency lysis buffer (50 mM Tris-HCl, pH 7.5, 0.5 mM EDTA, 0.5% NP-40, 150 mM NaCl) in the presence of protease inhibitor cocktail (Complete, Roche Molecular Biochemicals, Indianapolis, IN). FLAG-tagged

proteins were immunoprecipitated with anti-FLAG M2 agarose affinity gel (Sigma, St. Louis, MO), for 2 hours at 4°C from 1 mg of total cell lysate measured by the *Dc* Protein Assay Kit (Bio-Rad). Immunoprecipitated material was washed 3 times for 15 minutes each in low-stringency lysis buffer, and resuspended in 1X Laemmli buffer.

Nuclear and Cytoplasmic Extracts.

293T cells were transfected as described above and subjected to nuclear and cytoplasmic extraction as previously described (145) modified by the addition of 1% NP-40 to buffer C.

Histone Deacetylase Assay

Immunoprecipitated material was washed for an additional 15 minutes in SIRT2 deacetylase buffer (50 mM Tris-HCl, pH 9.0, 4 mM MgCl₂, and 0.2 mM DTT). Both immunoprecipitated material and recombinant SIRT2 were resuspended in 100 µl of SIRT2 deacetylase buffer containing NAD⁺ (Sigma) and [³H] acetylated histone H4 peptide (amino acids 1–23) (146). TSA (WACO BioProducts, Richmond, VA) was resuspended in DMSO, and nicotinamide (Sigma) was resuspended in ddH₂O, and added to reactions at the indicated concentration. Reactions containing TSA or nicotinamide were preincubated at room temperature with all components of the reaction in the absence of NAD⁺ for 10 minutes at room temperature. The enzymatic reactions were started by addition of NAD⁺. Reactions were incubated for 2 hours at 37°C and stopped by addition of 25 µl 0.1 M HCl and 0.16 M acetic acid. Released acetate was extracted in 500 µl of ethyl acetate, and vortexed for 15 min. After centrifugation at 14,000 rpm for 5

minutes, 400 μ l of the ethyl acetate fraction was mixed with 5 ml of scintillation fluid and counted.

Western Blotting

Samples were separated on 10% SDS-PAGE gels and transferred to Hybond ECL nitrocellulose membrane (Amersham Pharmacia Biotech, Inc.). Membranes were blocked with 5% blocking reagent (Bio-Rad) in TBS-Tween (10 mM Tris, pH 7.5, 150 mM NaCl, and 0.1% Tween-20), and were probed with anti-acetylated α -tubulin 6-11B-1, anti- α -tubulin B-5-1-2, or anti-FLAG M2 (Sigma), each diluted 1:2000, anti-HA, anti-p65 (Santa Cruz Biotechnology, Santa Cruz, CA), anti-lamin A (Cell Signaling Technology, Inc., Beverly, MA) each diluted 1:1000, anti-SIRT2 diluted 1:250, or anti-HDAC6 ((Santa Cruz Biotechnology) diluted 1:500. Secondary detection was performed using horseradish peroxidase-coupled sheep anti-mouse IgG (Amersham Pharmacia Biotech, Inc.), goat anti-rabbit IgG (Pierce Chemical Co., Rockford, IL), or goat anti-chicken IgY (Aves Labs, Inc.) diluted 1:5000 and ECL western blotting detection system (Amersham Pharmacia Biotech, Inc.).

Immunofluorescence Microscopy

HeLa cells grown on coverslips were transfected with LipofectAMINE (Gibco InVitrogen Corp.) according to manufacturer's protocol. Transfected cells were incubated for 12 hours with 400 nM TSA (WACO BioProducts) or 20 μ M Taxol (Sigma) 24 hours after transfection. Cells on coverslips were washed twice in PBS for 10 minutes, fixed in 4% paraformaldehyde (EMS, Ft. Washington, PA) for 10 minutes, followed by

permeabilization in 0.5% Triton-X-100 in PBS for 10 minutes. After 3 washes for 10 minutes each in PBS, cells were incubated in 10% BSA for 10 minutes and then incubated for 1 hour with anti-acetylated α -tubulin 6-11B-1, anti- α -tubulin B-5-1-2 diluted 1:1000 in PBS, 0.1% Tween-20. Cells were washed 3 times 10 minutes in PBS, 0.1% Tween-20, followed by incubation with goat anti-mouse IgG (Fc specific) TRITC-conjugated secondary antiserum (Sigma) diluted 1:100 in PBS, 0.1% Tween-20. Cells were then incubated in 20 μ g/ml DAPI for 5 minutes, washed 3 times for 10 minutes each in PBS and once briefly in ddH₂O, and mounted on slides with Gel Mount (Biomedica Corp., Foster City, CA). For endogenous SIRT2 and HDAC6 immunofluorescence microscopy, human fibroblast cells were grown on coverslips and processed as described above. Anti-SIRT2 and anti-HDAC6 (Santa Cruz Biotechnology, Santa Cruz, CA) antisera were diluted at 1:10 and SIRT2 was visualized with goat anti-chicken IgY FITC-conjugated (Aves Labs, Inc.) and HDAC6 was visualized with goat anti-mouse IgG (Fc specific) TRITC-conjugated secondary antibodies. Slides were analyzed on a Nikon E600 microscope system equipped with a SPOT 2 Digital Camera. Confocal images were acquired by laser-scanning confocal microscopy with an Olympus BX60 microscope equipped with a Radiance 2000 confocal setup (Bio-Rad). For cell count experiments, six random fields were visualized, from which at least 150 cells were counted.

In Vitro α -Tubulin Deacetylation Assay

For SIRT experiments (figure 3), immunoprecipitates were resuspended in 100 μ l of SIRT deacetylase buffer containing 50 μ g of total cellular lysate from untransfected 293T cells and 1 mM NAD⁺. Reactions containing 400 nM TSA or 5 mM nicotinamide

(Sigma) were preincubated as described for histone deacetylase assay and incubated for 2 hours at room temperature with constant agitation after addition of NAD^+ . Reactions were stopped by adding 50 μl of 6X Laemmli buffer. Beads were pelleted by centrifugation at 14,000 rpm for 10 minutes and 10 μl of each supernatant was separated on 10% SDS-PAGE gels and western blotted as described above. For HDAC6 and SIRT2 experiments (figure 5), assays were performed as described above with the exception of being carried out in HDAC deacetylase buffer (10 mM Tris-HCl, pH 8.0 and 10 mM NaCl) for both HDAC6 and SIRT2, and were incubated with the following substrates. For purified tubulin heterodimers, tubulin (Pure, Cytoskeleton, Denver, CO) was either left as heterodimers or polymerized in PEM buffer (80 mM PIPES, pH 6.8, 1 mM MgCl_2 , 1 mM EGTA) in the presence of 20 μM Taxol (Sigma) and 1 mM GTP (Sigma) for 30 minutes at 37°C, MAP-rich tubulin (Cytoskeleton) in PEM buffer was polymerized by addition of 1 mM GTP (Sigma) and incubated as described above, and 293T total cellular lysates harvested by sonication in PEM buffer were either left as heterodimers or polymerized in the presence of 20 μM Taxol (Sigma) and 1 mM GTP (Sigma) as described above. 25 μg of substrate was added to each reaction and incubated for 2 hours at 37°C with or without 1 mM NAD^+ and stopped as described above.

α -Tubulin and Histone H3 Peptide Kinetics with Hst2p and SIRT2

Increasing concentrations of acetylated α -tubulin peptide MPSD(AcK)TIGG (20–900 μM), and 800 μM of NAD^+ were reacted in the presence of 0.8 to 1 μM recombinant SIRT2 in 50 mM Tris-HCl, pH 7.5, 1 mM DTT, and 10% methanol at 37°C. For Hst2p reactions, α -tubulin peptides and 500 μM NAD^+ were reacted in the presence of 9 to 19

μM recombinant Hst2p under the same conditions. Reactions were quenched with TFA to a final concentration of 1%. Time points were chosen to include initial velocity conditions. Samples were subjected to the High Performance Liquid Chromatography (HPLC) with a Beckman C18 analytical column. Upon injection, the system was run isocratically with solvent A (0.05% TFA in H_2O), followed by a gradient of 0–10% solvent B (0.02% TFA in CH_3CN) for 4 minutes, and followed by a gradient of 10–23% solvent B for 23 min. Deacetylated and acetylated peptides eluted at 16% and 18% CH_3CN , respectively. The elution of substrates and products was monitored by measuring the absorbance at 214 nm, and corresponding peaks were integrated using the Beckman System Gold Nouveau software. The amount of product was quantified by calculating the percentage of the deacetylated α -tubulin peptide from the total α -tubulin peptide based upon their integration values. Graphs of rate versus α -tubulin peptide concentrations were fitted to the Michaelis–Menten equation to obtain the kinetic parameters K_m , k_{cat} , and V/K .

The monoacetylated histone H3 peptide ARTKQTARKSTGG(AcK)APRKQL (AcLys-14 H3) was utilized as substrate for both Hst2p and SIRT2. H3 peptide was [^3H] labeled using the histone acetyltransferase PCAF and purified as described (125). Rate measurements utilized a charcoal-binding assay where 70 μl of HDAC reactions were quenched in 10 μl of charcoal slurry (1:3 charcoal volume to glycine buffer volume) containing 2 M glycine, pH 10.0. Reaction times were chosen (usually 2–5 minutes) such that steady-state initial velocities were maintained. Samples were immediately heated for ≥ 20 minutes to liberate free acetate from Ac-ADP-ribose before centrifugation. The supernatant was treated with 10 μl of charcoal slurry before determining the total free

acetate liberated (by liquid scintillation counting). Data were converted to initial rates and fitted to the Michaelis-Menten equation $v_0 = ([E]_0 k_{cat} \cdot [S]) / (K_m + [S])$. Control experiments indicated that [³H]-Ac-Lys H3 peptide was not hydrolyzed nonenzymatically. Also, addition of activated charcoal (at all pH values and temperatures examined) immediately stopped the enzymatic reaction. Heating at high pH was only necessary to liberate acetate from the Ac-ADP-ribose.

Core Histones as Substrates

Calf thymus core histones (Calbiochem, San Diego, CA) were acetylated using 7.5–10 mg/ml calf thymus histones, 100 μ M AcCoA (~150 cpm/pmol, NEN), and 10 μ M PCAF, in 5 mM DTT, 50 mM, Tris-HCl pH 7.5, for 1.5 hours at 23°C. Remaining acetyl-CoA was removed by gel filtration, and labeled histones were quantified by liquid scintillation counting. Deacetylation assays were performed using 30–50 nM enzyme, 500 μ M NAD, and ~1.2 μ M histones, pH 7.5, at 24 \pm 1°C. Product formation was calculated from the radioactive charcoal-binding assay.

siRNA Assay

A 19-nucleotide double-stranded siRNA was generated against HDAC6 using nucleotides 211–229 and SIRT2 using nucleotides 260–278 (Dharmacon Research). 293T cells were transfected by electroporation on a Gene Pulser II system (Bio-Rad) using 200 V and 950 μ F in a 4 mm gap electroporation cuvette with siRNA at a final concentration of 3.2 μ M. Cells were transfected three times over a period of 5 days and

harvested 48 hours after final transfection. Cell lysates were separated on 10% SDS-PAGE gels and analyzed by western blotting as described above.

Microtubule Stabilizing and Destabilizing Drug Treatments

293T, HeLa, and HepG2 cells were treated for 6 hours with 25 μ M Colchicine (Sigma), 400 nM TSA (Sigma) or 20 μ M Taxol (Sigma) and lysed in low-stringency lysis buffer. Lysates were equilibrated by total protein concentration and were separated on 10% SDS-PAGE gels and western blotted as described above.

Chapter 3:

Cell Cycle-dependent Localization of SIRT2

Introduction

Human sirtuins exhibit distinctive subcellular localizations. SIRT1, SIRT6, and SIRT7 are localized to the nucleus, and SIRT7 is found exclusively in the nucleoli (67). However, in pancreatic β -cells, SIRT1 is localized in the cytoplasm and is excluded from the nucleus (147). The mechanism regulating SIRT1 subcellular distribution in this context remains elusive. SIRT2 is often observed as distinctly localized to the cytoplasm (54, 86, 87, 91). SIRT3, SIRT4 and SIRT5 are all localized to the mitochondria, however, only SIRT3 and SIRT4 have been clearly demonstrated to be imported into to the mitochondrial matrix (67, 97, 98).

A complex sorting network controls the subcellular distribution of proteins to the cell membrane, cytoplasm, nucleus, and organelles such as the mitochondria, ER and golgi. Proteins destined for the cell surface typically contain leader signal sequences at their amino-terminus that directs localization into the endoplasmic reticulum upon which the protein is then trafficked through intracellular vesicles to the cell surface (148). Similarly, proteins destined for the mitochondria often contain amphipathic α -helices at their amino-terminus that directs their binding to the TOM receptor on the outer mitochondrial membrane and subsequent import into the mitochondria (149). Additionally, many proteins have distinct functions in the nucleus, and in the cytoplasm, that requires their trafficking to, and maintenance within, these compartments. A network of importin and exportin proteins regulates protein trafficking between these two compartments. The nuclear import machinery recognizes peptide sequences made up primarily of basic amino acids termed nuclear localization signal (NLS) sequences (150). Likewise, nuclear export machinery is required to maintain proteins containing nuclear

export signal (NES) sequences in the cytoplasm (150, 151). The nuclear import and export machinery is coupled to the regulation of RAN-GTP hydrolysis, in which there is a concentration gradient of Ran-GTP and Ran-GDP exists between the nucleus and cytoplasm due to the presence of the RanGEF (Ran guanine nucleotide exchange factor) RCC1 in the nucleus tethered to chromatin and RanGAP (Ran GTPase-activating protein) in the cytoplasm (reviewed in (152)).

In addition to its predominantly cytoplasmic localization, SIRT2 has been observed in the nucleus as well (87, 91). Furthermore, SIRT2 has been shown to have a role in controlling cell cycle progression likely during the process of mitosis, suggesting the possibility of novel localizations of SIRT2 to mitotic structures (89, 90). We set out to determine the process maintaining SIRT2 in the cytoplasm, and how SIRT2 is localized throughout the cell cycle. In this chapter, we demonstrate that SIRT2 has an NES sequence that mediates its localization to the cytoplasm, and during mitosis, SIRT2 is enriched on a number of microtubule derived mitotic structures.

Results

Nucleocytoplasmic Shuttling of SIRT2

We transfected SIRT2 tagged at the amino-terminus with GFP (GFP-SIRT2) into HeLa cells and observed a minor fraction of cells contained GFP-SIRT2 in a pancellular distribution (figure 3.1A). Scoring cells for GFP-SIRT2 localization, we found that 99.5% were exclusively cytoplasmic and 0.5% had a pancellular distribution (figure 3.1B). This data suggest that GFP-SIRT2 can localize similar to the endogenous SIRT2 protein and can be found localized within the nucleus in a fraction of cells.

With a majority of GFP-SIRT2 localized predominantly in the cytoplasm, we hypothesized that either SIRT2 is actively transported into the nucleus in a small fraction of cells or is being actively exported out of the nucleus in a majority of cells. To evaluate this hypothesis, we utilized the nuclear export inhibitor Leptomycin B (LMB). LMB inhibits the Crm1-dependent nuclear export pathway by binding to the region on Crm1 responsible for recognizing NES motifs found on cargo proteins (153-156). Scoring GFP-SIRT2 transfected HeLa cells treated with LMB or vehicle alone, we examined the subcellular distribution of SIRT2, and observed a substantial fraction of LMB treated cells had GFP-SIRT2 localized in the nucleus (figure 3.1C). Nuclear sequestration of SIRT2 was observed in 92.1% of LMB treated cells (figure 3.1D). In contrast, we observed nuclear localization in only 7.9% cells treated with vehicle alone (figure 3.1D). These results indicate that SIRT2 is actively being exported from the nucleus in a Crm1-dependent manner.

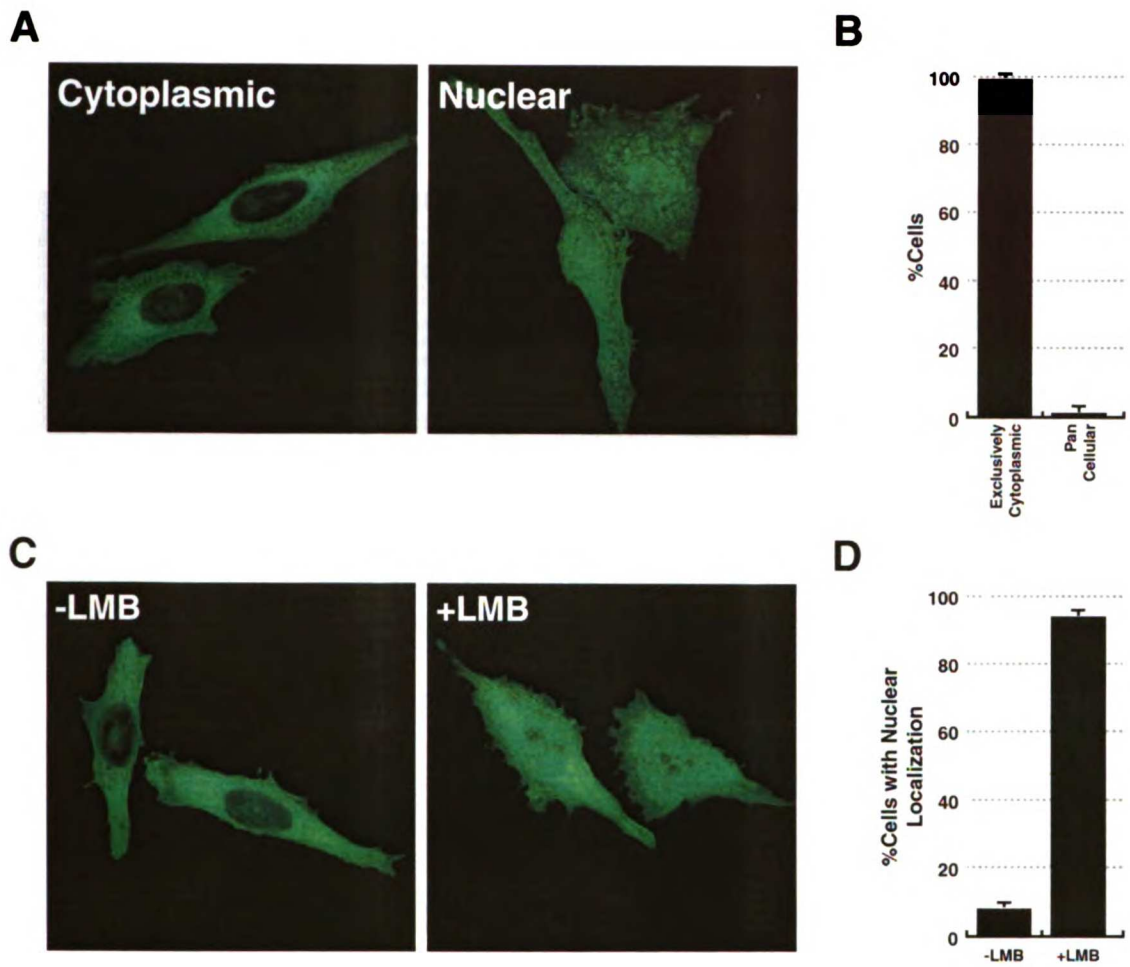


Figure 3.1. Cytoplasmic localization of SIRT2 is dependent on constitutive nuclear export. (A) HeLa cells were transfected with GFP-SIRT2 and visualized for cytoplasmic and pan cellular distribution. (B) Cells from (A) were scored for presence of cytoplasmic or pan cellular distribution. (C) HeLa cells were transfected with GFP-SIRT2 and treated with or without LMB. (D) Cells from (C) were scored for localization of GFP-SIRT2 in the nucleus.

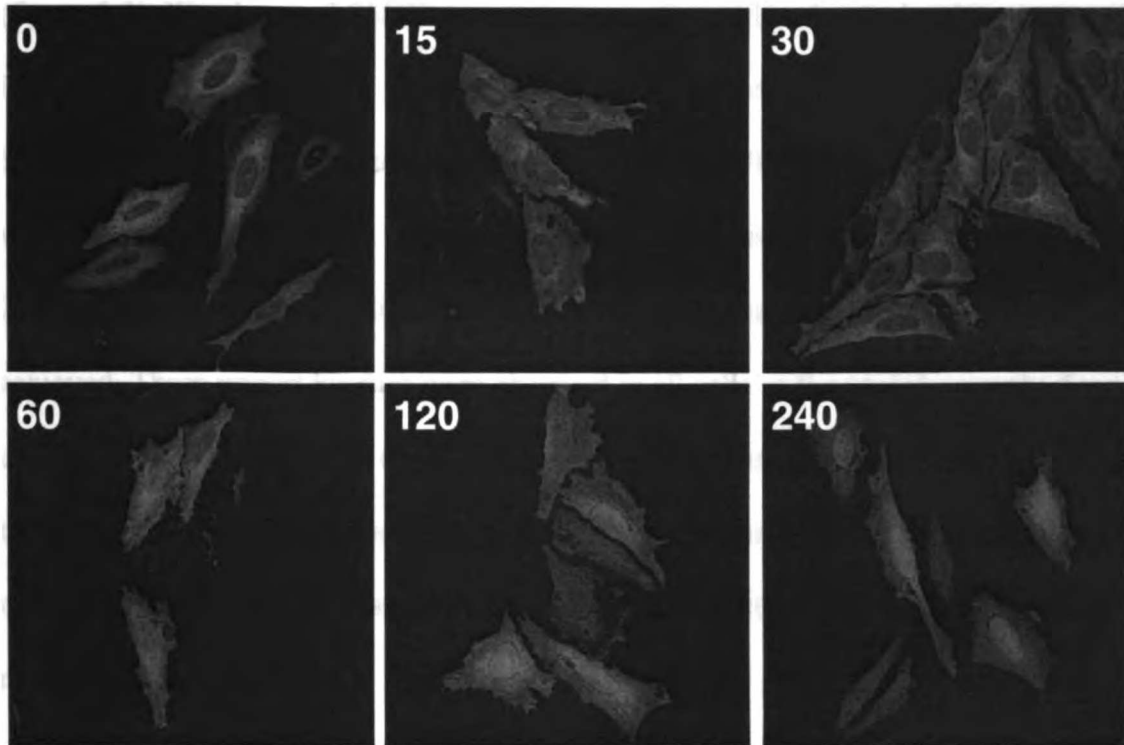
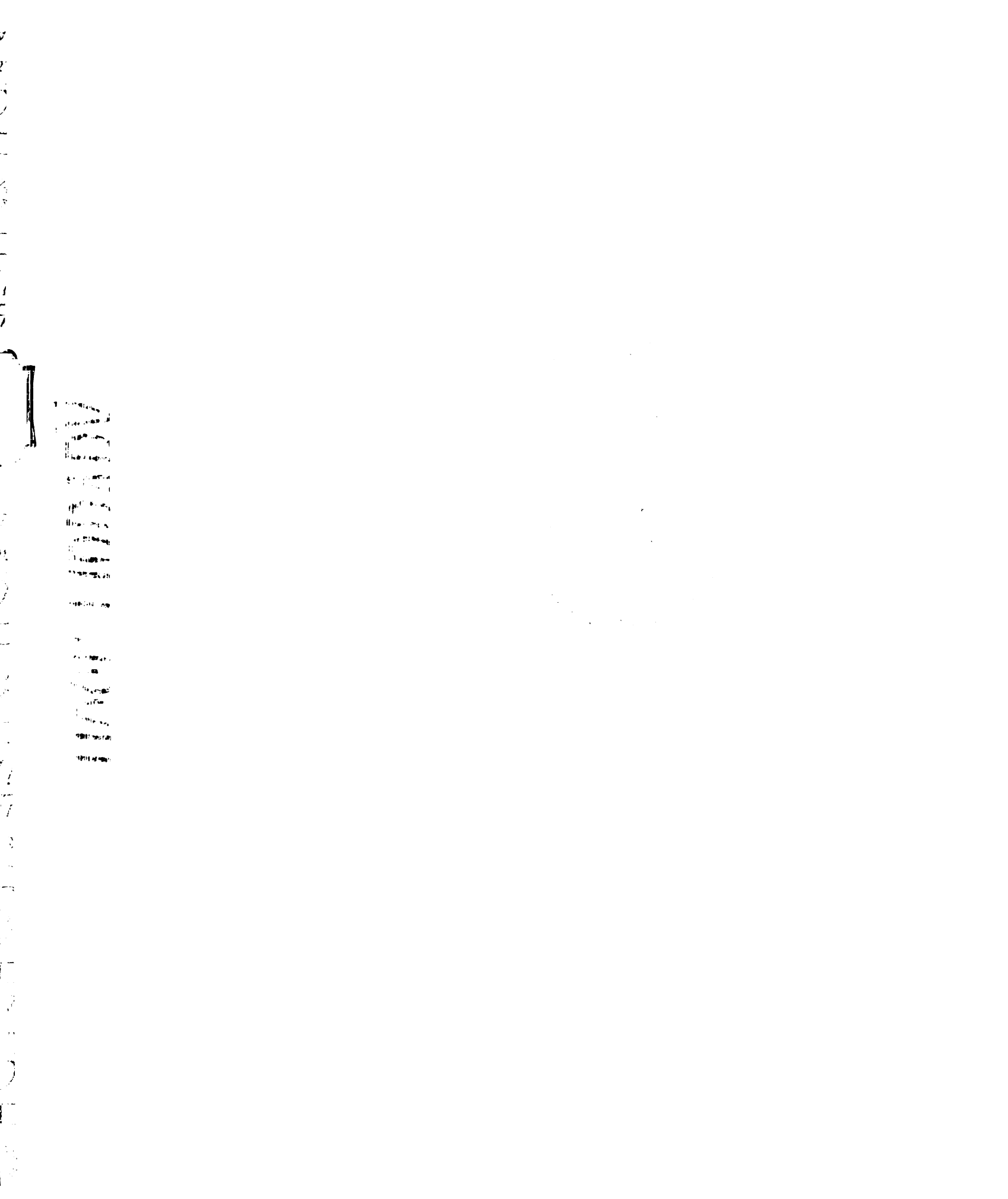


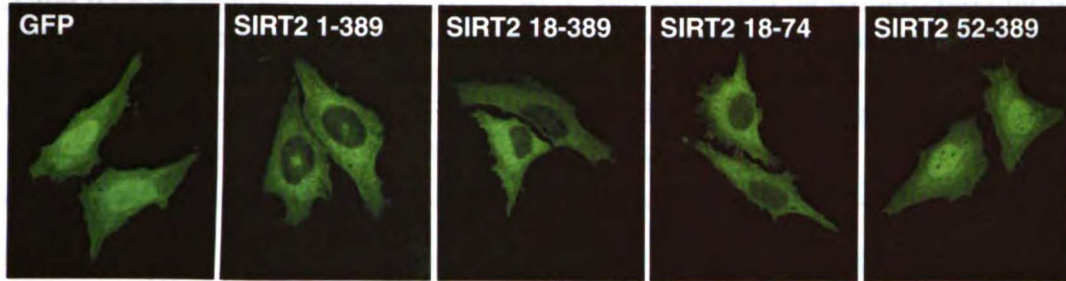
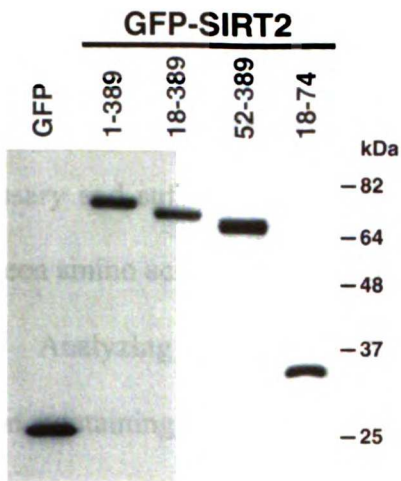
Figure 3.2. Nuclear import of SIRT2 is not dependent on transit through mitosis. HeLa cells were transfected with GFP-SIRT2 followed by treatment with LMB. At time points indicated cells were fixed and visualized for nuclear localization.



A possible explanation for the observations above is the nuclear localization we visualize in response to LMB is a consequence of cells that have transitioned through mitosis during the course of the LMB treatment rather than by nucleocytoplasmic shuttling of SIRT2. To address this possibility, we determined the subcellular distribution of GFP-SIRT2 in HeLa cells treated with LMB for 0, 15, 30, 60, 120 or 240 minutes (figure 3.2). We observed SIRT2 accumulation in the nucleus beginning 30 minutes after initiation of LMB treatment. Following 60 minutes, a dramatic increase in the amount of SIRT2 localized in the nucleus was observed, and at 120 minutes, a quantity of SIRT2 was observed in the nucleus that was not further enhanced with continued treatment for 240 minutes or 16 hours, indicating that by 120 minutes, steady-state nuclear import was achieved. These import kinetics were observed in all cells in the asynchronously dividing culture, indicating that the process of nuclear import and export is not dependent on cells transiting through mitosis, as only a low fraction of cells would have gone through mitosis in the time frame examined. Rather SIRT2 is continuously shuttling between the nucleus and the cytoplasm.

Identification of a Nuclear Export Signal in SIRT2

To determine the region within SIRT2 responsible for Crm1-dependent nuclear export we generated a deletion series of SIRT2 fused to the carboxy-terminus of GFP. As described above, fusion of SIRT2 to the pan-cellular-localized GFP protein resulted in targeting of GFP to the cytoplasm (figure 3.1 and 3.3A). Fusing the region of SIRT2 encompassing amino acids 18–74 resulted in cytoplasmic localization indicating that this region of SIRT2 is sufficient to maintain cytoplasmic localization (figure 3.3A). In contrast,

A**B****C**

SIRT2 Region	Subcellular Localization
1-389	Cytoplasmic
18-389	Cytoplasmic
18-74	Cytoplasmic
52-389	Nuclear

NES

D

Consensus NES: L-X₂₋₃-(F,I,L,V,M)-X₂₋₃-L-X-(L,I)

SIRT2 NES: 41 **L**RN**L**F**S**Q**T****L**S**L** 51

HIV-1 REV NES: 75 **L**-P**P****L**-E**R****L****T****L** 83

Cyclin B1: 142 **L**C**Q**A**F**S**D**-**V****I****L** 151

MAPKK: 32 **L**Q**K****K****L**-E**E****L****L** 41

PLC-δ: 165 **L**K**D****F****L**K**E**-**L****N****I** 174

Figure 3.3. A Crm1-dependent NES is in the amino-terminus of SIRT2. (A) HeLa cells were transfected with GFP or full-length and deletion mutants of GFP-SIRT2 and visualized for subcellular distribution. (B) 293T cells were transfected with cDNAs used in (A) and lysates were separated by SDS-PAGE and visualized by western blotting with an antiserum specific for GFP. (C) Schematic diagram of deletion analysis GFP-SIRT2 subcellular distribution. Region required for cytoplasmic localization is indicated. (D) Schematic of consensus Rev-like NES and proposed SIRT2 NES and NES sequences from proteins exported from the nucleus in a Crm1-dependent manner.

deletion of the first 52 amino acids from the amino-terminus of SIRT2 leads to a pan-cellular distribution of the GFP-SIRT2 protein (figure 3.3A). Generation of proper fusion proteins was confirmed by observing the expected protein size by SDS-PAGE and western blotting analysis (figure 3.3B). These results demonstrate that the sequence necessary and sufficient for nuclear export of SIRT2 is found in the region of SIRT2 between amino acids 18–52 (figure 3.3C).

Analyzing the region of SIRT2 encompassing amino acids 18–52, we found the region containing amino acids 41–51 conforms to a canonical Crm1-dependent NES sequence (figure 3.3D). We found the proposed SIRT2 NES sequence shares a high degree of similarity with known NES sequences from proteins previously characterized to shuttle in a Crm1-dependent manner (figure 3.3D) (157-160).

To assess the functionality of the proposed SIRT2 NES sequence in driving nuclear export of SIRT2, we generated a number of single and double point mutants of conserved residues within the SIRT2 NES sequence (figure 3.4). Alanine substitution of any of the conserved residues alone was not sufficient to functionally inhibit the NES. However, mutation of multiple sites within the SIRT2 NES sequence abolished its nuclear export capability, with the exception of L44,51A, which still demonstrated an exclusively cytoplasmic appearance to SIRT2. Lysates from transfected

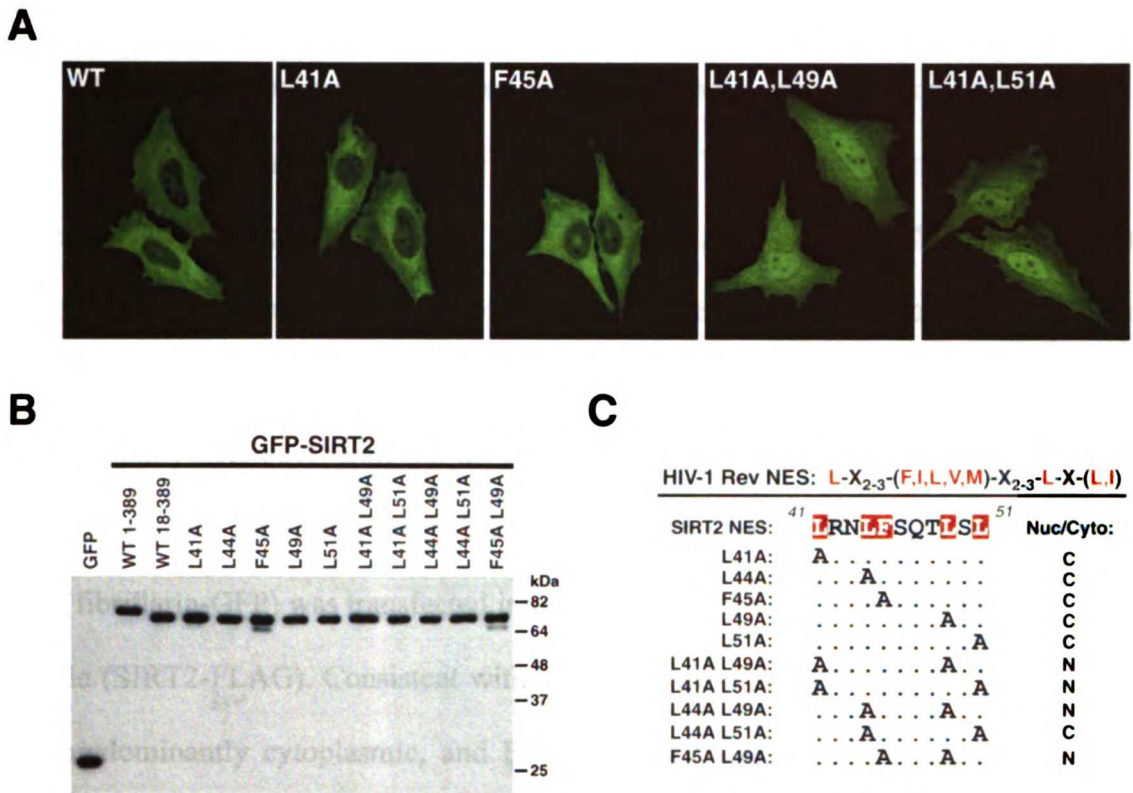


Figure 3.4. Mutational analysis of Crm1-dependent NES sequence in SIRT2. (A) HeLa cells were transfected with wild-type GFP-SIRT2 or single and double point mutants of the proposed NES sequence. (B) 293T cells were transfected with cDNAs used in (A) and lysates were separated by SDS-PAGE and visualized by western blotting with specific antisera for GFP. (C) Subcellular distribution results of all single and double mutants of SIRT2 NES analyzed in (A) and data not shown.

cells were analyzed by SDS-PAGE and western blotting to confirm the mutant proteins of the expected size were generated (figure 3.4B). These results demonstrate that SIRT2 is shuttling between the nucleus and cytoplasm via a Crm1-dependent NES sequence in its amino-terminus.

We found that nuclear-targeted GFP-SIRT2 was excluded from the nucleoli, a phenomenon not observed with GFP alone (figure 3.3A). Yeast Sir2p is localized to nucleoli via its association with the RENT complex, and the yeast SIRT2 homologue Hst2p, which is also localized predominantly in the cytoplasm, regulates yeast aging through suppression of recombination of the *rDNA* array (55). To confirm SIRT2 is predominantly excluded from the nucleoli, we coexpressed SIRT2 with the nucleolar-localized protein Fibrillarin (161, 162). Fibrillarin tagged at its carboxy-terminus with GFP (fibrillarin-GFP) was transfected into HeLa cells with SIRT2 tagged with the FLAG peptide (SIRT2-FLAG). Consistent with previous results for GFP-SIRT2, SIRT2-FLAG was predominantly cytoplasmic, and Fibrillarin-GFP was localized as expected to the nucleoli (figure 3.5) (161, 162). Upon LMB treatment, SIRT2-FLAG was sequestered in the nucleus but was excluded from the nucleoli, which were defined by the localization of Fibrillarin-GFP (figure 3.5). These results indicate that SIRT2 induced to localize to the nucleus is not targeted in significant quantities in the nucleoli; however, we cannot exclude the possibility that it might still regulate nucleolar processes indirectly.

Nuclear Entry of SIRT2 Prior to Mitosis

SIRT2 regulates cellular proliferation potentially by regulating mitotic progression, and furthermore, expression of SIRT2 is upregulated prior to entry into mitosis (89, 90). To

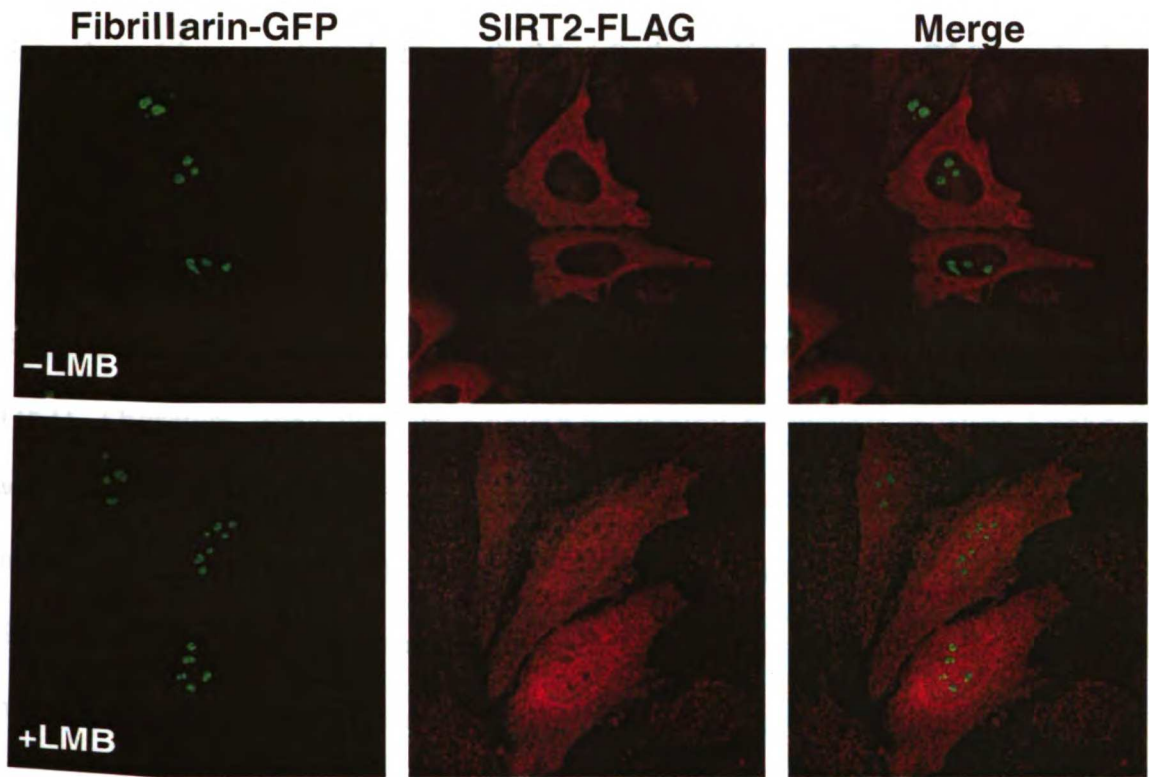
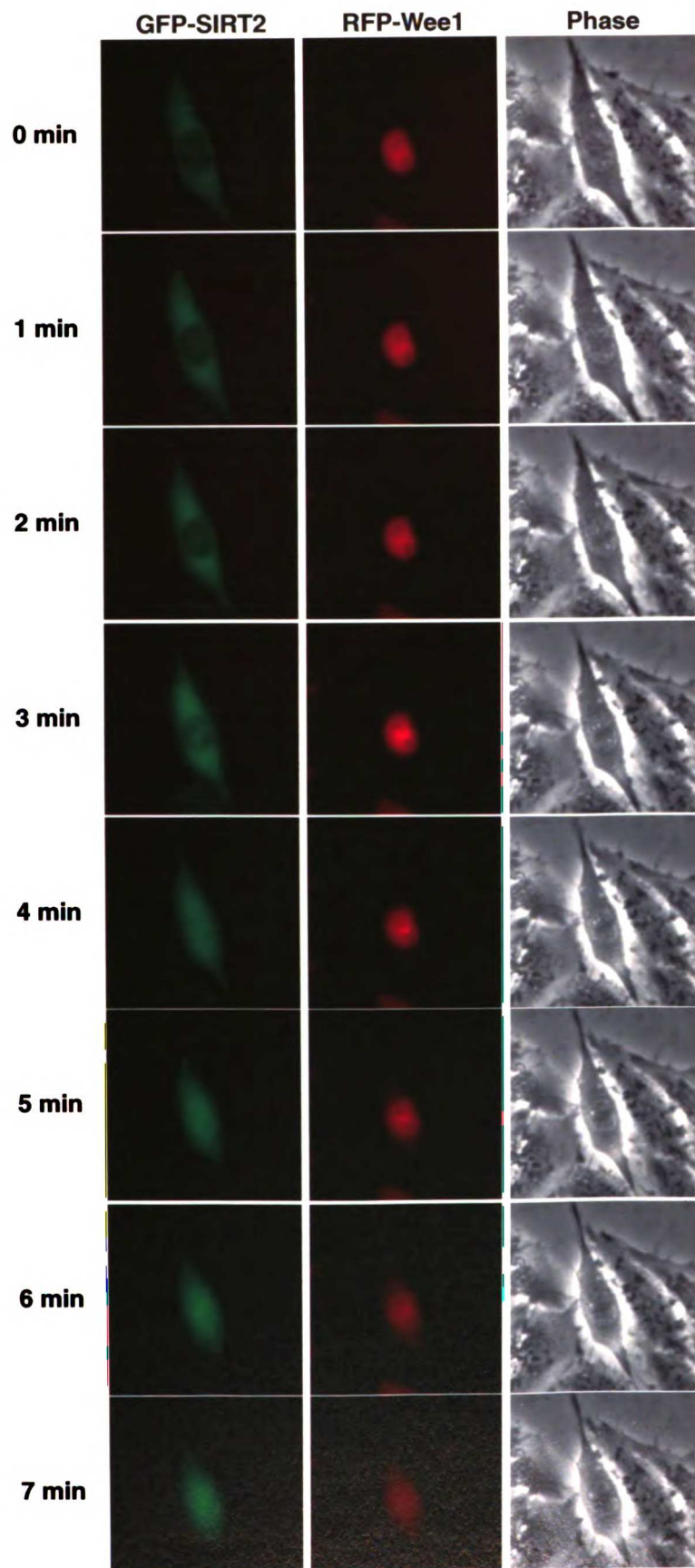


Figure 3.5. SIRT2 is excluded from the nucleoli when maintained in the nucleus. HeLa cells were transfected with SIRT2-FLAG and Fibrillarin-GFP and incubated with or without LMB for 2 hours and subsequently stained for FLAG and visualize by confocal microscopy.

determine if SIRT2 localization varied in cells as they progress through the cell cycle, we utilized time-lapse microscopy to visualize cells transfected with GFP-SIRT2 transit through the cell cycle. Using RFP-Wee1 to mark the nucleus of transfected cells, we observed SIRT2 was localized and maintained preferentially in the cytoplasm during interphase (data not shown). Interestingly, as cells transitioned from G2 into mitosis, we observed GFP-SIRT2 entering into the nucleus just prior to nuclear envelope breakdown (figure 3.6). Although Wee1 is localized exclusively in the nucleus, it is not efficiently anchored by interaction with nuclear structural components; therefore upon the breakdown of the nuclear envelope, Wee1 assumes a whole cell localization pattern (163). Therefore, using Wee1 as a timing mechanism for nuclear envelope breakdown, we found that GFP-SIRT2 began accumulating in the nucleus ($t=3$ min) prior to Wee1 release ($t=6$ min) (figure 3.6). These results suggest that either the NES sequence of GFP-SIRT2 is down-regulated or nuclear import process is up-regulated prior to entry into mitosis altering the steady state levels of SIRT2 in either compartment.

Localization of SIRT2 During Mitosis

We observed in HeLa cells stained with an antiserum for SIRT2, an enrichment of SIRT2 on the centrosome during early prophase, which was confirmed by costaining for Aurora A, which has previously been described as a component of the centrosome (figure 3.7A) (164). During metaphase, SIRT2 continued to be enriched at the centrioles and spread along the spindle fibers (figure 3.7B). With the observation that the localization of SIRT2 and Aurora A are both enriched on the centrosome and spindle fibers, we wanted to determine if these two proteins might be found in a multiprotein complex.

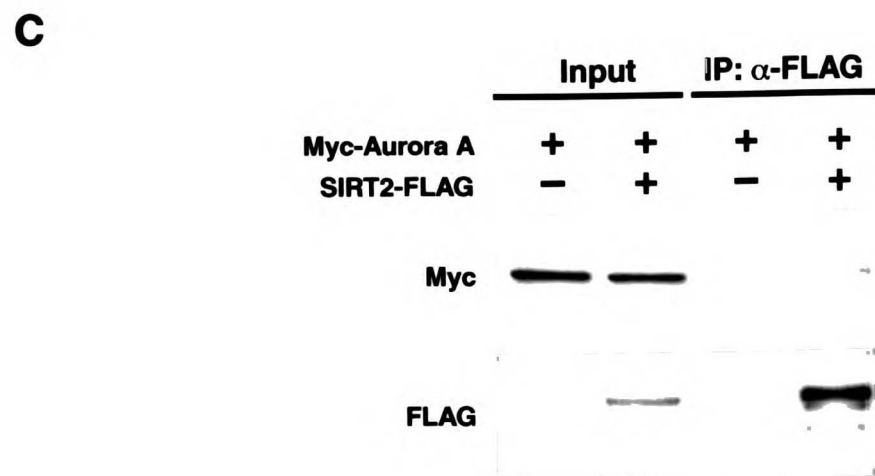
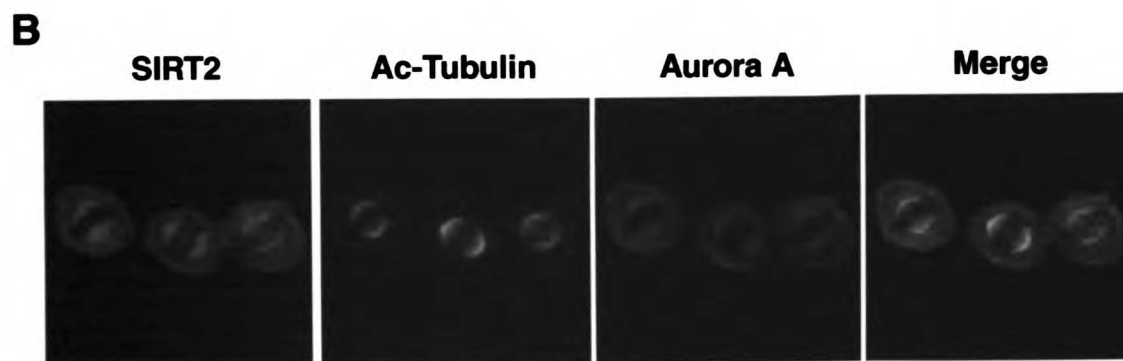
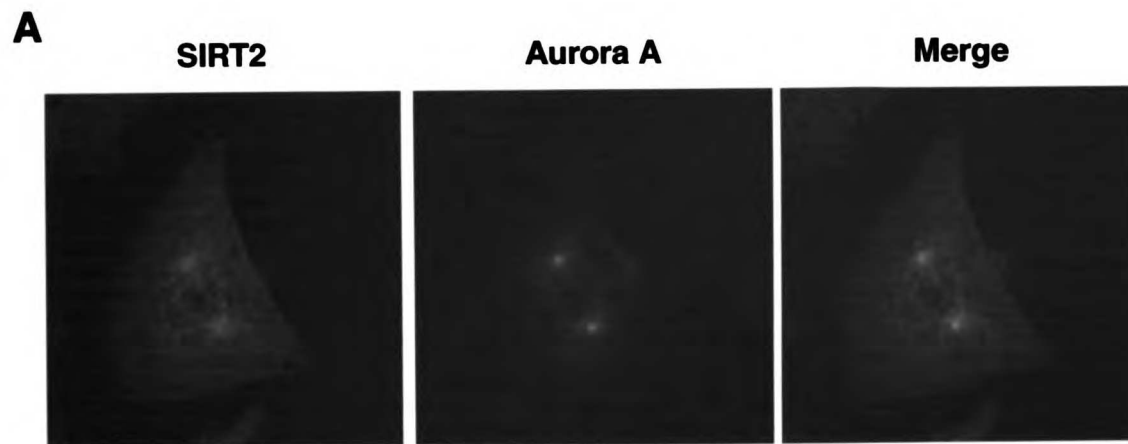


UNIVERSITY OF CALIFORNIA

Figure 3.6. Nuclear import of SIRT2 prior to nuclear envelope breakdown during mitotic entry. HeLa cells grown on a coverslip were transfected with GFP-SIRT2 and RFP-Wee1 and analyzed by time-lapse microscopy following release from a double thymidine block. GFP, RFP, and phase images were acquired each minute. Eight time points, of a cell at the G2 to M transition, is shown.

Coimmunoprecipitation experiments between SIRT2 and Aurora A were carried out, in which we transfected Myc-Aurora A with or without SIRT2-FLAG. Following immunoprecipitation of SIRT2-FLAG with an anti-FLAG antiserum, we probed for the presence of Aurora A by western blotting analysis. We observed that Aurora A interacted with SIRT2-FLAG and was not observed to interact with the antiserum alone control immunoprecipitation (figure 3.7C). These results indicate that SIRT2 is found on the centrosome and spindle fibers, confirmed by colocalization and interaction with a protein component previously demonstrated to associate with these structures.

In addition to detecting an enrichment of SIRT2 on early mitotic structures such as the centrosome and mitotic spindle, we also observed SIRT2 on late mitotic structures. By indirect immunofluorescence we observed SIRT2 localized at the midbody, a structure formed by the bundling of microtubules originating from polar microtubules formed during metaphase. To confirm localization at the midbody, we costained with the midbody localized Aurora B protein, a homologue of Aurora A (165). As observed with Aurora A, we found SIRT2 colocalized with Aurora B, confirming that SIRT2 is indeed targeted to the midbody (figure 3.8A). In addition, we carried out coimmunoprecipitation experiments as described above and observed interaction between SIRT2 and Aurora B, indicating that SIRT2 is localized at the midbody and found in a midbody-associated multimeric complex (figure 3.8B).



UWDT 1000

Figure 3.7. Colocalization and coimmunoprecipitation of SIRT2 and Aurora A on the centrosome and spindle fibers. (A) Enrichment of SIRT2 and Aurora A on the centrosome. HeLa cells were stained with antisera for SIRT2 (Green), and Aurora A (Red) and analyzed by confocal microscopy. (B) Enrichment of SIRT2 and Aurora A on the spindle fibers. HeLa cells were stained with antisera for SIRT2 (Green), acetylated α -tubulin (Red), and Aurora A (Blue) and analyzed by confocal microscopy (C) 293T cells were transfected with Myc-Aurora A with or without SIRT2-FLAG. Cellular lysates were immunoprecipitated with anti-FLAG and probed by western blotting with antisera specific for FLAG and Myc. 10% of protein input was analyzed by western blotting with antisera for FLAG or Myc.

Defined Enzymatic Activity of SIRT2 Controls Efficient Cytokinesis

With the observation that SIRT2 is found on various mitotic structures including the centrosome, metaphase mitotic spindle, and the midbody, we hypothesized that overexpression of SIRT2 might affect the integrity of cell division. Alterations of proteins localized to the midbody often have subtle defects in cytokinesis, as was recently observed for CD2AP (166). To determine if SIRT2 expression affects cell division, we transfected cells with GFP, or GFP-SIRT2 (wild-type or the catalytically inactive mutant H187Y). We observed an increase in the percentage of cells containing more than one nucleus in cells transfected with GFP-SIRT2. Two days post-transfection we scored cells containing two or more distinct nuclei to determine defective cytokinesis (figure 3.9). We observed that overexpression of wild-type GFP-SIRT2 resulted in a 3-fold increase and overexpression of catalytically inactive GFP-SIRT2 resulted in a 5.5-fold increase in multinucleation. These results indicate that SIRT2 regulates efficient cytokinesis, and that SIRT2 enzymatic activity may be finely tuned both temporally and spatially during mitosis.

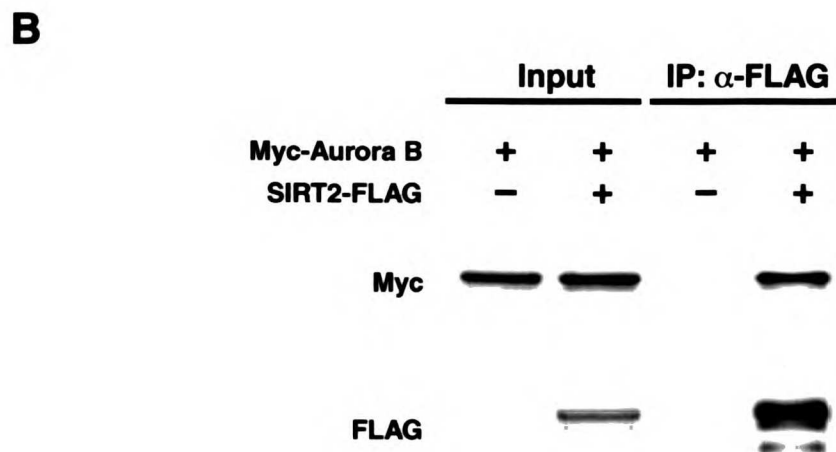
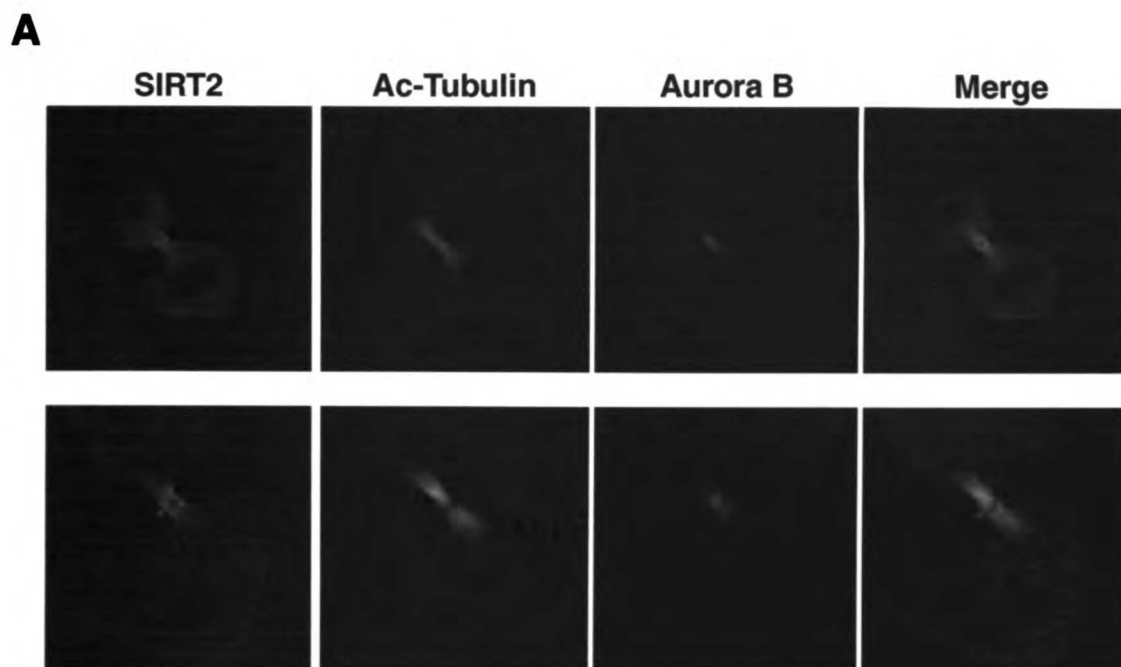


Figure 3.8. Colocalization and coimmunoprecipitation of SIRT2 and Aurora B at the midbody. (A) HeLa cells were stained with antisera for SIRT2 (Green), acetylated α -tubulin (Red), and Aurora B (Blue) and analyzed by confocal microscopy. Enrichment of the three proteins on the midbody are shown in the merge images. Two cells are shown (top and bottom rows) (B) 293T cells were transfected with Myc-Aurora B with or without SIRT2-FLAG. Transfections were immunoprecipitated and analyzed as in figure 3.7B.



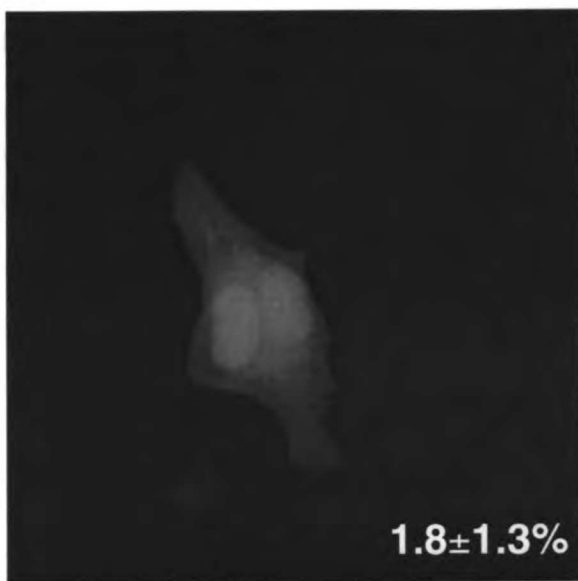
1
 2
 3
 4
 5
 6
 7
 8
 9
 10
 11
 12
 13
 14
 15
 16
 17
 18
 19
 20
 21
 22
 23
 24
 25
 26
 27
 28
 29
 30
 31
 32
 33
 34
 35
 36
 37
 38
 39
 40
 41
 42
 43
 44
 45
 46
 47
 48
 49
 50
 51
 52
 53
 54
 55
 56
 57
 58
 59
 60
 61
 62
 63
 64
 65
 66
 67
 68
 69
 70
 71
 72
 73
 74
 75
 76
 77
 78
 79
 80
 81
 82
 83
 84
 85
 86
 87
 88
 89
 90
 91
 92
 93
 94
 95
 96
 97
 98
 99
 100

1
 2
 3
 4
 5
 6
 7
 8
 9
 10
 11
 12
 13
 14
 15
 16
 17
 18
 19
 20
 21
 22
 23
 24
 25
 26
 27
 28
 29
 30
 31
 32
 33
 34
 35
 36
 37
 38
 39
 40
 41
 42
 43
 44
 45
 46
 47
 48
 49
 50
 51
 52
 53
 54
 55
 56
 57
 58
 59
 60
 61
 62
 63
 64
 65
 66
 67
 68
 69
 70
 71
 72
 73
 74
 75
 76
 77
 78
 79
 80
 81
 82
 83
 84
 85
 86
 87
 88
 89
 90
 91
 92
 93
 94
 95
 96
 97
 98
 99
 100

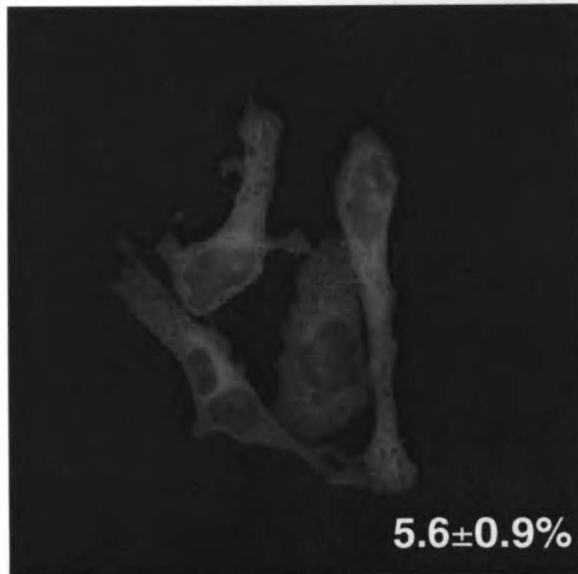
1
 2
 3
 4
 5
 6
 7
 8
 9
 10
 11
 12
 13
 14
 15
 16
 17
 18
 19
 20
 21
 22
 23
 24
 25
 26
 27
 28
 29
 30
 31
 32
 33
 34
 35
 36
 37
 38
 39
 40
 41
 42
 43
 44
 45
 46
 47
 48
 49
 50
 51
 52
 53
 54
 55
 56
 57
 58
 59
 60
 61
 62
 63
 64
 65
 66
 67
 68
 69
 70
 71
 72
 73
 74
 75
 76
 77
 78
 79
 80
 81
 82
 83
 84
 85
 86
 87
 88
 89
 90
 91
 92
 93
 94
 95
 96
 97
 98
 99
 100

1
 2
 3
 4
 5
 6
 7
 8
 9
 10
 11
 12
 13
 14
 15
 16
 17
 18
 19
 20
 21
 22
 23
 24
 25
 26
 27
 28
 29
 30
 31
 32
 33
 34
 35
 36
 37
 38
 39
 40
 41
 42
 43
 44
 45
 46
 47
 48
 49
 50
 51
 52
 53
 54
 55
 56
 57
 58
 59
 60
 61
 62
 63
 64
 65
 66
 67
 68
 69
 70
 71
 72
 73
 74
 75
 76
 77
 78
 79
 80
 81
 82
 83
 84
 85
 86
 87
 88
 89
 90
 91
 92
 93
 94
 95
 96
 97
 98
 99
 100

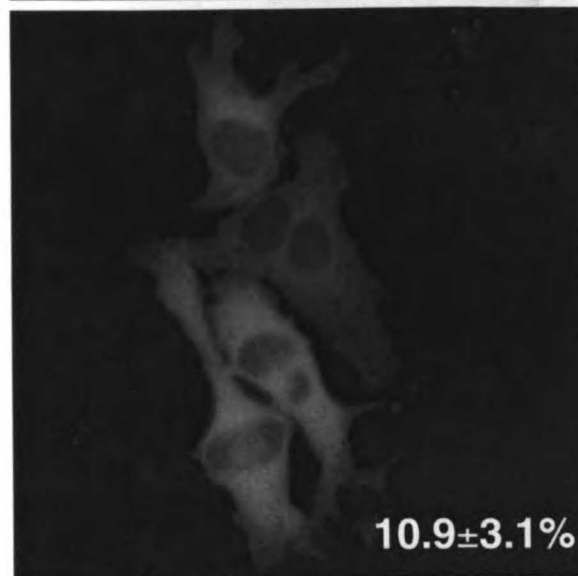
GFP



GFP-SIRT2 WT



**GFP-SIRT2
H187Y**



WOL. LUDWIG

Figure 3.9. Compromised cytokinesis by overexpression of SIRT2. HeLa cells were transfected with GFP, wild-type or H187Y GFP-SIRT2. 48 hours posttransfection, cells were scored for presence of multinucleation. Percentages represent average of counting ~200 cells in three transfections with error bars representing standard deviation.

WOL LAMTII
1000

Discussion

Although SIRT2 is predominantly localized in the cytoplasm, a fraction of the protein can be periodically observed in the nucleus (87, 91). It has been unclear if SIRT2 is constitutively targeted in the cytoplasm and selectively imported into the nucleus in a subset of cells, or if SIRT2 is actively shuttling between the cytoplasm and nucleus. In this chapter we report that SIRT2 is constantly shuttling between the cytoplasm and nucleus, and is excluded from the nucleus via a Crm1-dependent NES sequence in the amino-terminus of SIRT2. The rate of nuclear export exceeds the rate of nuclear import giving the appearance of constitutive localization of SIRT2 in the cytoplasm.

Identification of a Nuclear Export Signal Sequence in SIRT2

We found in a population of cells transfected with SIRT2, that a low percentage of cells had a pancellular distribution of SIRT2. This observation led us to hypothesize that SIRT2 is actively exported out of the nucleus in a majority of cells. We treated asynchronous growing cells with the nuclear export inhibitor LMB, which resulted in accumulation of SIRT2 within the nucleus. LMB binds to the exportin Crm1 and inhibits Crm1 from recognizing NES sequences within cargo proteins. Under these conditions, SIRT2 protein that enters into the nucleus is subsequently blocked from binding to Crm1 and is inhibited from being exported, sequestering SIRT2 in the nucleus. These results indicate that SIRT2 is actively exported out of the nucleus and that its localization in the cytoplasm is mediated by Crm1-dependent nuclear export machinery. We were unable to determine the presence of a nuclear localization signal (NLS) sequence within SIRT2, suggesting that SIRT2 is either imported by an undefined or multiple NLS sequences,

11/11/11 10:11 AM

piggy-backs onto another protein to mediate its import, or is only found in the nucleus following reformation of the nucleus after mitosis. As cells enter mitosis, the nuclear envelope is broken down in prophase allowing proteins from the two compartments to combine. Following the segregation and decondensation of the DNA at the end of mitosis, the nucleus is reformed requiring distinctly cytoplasmic proteins to be exported out of the nucleus to maintain the integrity of their localization pattern. To address this possibility, we treated transfected cells with LMB over a brief time course and found that nearly all cells in the asynchronous culture had SIRT2 in the nucleus following 30–120 minutes of treatment. Within this time frame, few cells would have undergone mitosis, indicating that SIRT2 is constantly shuttling between the nucleus and cytoplasm during interphase.

The canonical NES recognized by Crm1 consist of the leucine rich motif, characterized initially within the HIV-1 Rev protein. Using a series of deletion mutants of SIRT2 tagged to GFP, we localized the NES of SIRT2 to the amino-terminus between amino acids 41–51. This sequence conformed to the canonical Crm1-depenent NES consensus sequence, and subsequent mutagenesis studies indicated that this NES sequence is required for efficient cytoplasmic targeting of SIRT2. Interestingly, we found that neither LMB treatment, nor mutation of the NES, resulted in complete localization of SIRT2 into the nucleus. In fact, there continues to be a significant amount of the protein maintained in the cytoplasm, even after extended LMB treatments. These results indicate the potential of a second, LMB insensitive export pathway used by SIRT2 or a sequestration of SIRT2 within the cytoplasm by interacting with strictly cytoplasmic proteins.

11/17/11
11/17/11
11/17/11

Nuclear Import of SIRT2 During Mitotic Entry

We wanted to assess when SIRT2 may enter into the nucleus, therefore, we visualized cells transfected with GFP-SIRT2 throughout the cell cycle using time-lapse microscopy. We observe that SIRT2 maintained cytoplasmic localization throughout interphase, however, prior to mitotic entry SIRT2, appears to enter into the nucleus just prior to nuclear envelope breakdown. These results suggest that SIRT2 might target a factor in the nucleus for deacetylation that may function in mitotic entry. In this regard, Cyclin B1 behaves similarly to SIRT2, in which Cyclin B1 is constitutively shuttling between the nucleus and cytoplasm and has a functional Crm1-dependent NES. Similar to SIRT2, the rate of nuclear export of Cyclin B1 exceeds its rate of nuclear import, giving the perception that Cyclin B1 is a cytoplasmic protein (160, 167, 168). It will be of interest in future experiments to determine the mechanism of regulation and functional consequence of SIRT2 shuttling, and what factors it might target in the nucleus prior to mitotic entry.

Enrichment of SIRT2 on Microtubule Structures During Mitosis

In addition to its controlled cytoplasmic localization during interphase, we observe a distinct localization pattern of SIRT2 during mitosis. SIRT2 is phosphorylated in a mitotic specific manner, indicating a potential role for SIRT2 during this stage of the cell cycle (90). We find SIRT2 is enriched on the centrosome in prophase and then is found on the growing spindle fibers throughout metaphase. SIRT2 colocalizes and interacts with Aurora A on these structures, suggesting that it is part of a multiprotein complex at these sites. Following anaphase, and as cells progress through telophase and into cytokinesis, SIRT2 is found on the midbody where it assembles and interacts with Aurora

B. Interestingly, in some images, SIRT2 appears to be encircling the midbody, suggesting that it might not be directly associated with the microtubules forming the midbody, but might be localized to the cleavage furrow.

Surprisingly, all the structures SIRT2 associates with during mitosis are primarily composed of microtubules, a *bona fide* substrate for SIRT2. However, the acetylation status of these microtubules appears enriched, as opposed to reduced as would have been anticipated. In addition, overexpression of either wild-type or catalytically inactive SIRT2 results in defects in cytokinesis. These results suggest that SIRT2 enzymatic activity is regulated during mitosis, and although it is found on these structures, it might be maintained in a finely tuned state of inactivity. SIRT2 activity is required for mitotic progression (160, 167, 168), but its activity might be temporally and spatially controlled to function in the faithful completion of mitosis.

WU. LUNN

Experimental Procedures

Tissue Culture

293T and HeLa cells were obtained from American Type Culture Collection (ATCC), grown in Dulbecco's modified Eagle's medium (DMEM, Mediatech, Inc., Herndon, VA) supplemented with 10% fetal bovine serum (Gemini Bio-products, Woodland, CA) in the presence of penicillin, streptomycin and 2 mM L-Glutamine (Gibco Invitrogen Corp., Carlsbad, CA).

Plasmids and Mutagenesis

Human SIRT2, full length and deletion constructs were cloned into pEGFP-C1 vector (Clontech, Mountain View, CA), and in a derivative of the pcDNA3.1(+) backbone containing either the FLAG peptide sequence (FLAG vector) or HA peptide sequence, to generate carboxy-terminal FLAG-tagged fusion, or carboxy-terminal HA-tagged fusions, respectively, by standard PCR-based strategies. Site-directed mutagenesis for SIRT2 constructs were performed with QuikChange Site-Directed Mutagenesis Kit (Stratagene, La Jolla, CA) as recommended by the manufacturer. Fibrillarin-GFP was a kind gift from Dr. Tom Mistelli (161, 162). Red-Wee1 was a kind gift from Drs. Carlos De Noronha and Warner C. Greene (163). Myc-epitope tagged Aurora A and Aurora B were a kind gift from Dr. Hongtao Yu (169).

Transient Transfections and Immunoprecipitations

293T cells were transfected by the calcium phosphate DNA precipitation method and lysed 48 hours after transfection in low-stringency lysis buffer (50 mM Tris-HCl, pH 7.5,

UWA LIBRARY

minutes. After 3 washes for 10 minutes each in PBS, cells were incubated in 10% BSA for 10 minutes and then incubated for 1 hour with anti-FLAG diluted 1:5000 in PBS, 0.1% Tween-20. Cells were washed 3 times for 10 minutes each in PBS, 0.1% Tween-20, followed by incubation with goat anti-mouse IgG (Fc specific) TRITC-conjugated secondary antiserum (Sigma) diluted 1:100 in PBS, 0.1% Tween-20. Cells were then incubated in 20 μ g/ml DAPI for 5 minutes, washed 3 times for 10 minutes each in PBS and once briefly in ddH₂O, and mounted on slides with Gel Mount (Biomedica Corp., Foster City, CA). Confocal images were acquired by laser-scanning confocal microscopy with an Olympus BX60 microscope equipped with a Radiance 2000 confocal setup (BioRad). For cell count experiments, six random fields were visualized, from which at least 150 cells were counted.

For LMB and cytokinesis experiments, following 32 hours transfection with GFP-SIRT2, cells were treated with or without LMB (Sigma) and incubated for the times indicated or for 16 hours. Cells were washed and fixed as described above, and images acquired by confocal microscopy. Cell counts were performed on greater than 200 transfected cells, and results shown are a representative of three independent experiments.

For indirect immunofluorescence of endogenous proteins, HeLa cells were grown on coverslips for 24 hours, followed by processing for immunofluorescence as described above. Chicken anti-SIRT2 was diluted at 1:10, rabbit anti-aurora A and aurora B (Abcam, Cambridge, MA) were diluted 1:1000, and mouse anti-acetylated- α -tubulin 6-11B-1 (Sigma) was diluted 1:500. Secondary detection was performed using anti-mouse-

TRITC (Sigma), anti-chicken-Cy2 (Jackson ImmunoResearch Labs, West Grove, PA) and anti-rabbit-Cy5 (Jackson ImmunoResearch Labs), all diluted 1:500.

Time Lapse Microscopy

HeLa Cells were plated on 40 mm-diameter coverslips (Bioptechs Inc., Butler, PA) and 24 hours after seeding, cells were subjected to a double thymidine block and transfected. Briefly, cells were treated for 15 hours with 2 mM thymidine. Following first thymidine treatment, cells were washed in PBS and grown in fresh media. Following replacement of fresh media, cells were transfected with vectors for GFP-SIRT2 and RFP-Wee1 and grown in standard culture conditions for 8 hours. Cells were then retreated in 2 mM thymidine for 17 hours. Following second thymidine treatment, cells were washed twice in PBS and grown for 6 hours in fresh media, at which time the coverslip containing cells was transferred to a closed culture chamber system (Bioptechs) with CO₂-independent media and subjected to time-lapse microscopy with images acquired every minute on a Nikon elipse TE300 microscope controlled by Metamorph software.

Introduction

SIRT2 has been implicated in the control of cellular proliferation (89, 90). SIRT2 overexpression in the osteosarcoma cell line Soas2 induces a delay in mitotic exit that is dependent on SIRT2 enzymatic activity (90). In addition, SIRT2 has been suggested to be a tumor suppressor gene since overexpression of SIRT2 negatively regulates cellular proliferation (89). SIRT2 expression is reduced in a high proportion of glioma cell lines. Furthermore, replacement of SIRT2 expression in these cell lines reduced cellular proliferation as measured by colony formation assay (89). These data collectively suggest that SIRT2 functions to negatively regulate cell cycle progression.

Yeast Sir2p functions at three distinct loci for transcriptional repression, including the *rDNA* array, where it associates with Cdc14p and Net1 in the RENT complex (47, 170). In yeast, during the anaphase stage of mitosis, the RENT complex is released from the nucleoli and functions in mitotic exit (47). Although a mammalian RENT-like complex has not been characterized, two homologs of Cdc14p have been identified (CDC14A and CDC14B) (171). CDC14B, like its yeast counterpart, is localized to the nucleoli, whereas CDC14A is found in the cytoplasm (172, 173). SIRT2 is phosphorylated in a cell cycle-dependent manner, and its stability was shown to be regulated by the phosphatase CDC14B (90). However, it is not clear if CDC14B regulation of SIRT2 stability is by direct regulation of SIRT2 phosphorylation. In addition, the nature of the kinase involved in SIRT2 phosphorylation, and its possible role in regulation of SIRT2 stability has not been elucidated. Of interest, Cdc14p in yeast functions to antagonize Cdk1 activity by dephosphorylating several Cdk1 targets during the transition from mitotic entry into mitotic exit (174). Regulation of mitotic entry is

controlled by a complex network centered on the Cdk1 kinase, and involves a number of key Cdk1 inducers and inhibitors that are coupled with chromosome replication, spindle pole duplication, morphogenesis, and DNA damage (175). Cdk1 activity is pivotal in promoting several critical cellular events associated with mitotic entry, including centrosome separation, golgi fragmentation, chromosome condensation, nuclear envelope breakdown, and spindle assembly (reviewed in (176)).

In this chapter we demonstrate that Cdk1 phosphorylates SIRT2 on serine-368, which can be dephosphorylated by both CDC14A and CDC14B, and furthermore, that phosphorylation at this site is required for SIRT2 mediated delay in cell cycle progression.

UNIVERSITY OF MICHIGAN

Results

Generation of Multiple Isoforms of SIRT2 by Alternative Translational Start Sites

The SIRT2 protein migrated as multiple species by SDS-PAGE after transfection of 293T cells with a SIRT2 cDNA construct (figure 4.1A). Lysates from mock-transfected cells were analyzed alongside lysates from SIRT2-FLAG transfected cells to confirm the proteins recognized by the FLAG antiserum are attributed exclusively to the exogenously expressed SIRT2-FLAG protein. In addition, the western blot was probed for actin to confirm that equivalent amounts of protein from each transfection were analyzed (figure 4.1A). SIRT2 is expressed as two isoforms resulting from alternative splicing (figure 4.1B). In isoform 1, all exons are spliced contributing to a translated protein of 389 amino acids. A second isoform arises when the second exon is spliced out, placing a stop codon located in exon 3 in frame with the first ATG. However it is suspected that the second ATG (M38) can be utilized for translation initiation based on the presence of a Kozak sequence surrounding this ATG (88). The SIRT2 utilized in these studies corresponded to isoform 1 and it is possible that both ATG codons are utilized for translation upon expression of this isoform in 293T cells. To test this possibility, we mutated the second ATG (M38) into alanine, and observed that the two lower molecular weight proteins were no longer present. This observation indicates that the second ATG (M38) is utilized for translation as well as the first (figure 4.1C). As a control, the third ATG (M78) was mutated, which did not affect the translation products of SIRT2. These results indicate that exogenously expressed SIRT2 can be represented *in vivo* as two isoforms, and that the different variants that may exist from endogenously expressed SIRT2 may be the result of either alternative splicing or alternative translational start sites.

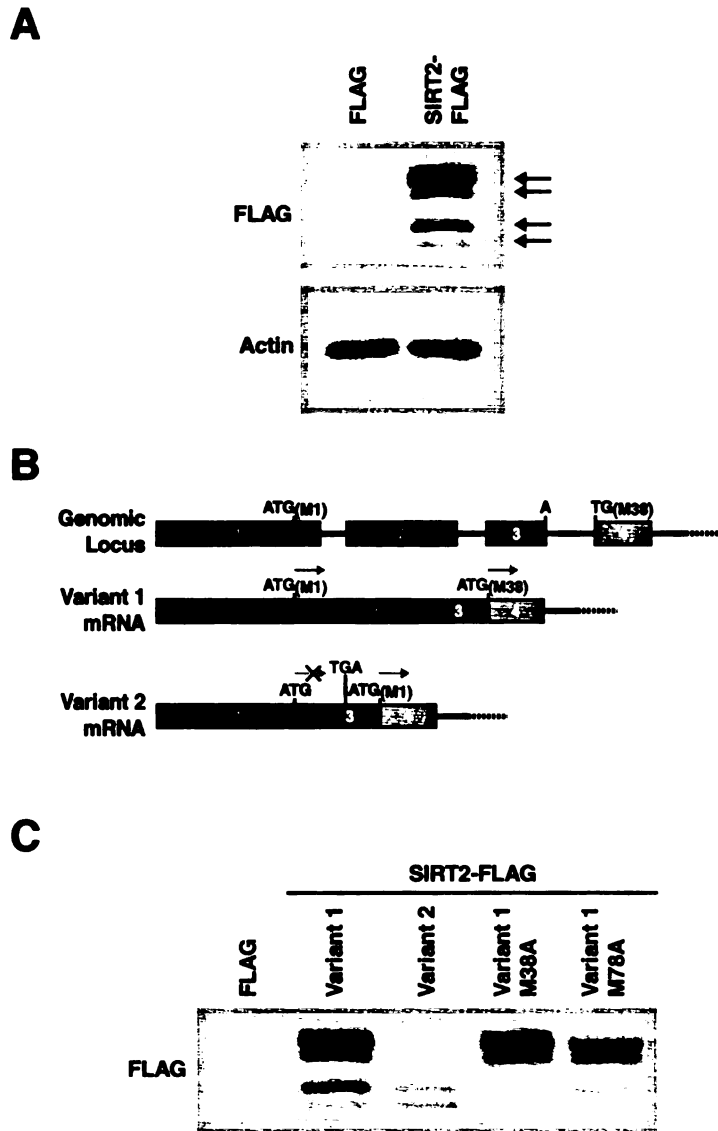


Figure 4.1. Exogenous SIRT2 migrates as multiple species on SDS-PAGE. (A) 293T cells were either mock transfected or transfected with SIRT2-FLAG and cellular lysates were separated by SDS-PAGE and probed by western blotting with antisera specific for FLAG or actin. (B) Schematic diagram of genomic and alternatively spliced transcripts of SIRT2. Location of two ATG codons that both serve as translational start sites are indicated. (C) 293T cells were either mock transfected or transfected with indicated SIRT2-FLAG vectors. Cellular lysates were analyzed with antisera specific for FLAG as in (A).

SIRT2 is Targeted for Phosphorylation

In addition to the two major isoforms expressed off the exogenous SIRT2-FLAG construct, each isoform consisted of two migratory species. To determine if phosphorylation was responsible for these multiple migratory species, immunoprecipitated SIRT2-FLAG was treated *in vitro* with calf intestinal phosphatase (CIP). Incubation of SIRT2-FLAG with increasing concentrations of CIP resulted in a shift in migration of SIRT2-FLAG to a faster migratory species, indicating that phosphorylation is responsible for the various species we visualize by SDS-PAGE (figure 4.2A). As a control, we incubated the *in vitro* phosphatase assay with the phosphatase inhibitor sodium pyrophosphate to confirm that the loss of the slower migratory species was due to the phosphatase activity of the CIP enzyme (figure 4.2A). These results indicate that SIRT2 is phosphorylated *in vivo*.

To determine which amino acids are phosphorylated in SIRT2, we probed immunoprecipitated SIRT2-FLAG with antibodies specific for phosphoserine, phosphothreonine, and phosphotyrosine amino acids. We observed that SIRT2 reacted strongly with the anti-phosphoserine and to a lesser degree with the anti-phosphothreonine antisera (figure 4.2B). We are unable to detect a significant phosphotyrosine signal in SIRT2-FLAG, however the IgG heavy chain from the immunoprecipitation procedure was potentially masking our ability to clearly discern a phosphotyrosine signal on the western blot. For this reason, as well as potential context-dependent site-specificity associated with phosphospecific antibodies, we are unable to conclusively determine the lack of phosphotyrosine residues within SIRT2 (figure 4.2B). These results confirm the presence of phosphorylation of SIRT2 and indicate that SIRT2

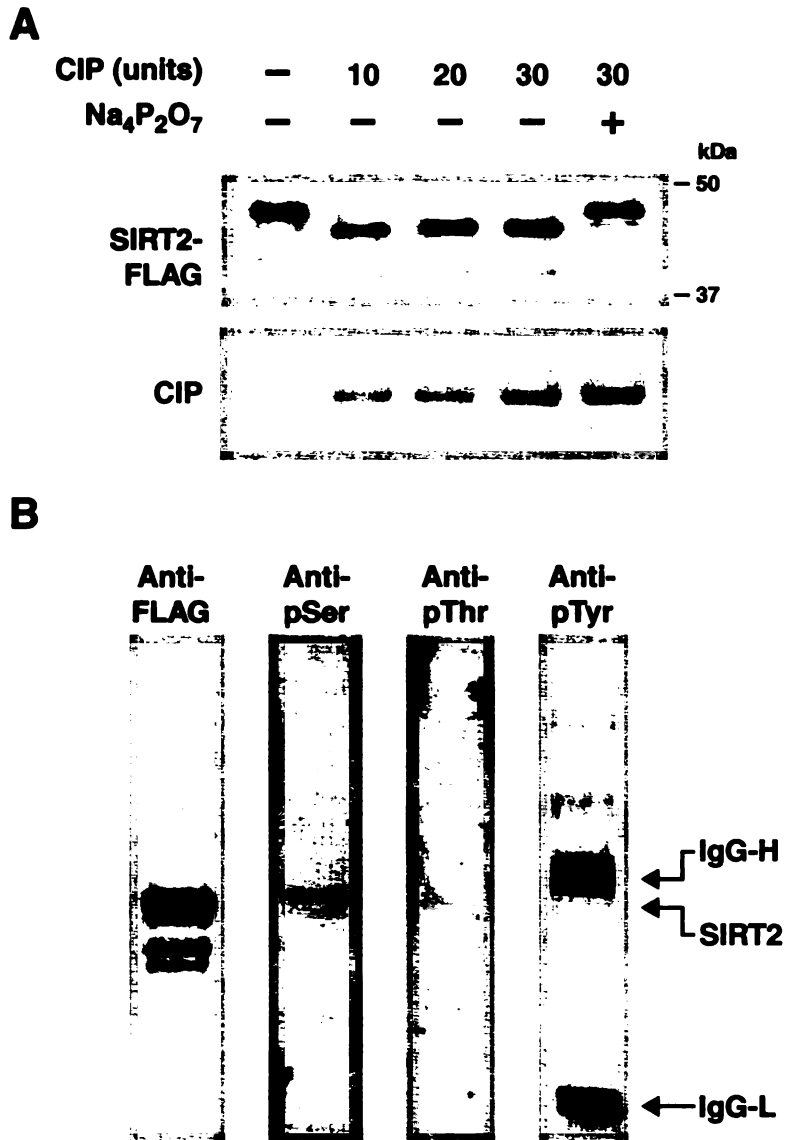


Figure 4.2. SIRT2 is targeted for phosphorylation *in vivo*. (A) 293T cells were transfected with SIRT2-FLAG, and lysates were subsequently immunoprecipitated with an anti-FLAG antiserum. Immunoprecipitated material was incubated with increasing concentrations of CIP with or without sodium pyrophosphate, followed by separation by SDS-PAGE and probed by western blotting with a FLAG specific antiserum. (B) Immunoprecipitated SIRT2 was prepared as in (A) and analyzed by western blotting with antisera specific for anti-FLAG, anti-phosphoserine, anti-phosphothreonine or anti-phosphotyrosine.

1

1. The first part of the document is a list of names and addresses of the members of the committee. The names are listed in alphabetical order, and the addresses are given in full. The list includes the names of the members of the committee, the names of the members of the sub-committee, and the names of the members of the advisory committee. The addresses are given in full, including the street name, the city, the state, and the zip code.

2. The second part of the document is a list of the names and addresses of the members of the committee. The names are listed in alphabetical order, and the addresses are given in full. The list includes the names of the members of the committee, the names of the members of the sub-committee, and the names of the members of the advisory committee. The addresses are given in full, including the street name, the city, the state, and the zip code.

3. The third part of the document is a list of the names and addresses of the members of the committee. The names are listed in alphabetical order, and the addresses are given in full. The list includes the names of the members of the committee, the names of the members of the sub-committee, and the names of the members of the advisory committee. The addresses are given in full, including the street name, the city, the state, and the zip code.

4. The fourth part of the document is a list of the names and addresses of the members of the committee. The names are listed in alphabetical order, and the addresses are given in full. The list includes the names of the members of the committee, the names of the members of the sub-committee, and the names of the members of the advisory committee. The addresses are given in full, including the street name, the city, the state, and the zip code.

5. The fifth part of the document is a list of the names and addresses of the members of the committee. The names are listed in alphabetical order, and the addresses are given in full. The list includes the names of the members of the committee, the names of the members of the sub-committee, and the names of the members of the advisory committee. The addresses are given in full, including the street name, the city, the state, and the zip code.

is potentially targeted for phosphorylation on serine and threonine residues.

Mapping of the Primary Phosphorylation Site in SIRT2 to Serine-368

To determine the site(s) of SIRT2 phosphorylation, we generated a deletion series of SIRT2 fused to the carboxy-terminus of GFP. We observed that GFP-SIRT2 deletion proteins containing the region of SIRT2 from amino acids 360–389 migrated as multiple protein species (figure 4.3A, lanes 8–13). However, fusions that did not contain the region encompassing amino acids 360–389 as well as GFP alone migrated as a single protein (figure 4.3A, lanes 3–7). Identification of the multiple migratory species is more evident in the smaller deletions, as the separation of smaller proteins is more pronounced with the SDS-PAGE conditions utilized. These data indicate that the phosphorylation dependent alteration in migration of SIRT2 is due to phosphorylation at the carboxy-terminal 30 amino acid residues of SIRT2. Analysis of the region encompassing amino acids 360–389 of SIRT2 indicates the presence of a number of potential serine and threonine phosphorylation sites (figure 4.3B). To determine which sites may be phosphorylated, each of these potential phosphorylation sites were individually mutated to alanine residues. All mutants, with the exception of S368A, migrated indistinguishably from the wild-type protein (figure 4.3C). Mutation of serine-368 to alanine caused SIRT2 to migrate faster than the wild-type protein, consistent with the possibility that this site is phosphorylated (figure 4.3C). However, these data also indicate that serine-368 is not the only potential phosphorylation site leading to migratory differences in SIRT2, as mutation of serine-368 is not sufficient to collapse all SIRT2 to a single protein band (figure 4.3C).

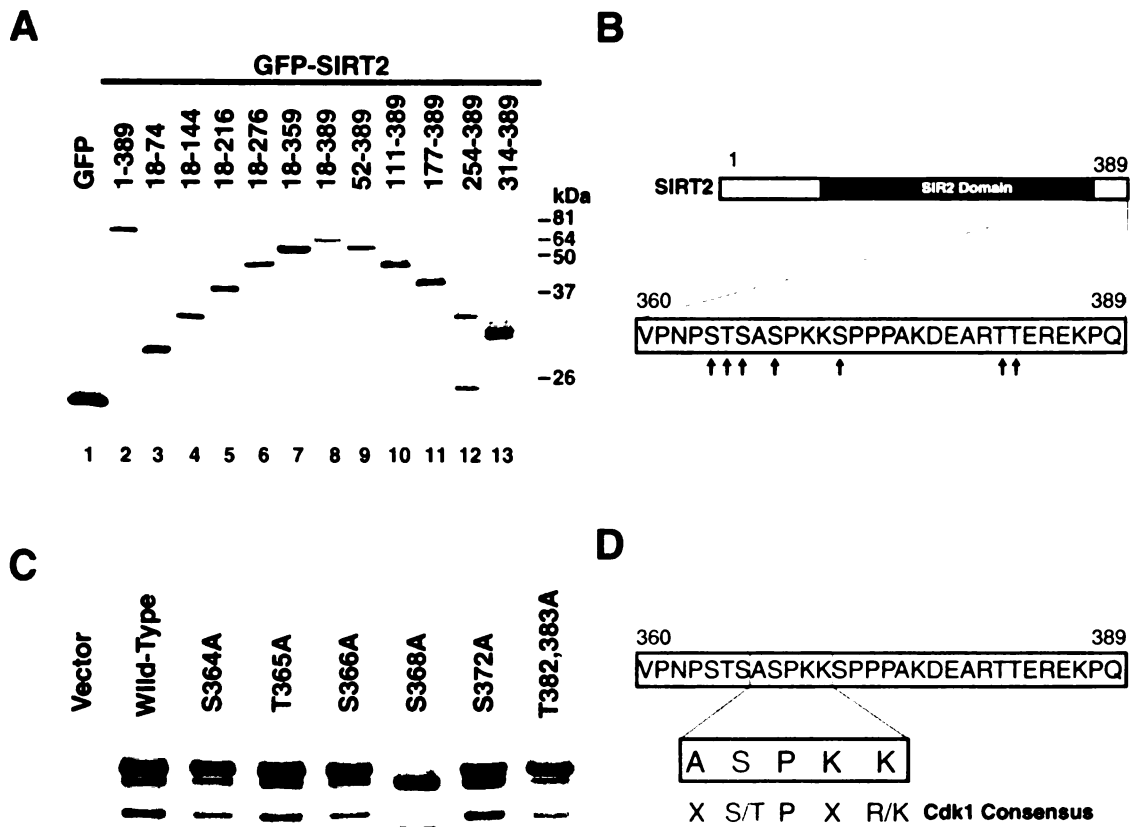


Figure 4.3. Phosphorylation of SIRT2 occurs on serine-368. (A) 293T cells were transfected with GFP or a series of GFP-SIRT2 deletion mutants. Cellular lysates were separated by SDS-PAGE and probed by western blotting with a GFP specific antiserum. (B) Schematic diagram of SIRT2 and amino acids 360-389, indicating potential sites of phosphorylation. (C) 293T cells were mock transfected or transfected with SIRT2-FLAG wild-type or single point mutations of potential phosphorylation sites. Cellular lysates were separated by SDS-PAGE and probed by western blotting with a FLAG specific antiserum. (D) Schematic diagram of SIRT2 amino acids 360-389, with Cdk1 consensus sequence shown.

1
2
3
4
5
6
7
8
9
10
11
12
13
14
15
16
17
18
19
20
21
22
23
24
25
26
27
28
29
30
31
32
33
34
35
36
37
38
39
40
41
42
43
44
45
46
47
48
49
50
51
52
53
54
55
56
57
58
59
60
61
62
63
64
65
66
67
68
69
70
71
72
73
74
75
76
77
78
79
80
81
82
83
84
85
86
87
88
89
90
91
92
93
94
95
96
97
98
99
100

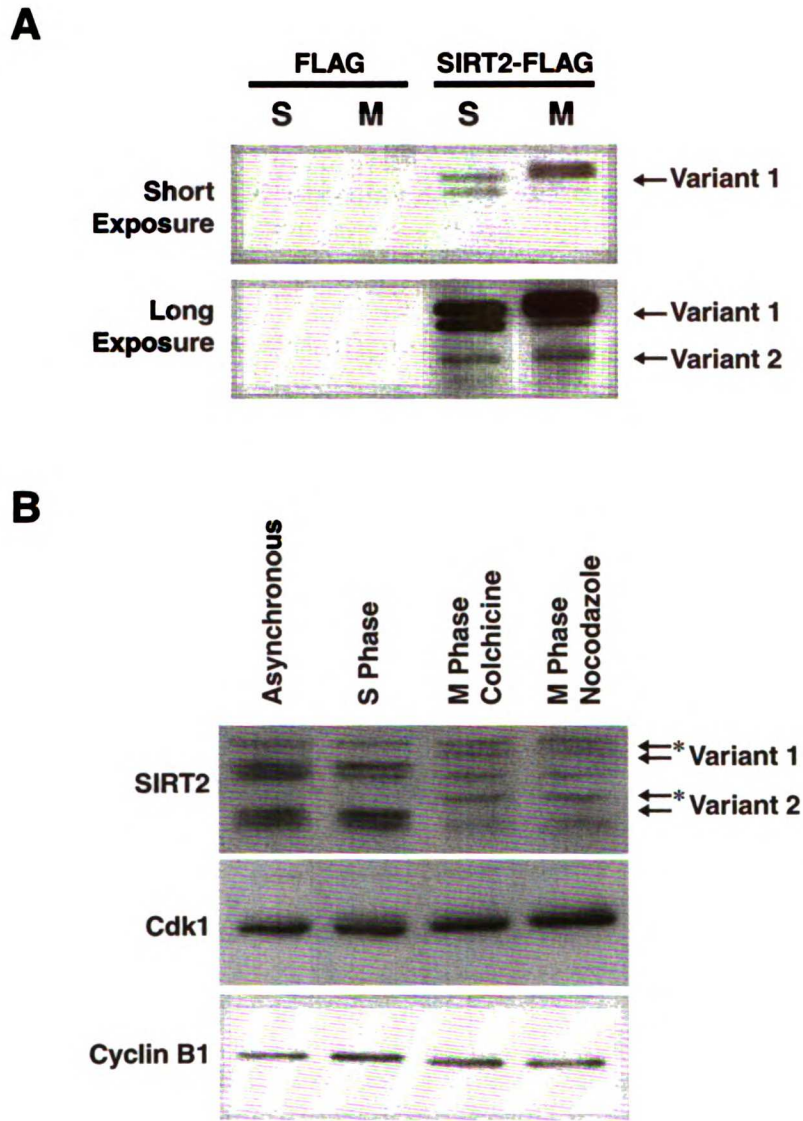


Figure 4.4. Phosphorylation of SIRT2 is enhanced during mitosis. (A) 293T cells were mock transfected or transfected with SIRT2-FLAG and arrested in either G1/S phase or M phase of the cell cycle. Cellular lysates were analyzed as in figure 4.3C. (B) 293T cells were allowed to grow asynchronously or arrested in either G1/S phase or M phase of the cell cycle. Cellular lysates were analyzed by western blotting as in figure 4.3C with antisera specific for SIRT2, Cdk1, and Cyclin B1.

Analysis of serine-368 and surrounding residues for potential kinase consensus sequence motif indicates that serine-368 is possibly targeted by CKI, GSK3, PKC, and Cdk1 for phosphorylation. Of interest was Cdk1, since serine-368 represented the only Cdk1 consensus site within the entire SIRT2 protein (figure 4.3D). In agreement with a possible role for Cdk1 in SIRT2 phosphorylation, we found that the phosphorylation status of exogenous SIRT2 was cell cycle-dependent, with an increase noted in SIRT2 phosphorylation during mitotic arrest (figure 4.4A). Cells were stained with propidium iodide and analyzed by flow cytometry to confirm that cells were arrested in G1/S and M phases of the cell cycle (data not shown). To determine the phosphorylation status of endogenous SIRT2, we arrested cells in G1/S phase or M phase, and compared them to asynchronously growing cells. We observed that endogenous SIRT2 was also hyperphosphorylated during mitotic arrest (figure 4.4B). These results indicate that SIRT2 phosphorylation is, in part, cell cycle-dependent.

Cdk1 Regulates SIRT2 Phosphorylation in vitro on Serine-368

To determine if Cdk1 can phosphorylate SIRT2, we purified 6x His-tagged wild-type and S368A recombinant SIRT2 (rSIRT2) protein expressed in *E. coli*, and incubated these rSIRT2 proteins with increasing concentrations of purified Cdk1-Cyclin B1 complex in the presence of [γ - 32 P]-ATP *in vitro*. Cdk1-Cyclin B1 efficiently phosphorylated wild-type rSIRT2 in a dose dependent manner (figure 4.5A, lanes 4–6). In contrast, the S368A mutant SIRT2 protein did not become phosphorylated upon incubation with Cdk1-Cyclin B1 (figure 4.5A, lanes 7–9).

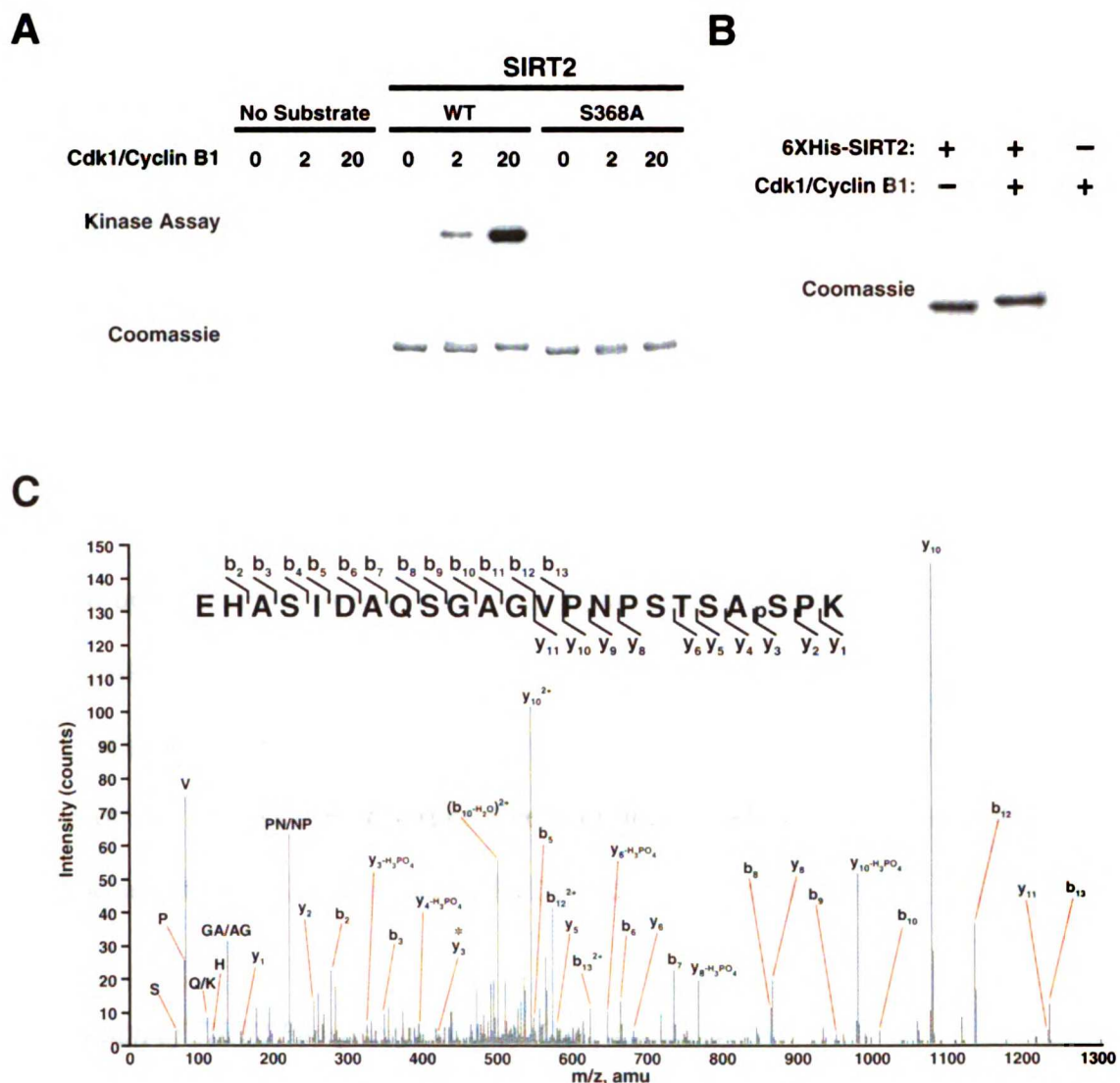


Figure 4.5. *In vitro* phosphorylation of SIRT2 by Cdk1 occurs on serine-368. (A) Increasing amounts of recombinant Cdk1-Cyclin B1 were incubated with or without wild type or S368A rSIRT2 with $[\gamma\text{-}^{32}\text{P}]\text{-ATP}$. Proteins were separated by SDS-PAGE and stained with coomassie blue, followed by autoradiography. (B) Wild-type rSIRT2 was incubated with or without Cdk1-Cyclin B1 to phosphorylate rSIRT2. Proteins were separated by SDS-PAGE and stained with coomassie blue. (C) rSIRT2 incubated with Cdk1-Cyclin B1 in (B) was excised from the gel and subjected to in-gel digestion with trypsin followed by analysis by tandem mass spectrometry.

To confirm that serine-368 was indeed the site targeted for phosphorylation by Cdk1, we incubated rSIRT2 with or without Cdk1-Cyclin B1. Incubation of rSIRT2 with Cdk1 resulted in a slower mobility of rSIRT2 when analyzed by SDS-PAGE (figure 4.5B). Both rSIRT2 bands (\pm Cdk1-Cyclin B1) were excised from the gel and subjected to in-gel digestion with trypsin. Resulting protein fragments were analyzed by tandem mass spectrometry (LC-MS/MS). Electrospray MS/MS spectrum of the triply charged molecular ion 763.4 derived from the phosphorylated peptide amino acids 348–370 was generated. The sequence of the peptide has been fully confirmed by overlapping ladders of the b and y ion series (figure 4.5C). The assignment of phosphorylation to serine-368 is based upon detection of ion y₃ carrying a phosphate group (figure 4.5C, indicated by an asterisk). The majority of the observed fragment ions could be matched to the predicted product ions and many internal product ions were also observed. The complete nature of the LC-MS/MS spectrum gives confidence that rSIRT2 phosphorylation by Cdk1 occurs at serine-368 and that rSIRT2 is indeed a substrate for Cdk1 *in vitro*.

Modulation of SIRT2 Phosphorylation by Cdk1-Cyclin B1

To determine if SIRT2 is phosphorylated by Cdk1 *in vivo*, we transfected cells with vectors encoding FLAG, SIRT2-FLAG wild-type or S368A and tested the effect of Purvalanol A, an inhibitor of Cdk1 activity on SIRT2 migration. Treatment of cells with Purvalanol A reduced the phosphorylation of SIRT2, as demonstrated by an increase in the amount of SIRT2 migrating as a faster protein species (figure 4.6A, lanes 3 and 4). As expected, no change was observed for the SIRT2 S368A mutant (figure 4.6A, lanes 5 and 6). Recent results have indicated that Purvalanol A can also inhibit the MAP

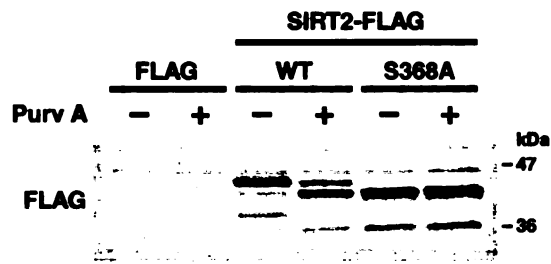
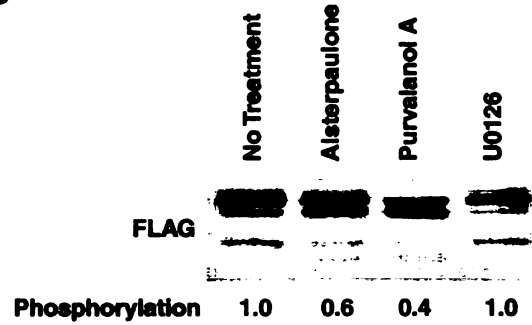
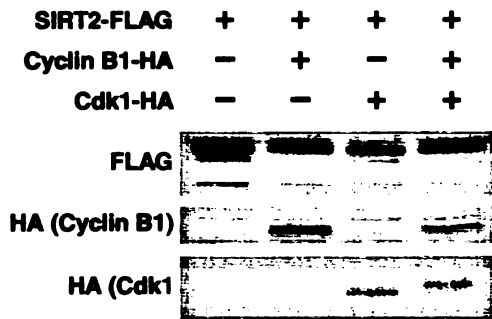
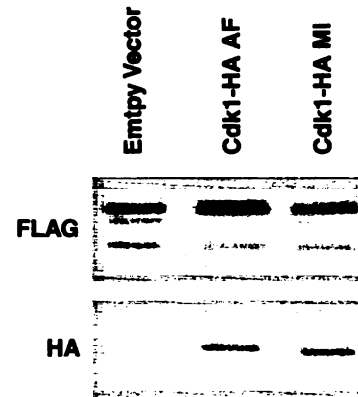
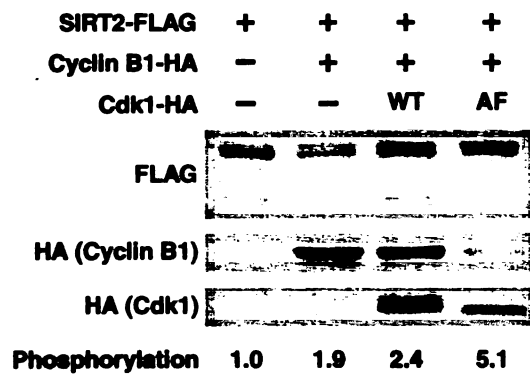
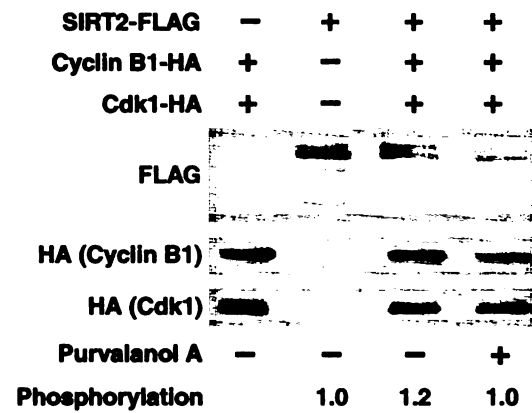
A**B****C****D****E****F**

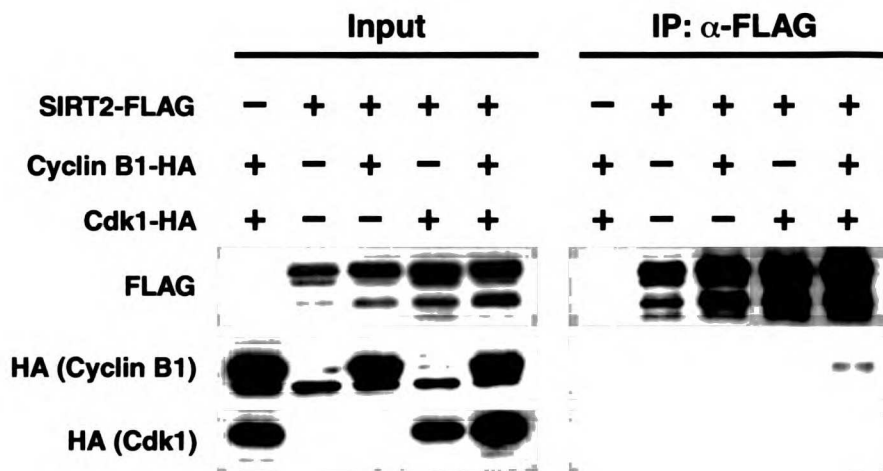
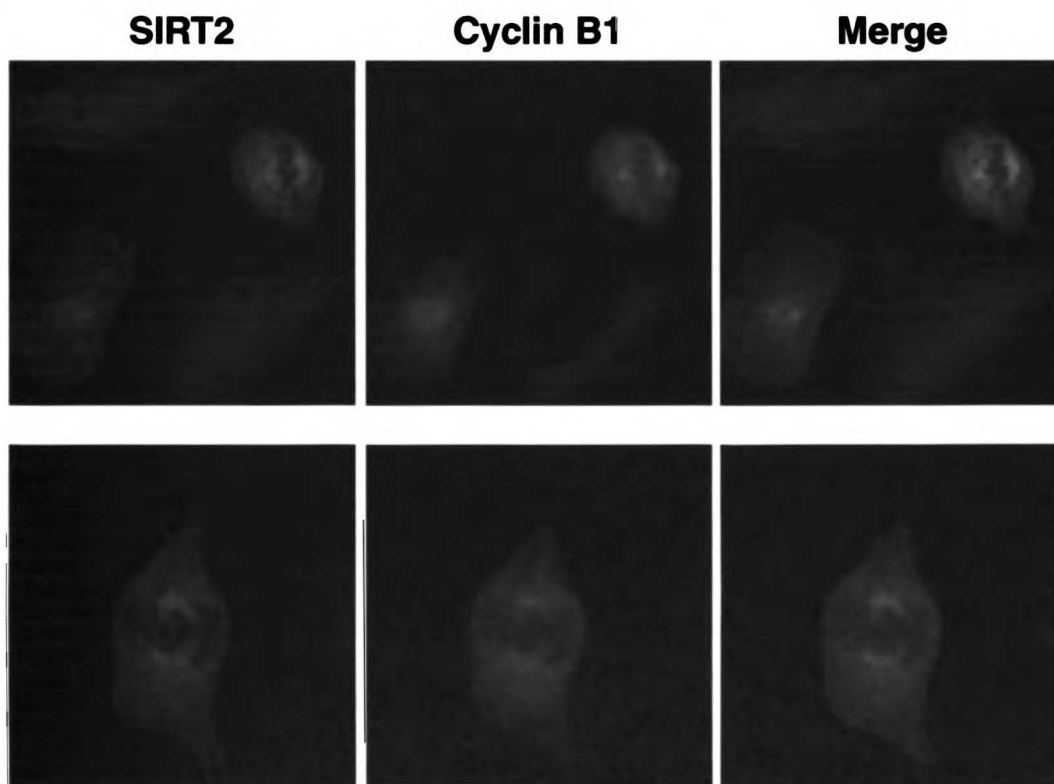
Figure 4.6. Reduction of SIRT2 phosphorylation by pharmacological inhibition of Cdk1 or expression of Cdk1-Cyclin B1 factors. (A) 293T cells were mock transfected or transfected with either SIRT2-FLAG wild-type or S368A, followed by treatment with or without Purvalanol A. Cellular lysates were separated by SDS-PAGE and probed by western blotting with a FLAG specific antisera. (B) 293T cells were transfected with SIRT2-FLAG and either mock treated or treated with Alsterpaullone, Purvalonal A, or U0126. Cellular lysates were analyzed as in (A). (C) 293T cells were either mock transfected or transfected with SIRT2-FLAG with or without Cdk1-HA, Cyclin B1-HA, or a combination of both. Cellular lysates were analyzed as in (A) with antisera specific for FLAG and HA. (D) 293T cells were transfected with SIRT2-FLAG with or without Cdk1-HA wild-type, AF or MI mutants. Cellular lysates were analyzed as in (A) with antisera specific for FLAG and HA. (E) 293T cells were transfected with SIRT2-FLAG with or without Cyclin B1-HA and Cdk1-HA wild-type or AF mutant. Cellular lysates were analyzed as in (A) with antisera specific for FLAG and HA, and quantification was performed on the FLAG western blot. (F) 293T cells were transfected with SIRT2-FLAG with or without Cyclin B1-HA and Cdk1-HA. Cells were treated with or without Purvalanol A for 3 hours. Cellular lysates were analyzed as in (A) with antisera specific for FLAG and HA, and quantification was performed on the FLAG western.

kinase pathway via inhibition of the p42/p44 Map Kinase Kinase (MAPKK or MEK1) (177). To confirm that reduction in phosphorylation of SIRT2 following Purvalanol A treatment is due to inhibition of Cdk1 and not MEK1, we treated cells with an additional, Purvalanol A unrelated Cdk1 inhibitor, Alsterpaullone, as well as the MEK1 inhibitor U0126. Alsterpaullone, like Purvalanol A, inhibited SIRT2 phosphorylation, however no reduction in SIRT2 phosphorylation due to the MEK1 inhibitor U0126 was observed (figure 4.6B). These results indicate that inhibition of Cdk1 results in a reduction of SIRT2 phosphorylation.

To determine if Cdk1-Cyclin B1 expression can directly affect SIRT2 phosphorylation, we overexpressed Cdk1-HA, Cyclin B1-HA, or both with SIRT2-FLAG. Expression of exogenous Cyclin B1 should lead to the activation of endogenous Cdk1 kinase activity. We found that expression of Cyclin B1 with or without Cdk1 resulted in an increase in SIRT2 phosphorylation, which was not observed with

overexpression of Cdk1 alone (figure 4.6C). These results indicate that Cyclin B1 can control the phosphorylation status of SIRT2 by activating endogenous Cdk1, whereas expression of wild-type Cdk1 alone is not sufficient to induce phosphorylation due to reduced Cyclin B1 expression found in asynchronous cells.

In addition to binding Cyclin B1, the kinase activity of Cdk1 is regulated itself by phosphorylation. For full activation of the Cdk1 kinase activity, Cdk1 needs to be phosphorylated on threonine-161, which is carried out by cyclin associated kinase (CAK) (178-180). Removal of the inhibitory phosphorylations on threonine-14 and tyrosine-15 is carried out by CDC25C (181-185). An increase in Cdk1 activity can be achieved by mutation of threonine-14 and tyrosine-15 to block the inhibitory phosphorylations on Cdk1. To generate a constitutively active Cdk1, we generated the nonphosphorylatable mutant, Cdk1 T14A,Y15F (Cdk1 AF), as previously reported (186). To determine if activated Cdk1 can cause a hyperphosphorylation of SIRT2 in the absence of exogenously expressed Cyclin B1, we cotransfected SIRT2 with Cdk1 AF or a catalytically inactive Cdk1 K33M,K34I (Cdk1MI). Coexpression of SIRT2 with Cdk1 AF, but not inactive Cdk1 MI, resulted in an increase in SIRT2 phosphorylation (figure 4.6D). To determine if the affect of Cdk1 AF on SIRT2 phosphorylation was further induced in the presence of Cyclin B1, we cotransfected SIRT2 with or without Cyclin B1 in addition to either Cdk1 WT or Cdk1 AF. After quantification of the phosphorylation status of SIRT2, we found that Cyclin B1 alone induced a 1.9-fold increase in SIRT2 phosphorylation, whereas addition of Cdk1 WT caused a modest induction of 2.4-fold, and addition of Cdk1 AF potentiated this increase further to 5.1-fold (figure 4.6E). To confirm that hyperphosphorylation of SIRT2 was a consequence of Cdk1 activity, we

A**B**

www.nature.com/scientificdata/

Figure 4.7. Interaction and colocalization of SIRT2 and the Cdk1-Cyclin B1 complex. (A) SIRT2 and both Cyclin B1 and Cdk1 coimmunoprecipitate. 293T cells were either mock transfected or transfected with SIRT2-FLAG with or without Cdk1-HA, Cyclin B1-HA or both. Cellular lysates were immunoprecipitated with anti-FLAG and probed by western blotting with antisera specific for FLAG and HA. 10% of protein input was analyzed by western blotting with antisera for FLAG or HA. (B) Confocal microscopy analysis of SIRT2 colocalization with Cyclin B1. U2OS Cells were stained for SIRT2 (green) and Cyclin B1 (red).

coexpressed Cdk1 and Cyclin B1 with SIRT2 followed by a short treatment with or without Purvalanol A. We found that the hyperphosphorylation induced by Cyclin B1/Cdk1 expression was abrogated with Purvalanol A, indicating that the effect is mediated through Cdk1 activity (figure 4.6F).

Colocalization and Interaction of SIRT2 and Cdk1-Cyclin B1

To determine if SIRT2 and Cdk1-Cyclin B1 associate together in a complex we performed coimmunoprecipitation experiments. Cdk1-HA and Cyclin B1-HA were transfected alone or together, and with or without SIRT2-FLAG. We found that Cyclin B1-HA and Cdk1-HA coimmunoprecipitated with SIRT2-FLAG (figure 4.7A). Furthermore, interaction of SIRT2-FLAG with either Cyclin B1-HA or Cdk1-HA was not dependent on one another as SIRT2-FLAG coimmunoprecipitated with either of them when transfected independently. However, we cannot rule out the possibility that the endogenous component of the Cdk1-Cyclin B1 complex may be present within, and responsible for, these interactions.

Interaction of transiently expressed SIRT2 with Cyclin B1 and Cdk1 prompted us to test if the endogenous proteins were colocalized *in vivo*. Using indirect immunofluorescence with antisera against SIRT2 and Cyclin B1, we observed that both

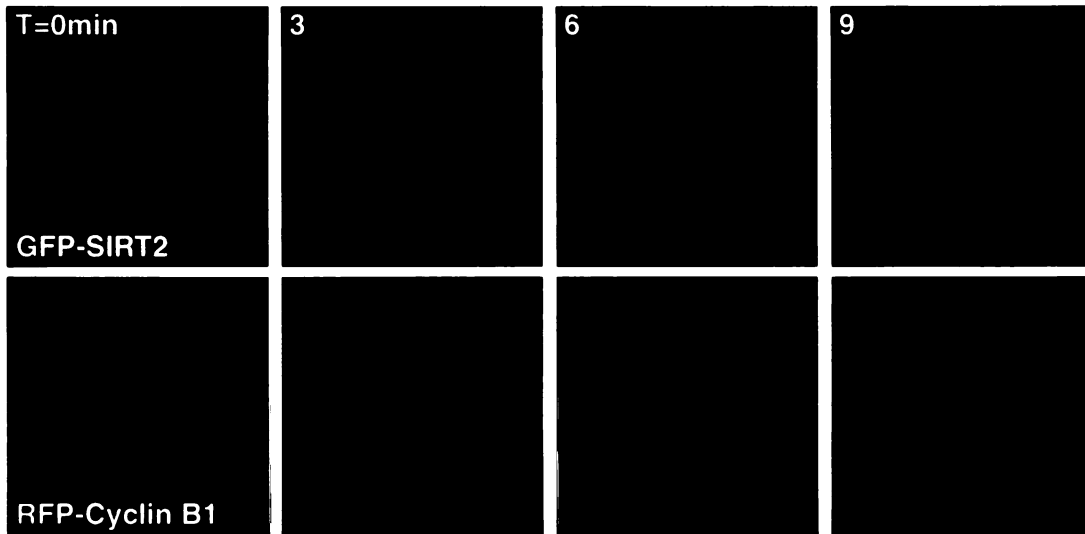


Figure 4.8. Colocalization of SIRT2 and Cyclin B1 during centrosome separation. HeLa cells grown on a coverslip were transfected with GFP-SIRT2 and RFP-Cyclin B1 and synchronized by double thymidine block. Images of both GFP and RFP were acquired each minute. Four time points, each three minutes apart, are shown of a cell at the G2 to M transition.

proteins were enriched on the centrosome during prophase and spindle fibers during metaphase (figure 4.7B). The merged images indicate that both endogenous SIRT2 and Cyclin B1 are colocalized on these structures (figure 4.7B).

To further define the localization of SIRT2 and Cyclin B1 during mitosis, we cotransfected SIRT2 tagged at the amino-terminus with GFP (GFP-SIRT2) and with Cyclin B1 tagged at the amino-terminus with DsRed (RFP-Cyclin B1), and followed these cells through the cell cycle with time-lapse microscopy (figure 4.8). We observed that exogenous GFP-SIRT2 was diffusely localized throughout the cytoplasm, however RFP-Cyclin B1 was localized predominantly on the centrosome as cells progressed through G2. Interestingly, just prior to and during the process of centrosome separation, both GFP-SIRT2 and RFP-Cyclin B1 were colocalized on the centrosome (figure 4.8). Together with the coimmunoprecipitation of these two proteins, these results suggest that SIRT2 forms a complex with Cyclin B1 during mitotic entry on the centrosome and that both proteins are concentrated on the spindle fibers during metaphase.

Dephosphorylation of SIRT2 by the Human CDC14 Phosphatases

To determine a potential role of CDC14A and/or CDC14B in dephosphorylation of SIRT2, we transfected SIRT2-FLAG with GFP, GFP-CDC14A or CDC14B-GFP. Extracts from these cells were probed with an antiserum specific for GFP to assess expression levels of CDC14A and B, as well as an anti-FLAG antiserum to detect SIRT2. We observed that coexpression of either CDC14A or CDC14B with SIRT2 resulted in the dephosphorylation of SIRT2 *in vivo* (figure 4.9). We reliably observe more complete

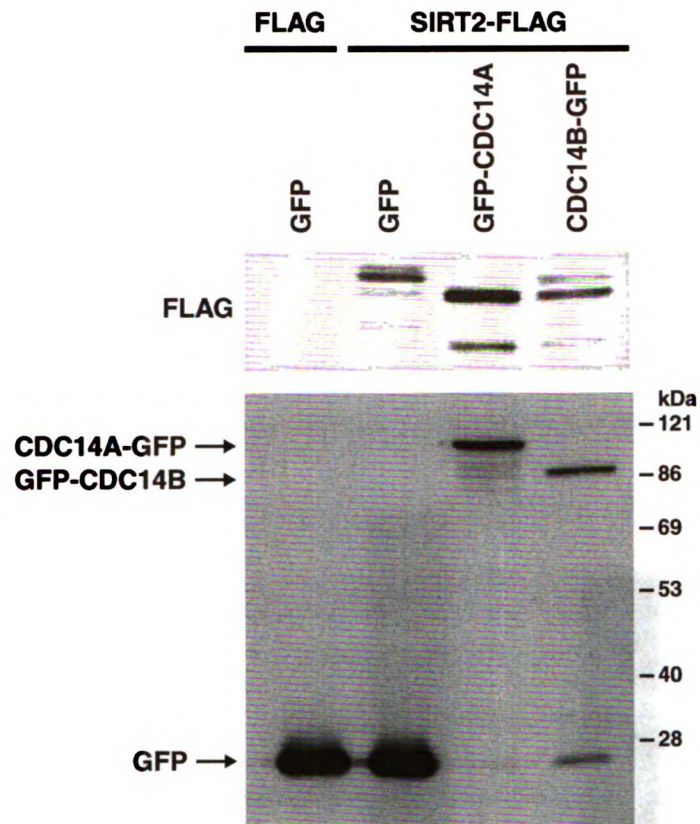
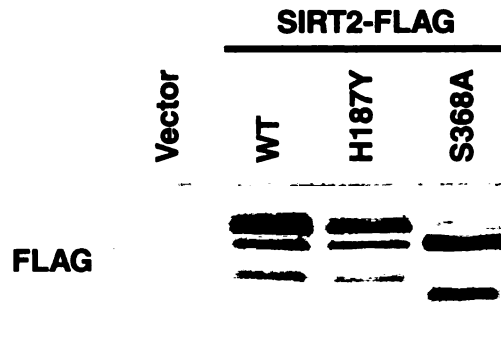


Figure 4.9. Dephosphorylation of SIRT2 by coexpression with CDC14A and CDC14B. 293T cells were mock transfected or transfected with SIRT2-FLAG with either GFP, GFP-CDC14A, or CDC14B-GFP. Cellular lysates were separated by SDS-PAGE and probed by western blotting with antisera specific for FLAG and GFP.

A



B

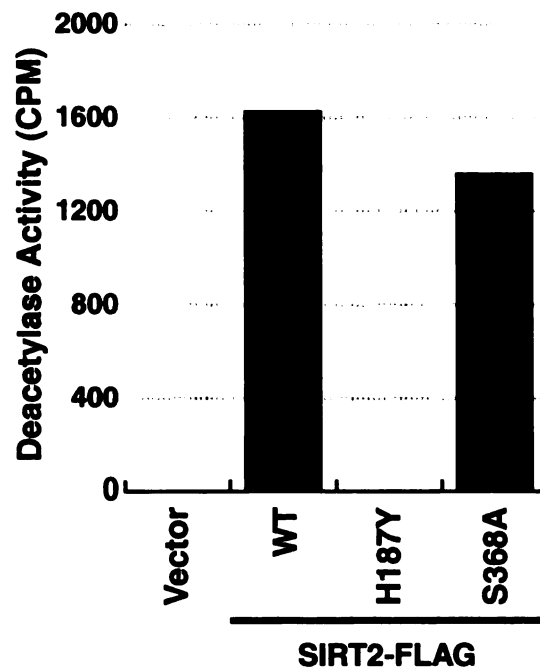


Figure 4.10. Serine-368 is not required for SIRT2 enzymatic activity *in vitro*. (A) 293T cells were either mock transfected or transfected with SIRT2 wild type, H187Y, or S368A. Cellular lysates were separated by SDS-PAGE and probed by western blotting with a FLAG specific antisera. (B) SIRT2-FLAG proteins from lysates in (A) were immunoprecipitated with anti-FLAG antiserum and utilized in an *in vitro* deacetylation assay.

dephosphorylation of SIRT2 with CDC14A. In contrast to published observations, we did not observe SIRT2 degradation in response to coexpression with either CDC14 proteins.

SIRT2-mediated Reduction in Cellular Proliferation is Dependent on Serine-368

To determine whether SIRT2 phosphorylation modifies its enzymatic activity, we tested if the S368A mutant protein was enzymatically active or inactive. We transfected SIRT2-FLAG wild-type, S368A, and the catalytically inactive H187Y in 293T cells and immunoprecipitated the SIRT2-FLAG proteins (figure 4.10A). The immunoprecipitated material was tested for enzymatic activity in an *in vitro* deacetylation reaction utilizing acetylated-Histone H3 peptide as a substrate. Both SIRT2 wild-type and the S368A mutant were able to deacetylate the acetylated Histone H3 substrate (figure 4.10B). In addition, both SIRT2 S368A and the phosphomimetic S368E are active *in vitro* on a histone peptide, and *in vivo* on α -tubulin deacetylation (data not shown). These results indicate that alteration of serine-368 does not affect SIRT2 intrinsic catalytic activity.

To determine whether serine-368 is required for SIRT2-mediated delay in cellular proliferation, we measured the rate of proliferation of cells transfected with SIRT2-FLAG wild-type or S368A. We utilized the cellular stain carboxyfluorescein succinimidyl ester (CFSE), a cell permeable dye that nonspecifically binds to cellular proteins with little or no effect on cell proliferation or viability (187). As cells proliferate, they separate the dye evenly between daughter cells, resulting in a dilution of dye as cells proliferate (figure 4.11A). We transfected a glioblastoma cell line U-87 MG (HTB-14) with the empty FLAG vector, SIRT2-FLAG wild-type or S368A, and with DsRed to mark transfected cells. Following transfection, cells were loaded with the CFSE dye and were subjected to

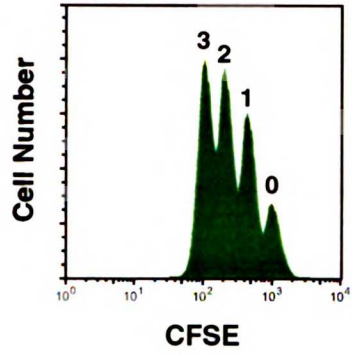
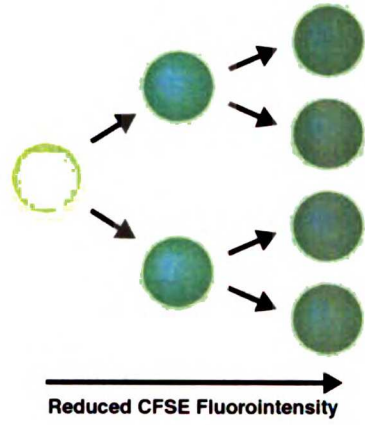
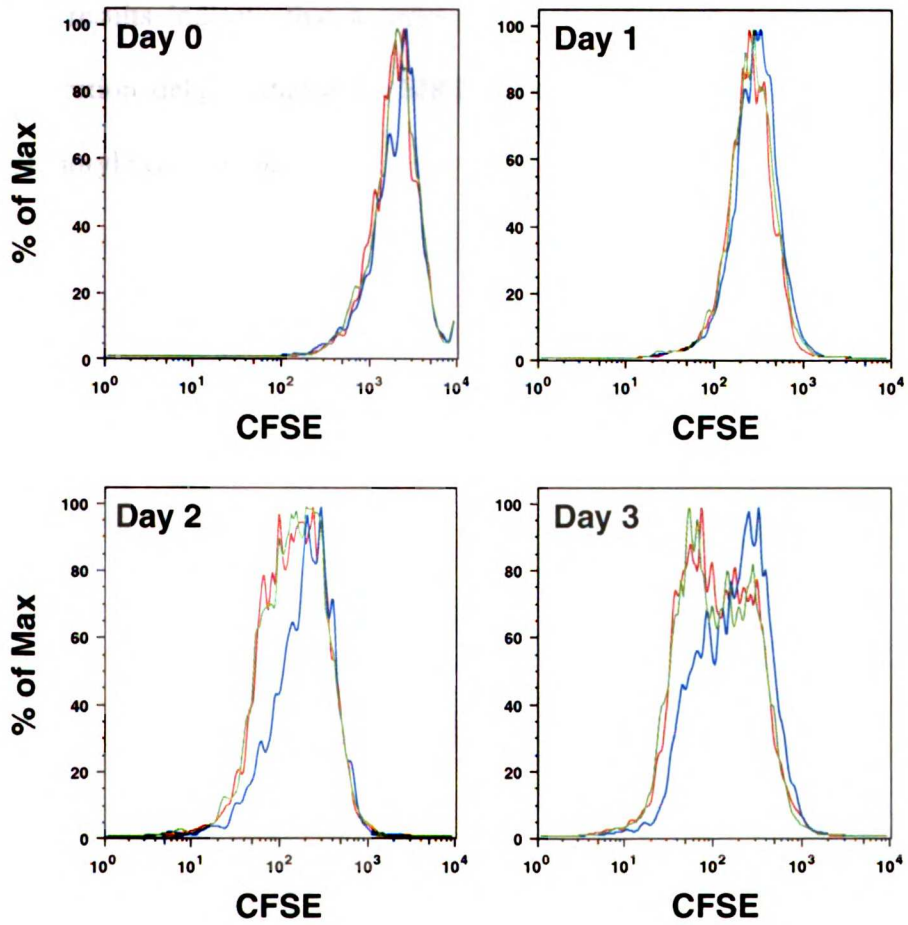
A**B**

Figure 4.11. Regulation of cellular proliferation by SIRT2 is dependent on serine 368 phosphorylation. (A) Schematic diagram of cell proliferation mediated CFSE dilution. (B) Glioma cells were mock transfected (red line) or transfected with SIRT2-FLAG wild-type (blue line) or S368A (green line), with DsRed as a marker for transfected cells. Transfected cells were stained with CFSE and reseeded. Cells were harvested at the indicated times and analyzed by flow cytometry.

flow cytometric analysis at Day 0 (immediately following loading with CFSE) or after 1, 2 and 3 days in culture. We observed that proliferation was suppressed in cells transfected with SIRT2-FLAG (blue line) in comparison to control cells transfected with the empty vector (red line) (figure 4.11B). However, cells transfected with the SIRT2-FLAG S368A vector did not suppress cellular proliferation (figure 4.11B, green line). These results indicate that a serine at amino acid 368 is required for the cell cycle proliferation delay induced by SIRT2 overexpression, potentially via its ability to be phosphorylated by Cdk1.

Discussion

Sirtuin proteins have garnered much interest in recent years as regulators of a vast number of cellular processes, including cell growth, apoptosis, metabolism, and aging (176). However, very little has been understood as to mechanisms utilized by the cell to regulate the function of these enzymes. In this chapter, we demonstrate the regulation of the biological function of SIRT2 via posttranslational modification.

Alternative Translational Start Sites in SIRT2

We found that translation of SIRT2 can occur from two different ATG codons, the first ATG in the mRNA and at the second downstream ATG (M38). Results from the cloning of the mouse gene suggest that translation might occur from the second ATG as it is preceded by a Kozak consensus sequence (88). Here we demonstrate that indeed SIRT2 can be translated off of two ATG codons by showing that mutation of the second ATG dramatically affects the isoforms of SIRT2 that are observed following transfection of full length SIRT2 cDNA. We have not been able to detect, in any of our assays, a differential function for the two variants. It will be of interest in the future to determine if the 5' or 3' untranslated regions of the SIRT2 cDNA, which are absent in our transient expression vectors might regulate ATG usage *in vivo*, as well as to understand what the functional differences between the two variants might be.

Phosphorylation of SIRT2 by Cdk1

In addition to translational initiation of SIRT2 from two different ATG codons resulting in the generation of two different isoforms of SIRT2, we also have demonstrated that

each isoform of SIRT2 migrates as multiple migratory species. We routinely see two different migratory species for each isoform. In addition, when larger quantities of protein are analyzed by western blotting, we are able to visualize a third, even slower migratory species (data not shown). By treatment of SIRT2 *in vitro* with calf intestinal phosphatase (CIP), we demonstrated that SIRT2 is targeted for phosphorylation. Furthermore, we localize the primary site of phosphorylation in SIRT2 to serine-368. However, our data suggest that serine-368 is not the only site for phosphorylation in SIRT2 primarily for two reasons. First, upon mutation of serine-368 to an alanine, we do not observe a complete collapse of the protein to a single band, indicating that a second site is potentially phosphorylated resulting in a similar mobility shift. Second, not all phosphorylation events result in a change in mobility as alteration of mobility due to phosphorylation is influenced by many factors.

Bioinformatic analysis indicated that serine-368 could serve as a site of phosphorylation by a number of different kinases. We found that serine-368 represents a consensus phosphorylation site for the mitotic kinase Cdk1. SIRT2 is targeted for phosphorylation in a mitosis-dependent manner, however a site for phosphorylation as well as potential kinases have not been identified (90). We found that Cdk1 can regulate the phosphorylation of serine-368 both *in vitro* and *in vivo*, indicating that the mitotic phosphorylation of SIRT2 is due, in part, to Cdk1 activity. Furthermore, we observed that SIRT2 and the Cdk1-Cyclin B1 complex interact and that they are found on similar mitotic structures, including the centrosome pre- and post-separation as well as the mitotic spindle during metaphase.

Phosphorylation Dependent Regulation of Cellular Proliferation by SIRT2

SIRT2 overexpression has been shown to regulate cell cycle progression. SIRT2 overexpression leads to slower progression of transfected cells through mitotic exit that is dependent on the enzymatic activity of SIRT2 (90). Furthermore, overexpression of SIRT2 in a glioma cell line reduces the number of colonies that form once transfected cells are placed in selection medium (89). We confirm previous results in which overexpression of SIRT2 reduces the rate of cellular proliferation. However, we found that expression of the nonphosphorylatable S368A mutant does not regulate cellular proliferation as observed with wild-type SIRT2. Our results suggest that SIRT2 overexpression suppresses proliferation in a manner dependent on the ability of SIRT2 to be phosphorylated at serine-368. Interestingly, we observe that both SIRT2 wild-type and S368A are fully functional as deacetylases. Therefore, the lack of regulation of cellular proliferation by SIRT2 S368A could be through its inability to properly interact within multiprotein complexes or recognize and function properly on a specific mitotic regulated substrate.

Finally, we observe that as for other Cdk1 targets, SIRT2 can be targeted for dephosphorylation by the phosphatases CDC14A and CDC14B. However, our data is not completely consistent with previously published results in which coexpression of SIRT2 with CDC14B but not CDC14A results in degradation of SIRT2 via trafficking through the 26S proteasomal degradation pathway (90). Due to the complete loss of protein in their experiments, Dryden et al were unable to determine if SIRT2 is in fact dephosphorylated by CDC14B. Here we demonstrate that SIRT2 can be

dephosphorylated by both CDC14A and CDC14B, and furthermore SIRT2 was not degraded when coexpressed with CDC14B.

Here we demonstrate that SIRT2 is phosphorylated by a mitotic kinase, however we do not know what role this phosphorylation has in regulating SIRT2 function. It is possible that, although not detected in an *in vitro* deacetylase activity assay, that phosphorylation of SIRT2 by Cdk1 could regulate SIRT2 enzymatic activity. We know that neither the SIRT2 S368A mutant that cannot be phosphorylated, nor serine-368 mutated to a glutamic acid (S368E), which potentially mimics phosphorylation, does not affect SIRT2 enzymatic activity at a considerable level either *in vitro* on a histone peptide substrate or *in vivo* on α -tubulin (data not shown). However, it is unclear if S368E does in fact mimic a phosphorylated serine residue in this context. In either case, serine-368, and potentially its regulation by phosphorylation is integral in the ability of SIRT2 to regulate cellular proliferation.

Experimental Procedures

Tissue Culture

293T, U-87 MG (HTB-14), U20S and HeLa cells were obtained from American Type Culture Collection (ATCC), grown in Dulbecco's modified Eagle's medium (DMEM, Mediatech, Inc., Herndon, VA) supplemented with 10% fetal bovine serum (Gemini Bioproducts, Woodland, CA) in the presence of penicillin, streptomycin and 2 mM L-Glutamine (Gibco Invitrogen Corp., Carlsbad, CA).

Plasmids and Mutagenesis

Human SIRT2 full length and variant 2, Cdk1 and Cyclin B1 cDNAs were sub-cloned to generate carboxy-terminal FLAG- or HA-tagged fusions in a derivative of the pcDNA3.1(+) backbone with the FLAG or HA peptide sequences, respectively. Wild-type and fragments of human SIRT2 were cloned into pEGFP-C1 vector (Clontech, Mountain View, CA) by standard PCR-based strategies to generate GFP-SIRT2 full length and deletion mutants. Site-directed mutagenesis for SIRT2 constructs were performed with QuickChange Site-Directed Mutagenesis Kit (Stratagene, La Jolla, CA) as recommended by the manufacturer. Cyclin B1 cDNA was cloned into DsRed-C1 (Clontech) to generate RFP-Cyclin B1. Full-length human SIRT2 wild-type and S368A cDNAs were cloned into the pTrcHis vector (Gibco, Invitrogen Corp.) for production of recombinant 6xHis-SIRT2. GFP-CDC14A and CDC14B-GFP were kind gifts from Peter K. Jackson.

Purification of Recombinant SIRT2

DH5 α F'IQ bacteria (Gibco InVitrogen Corp.) were transformed with pTrcHis-SIRT2 and induced with 0.1 mM IPTG (isopropyl- β -D-thiogalactopyranoside) at 37°C for 2 hours. The resulting 6xHis-tagged protein was purified as described previously (188). Recombinant protein was aliquoted and stored at -20°C.

Transient Transfections and Immunoprecipitations

293T cells were transfected either by the calcium phosphate DNA precipitation method or with Fugene 6 transfection reagent (Roche Applied Science, Indianapolis, IN) and lysed 48 hours after transfection in low-stringency lysis buffer (50 mM Tris-HCl, pH 7.5, 0.5 mM EDTA, 0.5% NP-40, 150 mM NaCl) in the presence of protease inhibitor cocktail (Complete, Roche Molecular Biochemicals, Indianapolis, IN). FLAG-tagged proteins were immunoprecipitated with anti-FLAG M2 agarose affinity gel (Sigma, St. Louis, MO), for 2 hours at 4°C from 1 mg of total cell lysate measured by the *Dc* Protein Assay Kit (Bio-Rad, Hercules, California). Immunoprecipitated material was washed 3 times for 15 minutes each in low-stringency lysis buffer, and agarose-immune complexes were resuspended in 1X Laemmli buffer.

Histone Deacetylase Assay

Immunoprecipitated material was washed for an additional 15 minutes in SIRT2 deacetylase buffer (50 mM Tris-HCl, pH 9.0, 4 mM MgCl₂, and 0.2 mM DTT). Immunoprecipitated material was resuspended in 100 μ l of SIRT2 deacetylase buffer containing NAD⁺ (Sigma) and [³H] acetylated histone H4 peptide (amino acids 1–23)

(146). The enzymatic reactions were started by addition of NAD^+ . Reactions were incubated for 2 hours at 37°C and stopped by addition of $25\ \mu\text{l}$ $0.1\ \text{M}$ HCl and $0.16\ \text{M}$ acetic acid. Released acetate was extracted in $500\ \mu\text{l}$ of ethyl acetate, and vortexed for 15 minutes. After centrifugation at $14,000\ \text{rpm}$ for 5 minutes, $400\ \mu\text{l}$ of the ethyl acetate fraction was mixed with 5 ml of scintillation fluid and counted.

Western Blotting

Samples were separated on 10% SDS-PAGE and transferred to Hybond ECL nitrocellulose membrane (Amersham Pharmacia Biotech, Inc.). Membranes were blocked with 5% blocking reagent (Bio-Rad) in TBS-Tween ($10\ \text{mM}$ Tris, pH 7.5, $150\ \text{mM}$ NaCl , 0.1% Tween-20) or in 5% BSA to block membranes prior to incubation with phosphospecific antisera. Subsequently, membranes were probed with anti-HA (H6908, Sigma), anti-FLAG (F7425; Sigma), anti-Actin (C4, ICN Biomedicals, Inc. Irvine, CA), anti-Cyclin B1 (mixed monoclonal, Upstate, Waltham, MA) and anti-Cdk1 (rabbit polyclonal, Upstate) and anti-GFP (Livingcolors monoclonal, Clontech) each diluted 1:5000, anti-phosphoserine, anti-phosphotyrosine, and anti-phosphothreonine (phospho-antibody pack, Zymed, Carlsbad, CA) diluted 1:1000, or anti-SIRT2 (87) diluted 1:500. Secondary detection was performed using horseradish peroxidase-coupled sheep anti-mouse IgG (Amersham Pharmacia Biotech, Inc.), goat anti-rabbit IgG (Pierce Chemical Co., Rockford, IL), or goat anti-chicken IgY (Aves Labs, Inc., Tigard, OR) diluted 1:5000 and ECL western blotting detection system (Amersham Pharmacia Biotech, Inc.).

Immunofluorescence Microscopy

U2OS and HeLa cells grown on coverslips were washed twice in PBS for 10 minutes, fixed in 4% paraformaldehyde (EMS, Ft. Washington, PA) for 10 minutes, followed by permeabilization in 0.5% Triton-X-100 in PBS for 10 minutes. After 3 washes for 10 minutes each in PBS, cells were incubated in 10% BSA for 10 minutes and then incubated for 1 hour with anti-SIRT2 diluted 1:20 and anti-Cyclin B1 (Upstate Biotech) diluted 1:1000 in PBS, 0.1% Tween-20. Cells were washed 3 times 10 minutes in PBS, 0.1% Tween-20, followed by incubation with goat anti-mouse IgG (Fc specific) TRITC-conjugated secondary antiserum (Sigma) and goat anti-chicken IgY FITC-conjugated (Aves Labs, Inc.) both diluted 1:500 in PBS, 0.1% Tween-20. Cells were washed 3 times for 10 minutes each in PBS and once briefly in ddH₂O, and mounted on slides with Gel Mount (Biomedica Corp., Foster City, CA). Confocal images were acquired by laser-scanning confocal microscopy with an Olympus BX60 microscope equipped with a Radiance 2000 confocal setup (Bio-Rad).

Cell Proliferation Measurements

The glioma cell line U-87 MG was transfected with vectors for SIRT2-FLAG wild-type, S368A, and the empty FLAG vector, along with a vector for DsRed (Clontech) at a ratio of 6:1 to mark transfected cells. 24 hours following transfection, cells were washed with PBS, trypsinized to remove cells from the plate, and washed again in PBS twice. Pelleted cells were incubated with 0.1 μ M of CFSE (Molecular Probes, Eugene, OR) at 37°C for 10 minutes. Cells were then washed twice in PBS and either subjected to flow cytometry or plated in culture medium and allowed to grow for 24, 48 or 72 hours. Following

indicated times, cells were harvested by trypsinization and subjected to flow cytometric analysis. Flow cytometry data were compensated and analyzed by FlowJo software.

In vitro Kinase Assays

Reactions were prepared in kinase assay buffer (50 mM Tris-HCl, pH 7.4, 100 mM KCl, 10 mM MgCl₂, 1 mM DTT, 30 μM ATP, with or without 10 μCi of [γ -³²P] ATP) containing 3 μg of rSIRT2 and indicated concentrations of Cdk1-Cyclin B1 (NEB or Upstate Biotechnology). Reactions were carried out at 30°C for 30 minutes, and stopped by addition of 6X Laemmli buffer to a final concentration of 1X.

In vitro Phosphatase Assay

SIRT2-FLAG was immunoprecipitated from transfected 293T cells as described above. Immunoprecipitated material was washed an additional 2 times for 15 minutes each in NEB buffer 3 (New England Biolabs, Beverly, MA). Immunoprecipitated material was resuspended in NEB buffer 3 with or without sodium pyrophosphate and incubated at 37°C for 10 minutes, followed by the addition of indicated amount of calf intestinal phosphates (CIP; NEB) and incubated at 37°C for an additional 30 minutes. Reactions were stopped by addition of 6X Laemmli buffer to bring reaction to a final concentration of 1X and subjected to SDS-PAGE and western blotting as described above.

Pharmacological treatments, cell cycle arrest and Cdk1 Inhibitors

For G1/S and M phase cell cycle arrest experiments, 293T cells were treated for 15 hours with 2 mM thymidine. Following treatment, cells were washed twice in PBS and replaced in fresh growth medium. Cells were then transfected with SIRT2-FLAG or the empty FLAG vector using Fugene 6, and incubated for 8 hours under standard cell culture conditions. Following incubation cells were retreated with either 2 mM thymidine (for G1/S phase block), 1 ng/mL Nocodazole (Sigma) or 10 µg/mL Colchicine (Sigma) (both for M phase block) and incubated for 17 hours. Cells were harvested and subjected to SDS-PAGE and western blotting as described above, or for cell cycle analysis with propidium iodide and flow cytometry.

For treatment of cells with Cdk1 inhibitors, 293T cells were transfected with SIRT2-FLAG using FuGENE 6. 24 hours post transfection, cells were treated with either 10 µg/mL Purvalanol A, 10 mM Alsterpaullone, or 10 mM U0126 (all from Calbiochem, San Diego, CA) for 12 hours, or with a short treatment with 40 µg/mL Purvalanol A for 3 hours. Cells were harvested and subjected to SDS-PAGE and western blotting as described above.

Time Lapse Microscopy

Hela Cells were plated on 40-mm coverslips (Biotechs) and treated for 15 hours with 2 mM thymidine. Following thymidine treatment, cells were washed in PBS and grown in fresh media. Following replacement of fresh media cells were transfected with vectors for GFP-SIRT2 and RFP-Cyclin B1 and grown in standard culture conditions for 8 hours, at which time cells were retreated for 17 hours in 2 mM thymidine. Following second

thymidine treatment, cells were washed twice in PBS and grown for 6 hours in fresh media, at which time cells were placed in a closed culture chamber system (Bioptechs) with CO₂-independent media and subjected to time lapse microscopy with images acquired every minute on a Nikon elipse TE300 microscope controlled by Metamorph software.

Tandem Mass spectrometry

Nanocapillary HPLC ESI MS and MS/MS analysis was performed utilizing an Ultimate 2000 HPLC system equipped with Switchos™ and Famos™ autosampler (Dionex/LC Packings) on-line with a QStar XL, QqTOF hybrid mass spectrometer (Applied Biosystems/MDS Sciex). The QSTAR was operated with a nanoelectrospray ion source (Protana) and PicoTip™ emitters (New Objective, Inc.). Protein digest volumes of 2–3 µL were desalted online using a Nano-Precolumn™ (Dionex/LC Packings; C18, 300Å pore size, 5-µm particle size, 5-mm, 300-µm i.d.) and peptides were separated on a self-packed column (packing material: Phenomenex Jupiter Proteo™; C12 end-capped, 4-µm particle size, 90Å pore size, 15-cm length, 75-µm id). The mobile phase flow rate was 250 nL/min. The column was equilibrated at 2% solvent B for 20 minutes before sample injection (solvent B: 80% acetonitrile/0.08% formic acid; solvent A: 2% acetonitrile/0.1% formic acid). Peptides were separated using a linear gradient of 2–50% solvent B over 20 min, followed by a column cleanup step at 95% solvent B for 5 min. Data was acquired automatically by operating the mass spectrometer in information dependent acquisition (IDA) mode which allowed for a 1-second MS survey scan followed by two 2-second MS/MS scans. Peptides were fragmented by low-energy

collision induced dissociation (CID). Nitrogen was used as the collision gas and the collision energy was automatically adjusted depending on the precursor ion charge state. The mass spectrometer was externally calibrated using product ions of Glu¹-Fibrinopeptide B (Sigma). Data analysis was facilitated by employing BioAnalyst software (Applied Biosystems/MDS Sciex) and Mascot (Matrix Science). Mass accuracy tolerance windows for Mascot searches were set at ± 100 ppm and ± 0.1 Da for precursor and product ions masses, respectively. The MS/MS spectra of phosphorylated peptides and their non-phosphorylated counterparts were manually verified. Selected ion chromatograms of phosphorylated and non-phosphorylated forms of peptides spanning amino acid regions 348–380 and 347–380 of rSIRT2 were generated to interrogate the HPLC MS/MS data for the presence of precursor ions that were not automatically selected for CID.

Rapid progress has been made in the understanding of the enzymatic properties and physiological roles of sirtuin proteins since the demonstration that these factors are protein deacetylases (8, 9). The focus of this thesis is on understanding the cell biology of the human SIRT2 protein. We have identified lysine-40 of α -tubulin as the first substrate for SIRT2 enzymatic activity *in vivo*. Furthermore, using our knowledge of SIRT2 and HDAC6 as α -tubulin deacetylases, we were able to demonstrate that one function of α -tubulin acetylation is to regulate the association of MIZ-1 with the microtubule network. In addition, we have observed that SIRT2 shuttles between the nucleus and the cytoplasm, and have characterized a functional Crm1-dependent NES sequence located in the amino-terminus of SIRT2. During interphase, SIRT2 shuttles constantly between the two compartments, however its rate of nuclear export exceeds its rate of nuclear import, thus giving the perception that SIRT2 is a cytoplasmically localized protein. During entry into mitosis, SIRT2 becomes localized to the nucleus, which occurs prior to nuclear envelope breakdown, suggesting a mitosis dependent regulation of its nucleocytoplasmic shuttling properties. During mitosis, we found that SIRT2 associates with a variety of microtubule based structures, including the centrosome, spindle fibers and midbody. And finally, we have identified that SIRT2 regulates cell cycle progression in a manner dependent on its ability to be phosphorylated by the Cdk1 kinase at serine-368.

Sirtuin Activity

It remains unclear whether all classes of sirtuins have deacetylase activity. For instance, only the class I human sirtuins (SIRT1–3) exhibit robust enzymatic activity when assayed *in vitro* on a peptide corresponding to the amino-terminal tail of histone H4. This is

consistent with the *S. cerevisiae* class I sirtuins Sir2p, Hst1p, and Hst2p, which also show activity toward histones (53, 54, 87). SIRT5, a class III sirtuin, has low but reproducibly detectable activity in comparison to the class I sirtuins (chapter 2 and (87)). Interestingly, the class III sirtuin from *A. fulgidus*, Sir2-Af1, also demonstrates low activity on a histone peptide but significantly stronger activity on an acetylated BSA substrate, suggesting some degree of substrate-specificity for this class (111, 113). Although there is variability in sirtuin deacetylase activity *in vitro*, non-histone substrates may be preferentially targeted *in vivo*. For instance, the Class U sirtuins are only present in gram-positive bacteria, an organism lacking histones (17), where sirtuins have been demonstrated to target propionyl- and acetyl-coenzyme A synthetase and the archaeal chromatin protein Alba for deacetylation (19-21). Likewise, the mammalian sirtuin SIRT3 contains potent activity on a histone peptide but is localized primarily in the mitochondrial matrix, a cellular compartment lacking histone proteins, and is expected to have novel targets within this organelle (66, 67, 97, 98). The list of non-histone substrates and biological implications for all sirtuins will no doubt continue to grow.

Many sirtuins possess ADP-ribosyltransferase activity in addition to deacetylase activity (18, 99, 121, 128). The sirtuin protein from the protozoan parasite *Trypanosoma brucei*, termed TbSIR2RP1, functions *in vivo* both as a deacetylase and as an ADP-ribosyltransferase towards Histones H2A and H2B, and regulates resistance to DNA damage (128). While SIRT2 was initially reported as an ADP-ribosyltransferase, it is likely that this is not its primary activity, but rather secondary to its potent deacetylase activity. However, whether SIRT2 functions as an ADP-ribosyltransferase or deacetylase may be substrate dependent (18). We have observed that SIRT4, 6, and 7 possess no

deacetylase activity on a histone peptide, suggesting they potentially function primarily as ADP-ribosyltransferases. Consistent with this hypothesis, SIRT6 has been shown to possess mono-ADP-ribosyltransferase activity. The catalytic mechanism of this reaction is intra-molecular, with individual molecules of SIRT6 directing their own modification (99). The targets of, and physiological roles, for SIRT6 ADP-ribosyltransferase activity, in addition to other mammalian sirtuins will be a compelling area of research in the future.

SIRT2 is a α -Tubulin Deacetylase

Our initial studies were focused on identification of substrates for SIRT2. We found that SIRT2 functions both *in vitro* and *in vivo* as an α -tubulin deacetylase, targeting lysine-40 (figure 5.1). We have not ruled out the possibility that other sites within α -tubulin might be targeted for reversible acetylation in addition to lysine-40. Evolutionarily, tubulin acetylation is not broadly conserved. For instance, α -tubulin in *S. cerevisiae* does not contain the lysine-40 motif found within mammalian α -tubulin. Furthermore, the yeast SIRT2 equivalent, Hst2p, does not efficiently deacetylate a human α -tubulin peptide corresponding to the amino acids surrounding lysine-40, but prefers a histone substrate, suggesting SIRT2 represents an evolutionarily developed mechanism to control microtubule function.

Although α -tubulin acetylation was identified in the early 1980s, little has been elucidated as to the functional consequences of this modification on microtubule function. Like histones, we can anticipate that regulation of α -tubulin acetylation is mediated by the opposing activities of HDACs and HATs. The lack of knowledge of the

enzymes involved in the regulation of α -tubulin acetylation has made understanding the biological implications of this modification difficult (131, 136, 189-192). Early studies seeking to identify a α -tubulin acetyltransferase found such an activity in a protein mixture from *Chlamydomonas*, and a 67 kDa protein was isolated and suspected to be responsible for this observed activity (190-192). Since then, no further characterization of the purified α -tubulin acetyltransferase has been carried out.

Studies in *Chlamydomonas reinhardtii* and *Tetrahymena*, in which α -tubulin is acetylated within a motif homologous to mammalian lysine-40, were carried out to elucidate a function for this modification. In the first study, no overt phenotype was observed in *Chlamydomonas* upon overexpression of α -tubulin containing a nonacetylatable residue in place of lysine-40 (193). However, the authors were only able to obtain 50–70% replacement of wild-type α -tubulin with the overexpressed mutant protein, and it is unclear what percentage of acetylatable α -tubulin incorporation into microtubules is sufficient to mediate proper function. In the second study, the α -tubulin gene was replaced in *Tetrahymena* with a mutant gene containing a K40R substitution. In this system, complete absence of α -tubulin acetylation did not compromise microtubule function (194). These studies found that, at least in these single celled organisms, α -tubulin acetylation was dispensable for normal microtubule function. Consequently, interest waned in the microtubule field for understanding the significance of α -tubulin acetylation.

Although little is known with regard to the mechanism(s) leading to, and functional consequences of, α -tubulin acetylation, this modification has consistently been utilized in the literature as a marker for stable microtubules. The potential correlation

between stability of microtubules and α -tubulin acetylation is primarily based on the fact that stable microtubule structures, such as those found in flagella and cilia, are hyperacetylated (136). However, no solid relationship has been established between α -tubulin acetylation and microtubule stability (195). In fact, functional significance of α -tubulin acetylation on microtubule stability was found to be minimal (192, 196). It is generally accepted that stable microtubules are hyperacetylated because the tubulin acetyltransferase prefers polymerized α -tubulin over α -tubulin dimers as a substrate (130, 192). With the identification of HDAC6 as a tubulin deacetylase, a role for microtubule acetylation in potentiating microtubule stability was again suggested (140, 141). However, these conclusions were challenged by a report published shortly thereafter (197), and the current model is again consistent with earlier studies demonstrating that acetylation is a consequence, not a direct cause, of microtubule stability (194, 198, 199). Further studies on the subtle affects of acetylation on microtubule function will no doubt again raise questions on the effect of α -tubulin acetylation on microtubule stability.

Two α -Tubulin Deacetylases in One Complex

The demonstration that HDAC6 is localized along the microtubule network, and is involved in the regulation of α -tubulin acetylation, has provided an explanation for the fact that α -tubulin becomes hyperacetylated in response to Trichostatin A (140-142). We found that SIRT2 also regulates α -tubulin acetylation, by directly deacetylating lysine-40 both *in vitro* and *in vivo*. Interestingly, endogenous SIRT2 and HDAC6 colocalize along the microtubule network, and both proteins interact in coimmunoprecipitation

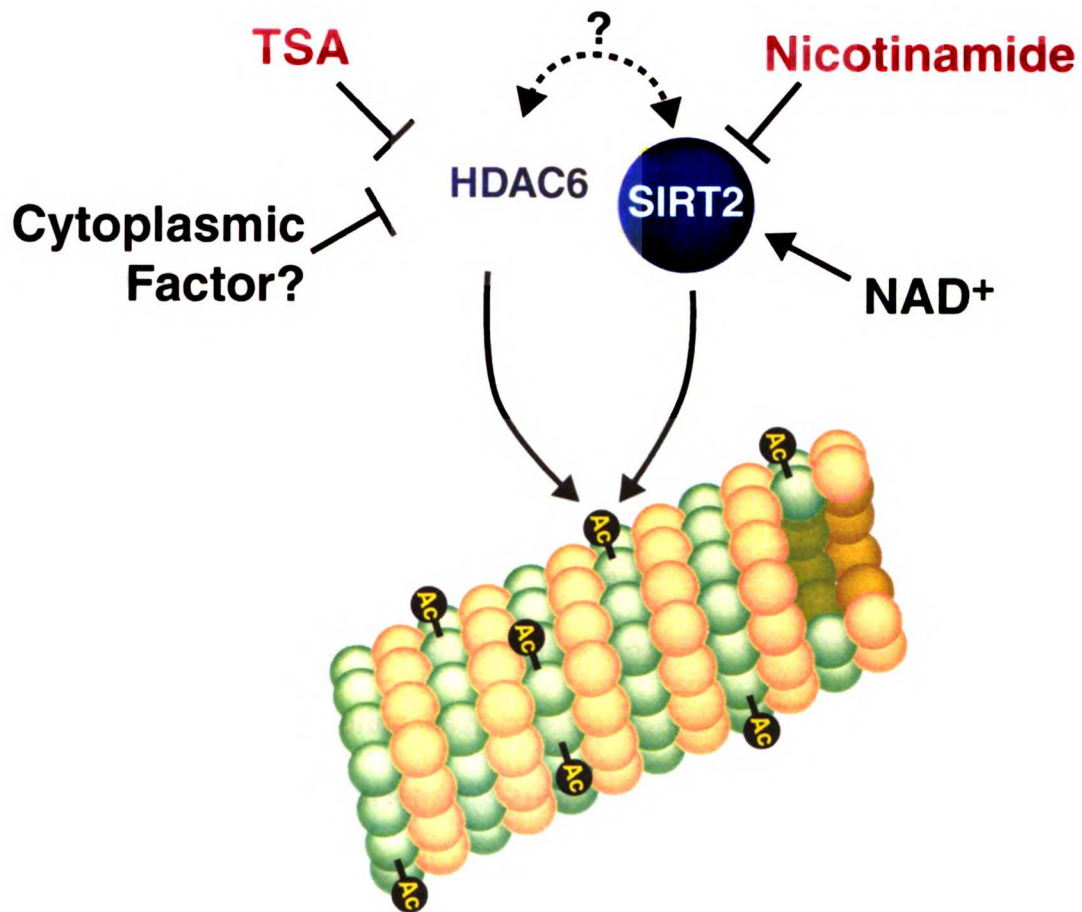


Figure 5.1. Schematic diagram of α -tubulin deacetylation by HDAC6 and SIRT2. Both HDAC6 and SIRT2 are found in a common multimeric complex, but are capable of α -tubulin deacetylation independently of one another. Enzymatic activity of both proteins is inhibited by distinct small molecules.

experiments (figure 5.1). Interaction between HDAC6 and SIRT2 is not dependent on the presence of microtubules, as coimmunoprecipitated material was devoid of α -tubulin. These results were further confirmed by colocalization studies of SIRT2 and HDAC6 and with tubulin. We found that SIRT2 and HDAC6 colocalize together to a greater extent than each protein individually colocalizes with tubulin. These observations are consistent with the model that both proteins are part of a single multiprotein complex. However, HDAC6 and SIRT2 might differ in their microtubule structural specificities or mechanisms of regulation. Both enzymes deacetylate tubulin heterodimers and microtubules composed of purified tubulin with similar efficiencies. In contrast, SIRT2 deacetylates tubulin (dimers or microtubules) assembled from cell lysates to a greater extent than HDAC6. This observation might indicate the presence of a selective HDAC6 inhibitor in cellular lysate microtubules. It will be important to establish in future experiments the relative role of each protein in α -tubulin deacetylation, the nature of the multiprotein complex harboring both proteins, the physiological role of the NAD⁺-dependency of SIRT2 on microtubule biology and, as discussed above, the possible regulation of HDAC6 activity by cytoplasmic proteins. However, it should be noted that inhibition of each protein alone, either via siRNA or via selective inhibitors, is sufficient to induce a global hyperacetylation of α -tubulin. This observation suggests that both proteins function autonomously in tubulin deacetylation despite their ability to interact.

The observation that members of two different classes of HDAC enzymes interact and target a common substrate has been observed for many other acetylated substrates (87, 140-142). In yeast, the Set3 complex was demonstrated to contain both NAD⁺-dependent and independent deacetylase enzymes (Hst1 and Hos2), however the

significance of the presence of both of these enzymes within a single complex remains to be determined (138). The transcription factors p53 and NF- κ B, histone proteins, and Ku70 are also targeted for deacetylation by two distinct classes of HDAC enzymes (69-72, 77, 123, 200-202). The biological relevance of having two distinct HDAC enzymes carry out deacetylation of an identical residue remains elusive. It is tempting to speculate that the two enzymes are differentially regulated resulting in physiological situations where one predominates over the other. In addition, tissue distribution of the various enzymes may contribute to the preferential use of one enzyme over the other. Given the NAD⁺-dependence of the class III HDACs, it is reasonable to speculate that these enzymes may regulate substrate deacetylation depending on the metabolic state of the cell.

Acetylation-dependent Association of Factors with the Microtubule Network

Our studies and those of others have highlighted a potential role of α -tubulin acetylation in regulating interaction between microtubule-associated proteins and microtubules. The transcription factor MIZ-1 binds to microtubules and microtubule stabilization results in sequestration of MIZ-1 in the cytoplasm (143). Furthermore, release of MIZ-1 from the microtubule and subsequent import of MIZ-1 into the nucleus is observed upon drug-induced microtubule depolymerization, resulting in an increase in MIZ-1-dependent gene transcription. We found a decrease in α -tubulin acetylation following treatment with microtubule depolymerizing agents. However, drug-induced microtubule depolymerization is equally efficient both in the presence or absence of Trichostatin A, an inducer of α -tubulin acetylation (data not shown). These results suggest that α -tubulin

deacetylation is coupled to, but not required for, microtubule depolymerization. Using SIRT2 to deacetylated α -tubulin, we observed that MIZ-1 binds to microtubules in an acetylation-dependent manner, suggesting a role for reversible α -tubulin acetylation in controlling MIZ-1 function by interaction with microtubules and sequestration in the cytoplasm. Consistent with the role for α -tubulin acetylation in regulating protein: microtubule interaction, HDAC6 overexpression, resulting in reduced α -tubulin acetylation levels, was shown to disrupt the localization of p58, a protein that mediates binding of golgi elements to microtubules (203). These findings indicate a potential role for acetylation of α -tubulin in controlling the binding of factors to the microtubule network. Such regulation could allow for proteins to be associated to microtubules in an acetylation-dependant manner versus regulation strictly by microtubule polymerization status, which is under the influence of dynamic instability and is not likely to be capable of fine tuned regulation. Therefore it is tempting to speculate that an alternative mechanism to sequester proteins in the cytoplasm might be mediated by interaction with microtubules in addition to other characterized methods such as 14-3-3 binding. In support of this model, a number of additional proteins are maintained in the cytoplasm by interaction with the microtubule network, such as PREP2, Runx2, and p/CIP (204-206). However the mechanisms inducing the binding and/or release of these proteins have not been elucidated. One could speculate that acetylation of α -tubulin could regulate these interactions, like it does with MIZ-1 and p58. Regulation of microtubule interaction via posttranslational modifications of tubulin, including acetylation, could provide the cell a versatile tool to regulate the binding of factors to the microtubule network.

A Tubulin Code for Microtubule Posttranslational Modifications?

Like tubulin, histones are modified by a variety of posttranslational modifications. These include acetylation, phosphorylation, methylation, ubiquitination, and ADP-ribosylation. Histone modifications are precisely coordinated during transcriptional silencing, transcriptional activation, and DNA replication. The “histone code hypothesis” proposes that these modifications are precisely codified to mediate specific biological responses and are recognized by specific reading proteins that translate the code (207-210). Tubulin is also subject to a number of posttranslational modifications, and we propose that a tubulin code mediated by specific tubulin posttranslational modifications might also exist. Therefore, acetylation in coordination with other posttranslational modifications of tubulin could play a significant role in the regulation of protein binding to the microtubule network resulting in effects on the regulation of cell shape, intracellular transport, cell motility, and cell division.

SIRT2 is Exported from the Nucleus

In addition to the characterization of α -tubulin deacetylation within the cytoplasm by SIRT2, we find the localization of SIRT2 in the cytoplasm is dependent on the integrity of an NES sequence within SIRT2. We have identified a Rev-like Crm1-dependent NES sequence between amino acids 41–51. SIRT2 is rapidly shuttling between the nucleus and the cytoplasm, but the rate of export exceeds the rate of import, thus a constitutively cytoplasmic appearance is observed. However, how SIRT2 enters into the nucleus and its function in this compartment remains to be elucidated. Although the relative ability of SIRT2 to deacetylate a histone peptide is less than an α -tubulin peptide, SIRT2 remains

an effective histone deacetylase (87, 90, 133). It is therefore reasonable to speculate that SIRT2 also plays a role in histone deacetylation in addition to potentially other nuclear proteins that are modified by acetylation.

We observed that SIRT2 accumulates in the nucleus as cells transition from G2 into mitosis. The mechanism regulating the steady-state levels of SIRT2 in the nucleus and cytoplasm remains unclear. Cyclin B1 behaves similar to SIRT2 in that it shuttles between the nucleus and cytoplasm during interphase and accumulates in the nucleus prior to nuclear envelope breakdown. Cyclin B1 binds to and is required for activation of the mitotic kinase Cdk1. One of the many functions of the Cdk1-Cyclin B1 complex during mitotic entry is to phosphorylate the nuclear lamin proteins, a step that is necessary, but not sufficient, for lamin matrix disassembly and subsequent breakdown of the nuclear envelope (211-214). It is believed that Cyclin B1 is phosphorylated by the Polo-like kinase 1 (Plk1) near its NES prior to nuclear envelope breakdown. This phosphorylation leads to downregulation of NES function and subsequent nuclear accumulation of the Cdk1-Cyclin B1 complex (215). Although we have tested the ability of a number of kinases, including Plk1, to induce nuclear accumulation of SIRT2, we were unable to determine if phosphorylation, or expression of a kinase, regulated SIRT2 nuclear import.

It is not clear why SIRT2 translocates into the nucleus prior to nuclear envelope breakdown. It is widely appreciated that regulated nuclear translocation of signaling proteins increases the speed and specificity of signal transduction pathways, creating a switch-like response (216). A switch-like, all or nothing response, regulates the onset of mitosis, where mitotic entry is coupled with translocation of both Cdk1-Cyclin B1 and its

activator, CDC25C into the nucleus (216, 217). Similarly, we can speculate that SIRT2 has a functional target within the nucleus upon which deacetylation is coupled to processes influencing the switch-like onset of mitosis. Identifying the mechanism leading to SIRT2 nuclear accumulation as well as mitotic specific SIRT2 targets will lead to further understanding of the reason behind the unique localization pattern of SIRT2 during mitosis.

Mitotic Localization of SIRT2

During mitosis, SIRT2 is localized at the centrosome, the metaphase spindle fibers, and the midbody during cytokinesis. It is intriguing that these sites all contain relatively hyperacetylated α -tubulin. Why a α -tubulin deacetylase is enriched at sites of α -tubulin hyperacetylation remains puzzling. One could speculate that SIRT2 enzymatic activity is regulated, and that these microtubule structures require a tight regulation of α -tubulin acetylation to faithfully segregate the genomic DNA and carry out cytokinesis during mitosis. In support of this hypothesis, we find that overexpression of either a wild-type or catalytically inactive SIRT2 leads to a multinucleation phenotype, suggesting a role for both active and inactive SIRT2 in mediating the faithful completion of mitosis. Further studies should focus on determining the possible spatial and temporal regulation of SIRT2 enzymatic activity during both interphase and mitosis.

The presence of SIRT2 on these mitotic structures raises intriguing questions regarding potential regulation of α -tubulin or other mitotic regulatory proteins by acetylation. We have been unable to determine if alteration in α -tubulin acetylation on lysine-40 can modify mitotic progression. Indeed, overexpression of a mutant α -tubulin

that cannot be acetylated (K40A) does not have a significant consequence on cell cycle progression (data not shown). However, given the high expression level of endogenous tubulin, it is hard to determine what percentage of the exogenously expressed mutant α -tubulin is being incorporated into the polymerized microtubules, and furthermore what level of reduction in α -tubulin acetylation would be sufficient to uncover a functional relevance to this modification. In addition, it is likely that SIRT2 has a number of additional acetylated substrates that may be uniquely targeted during mitosis. Identification of novel substrates of SIRT2 would therefore be of considerable interest in further determining the function of SIRT2 during the cell cycle.

Regulation of SIRT2 Function by Phosphorylation

Much of the focus on mammalian sirtuins has been on the identification of substrates for deacetylation, and mechanisms regulating sirtuin activity have remained elusive. Our results on SIRT2 are shedding light on the role of posttranslational modifications in regulating sirtuin activity. SIRT2 is phosphorylated in a mitotic-specific manner (98). We find Cdk1 targets SIRT2 for phosphorylation both *in vitro* and *in vivo*, indicating that SIRT2 is a potential effector molecule of Cdk1 in the control of mitotic progression (figure 5.2). SIRT2 activity was reported to control mitotic exit (98). Furthermore, SIRT2 is absent in a high percentage of glioma cell lines, suggesting that it plays a role in controlling glioma tumorigenesis (89). Adding SIRT2 back to these cells reduces their proliferation rate, indicating that SIRT2 may function as a tumor suppressor. However, it is unclear if regulation of glioma proliferation by SIRT2 is through regulation of mitotic exit or an unrelated stage in the cell cycle.

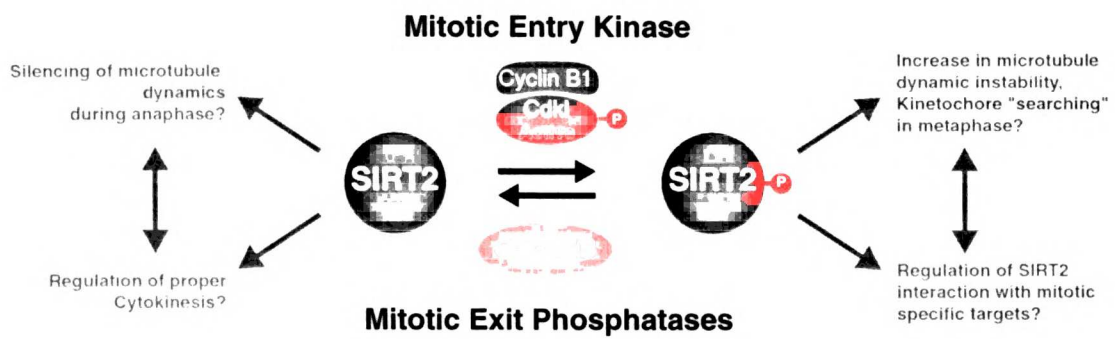


Figure 5.2. Regulation of SIRT2 by phosphorylation. SIRT2 phosphorylation is mediated by opposing activities of the Cdk1 kinase and the CDC14 family of phosphatases.

How does phosphorylation affect SIRT2 function? The solved structures of Sir2-Af1, Sir2-Af2, and SIRT2 correspond primarily to the catalytic domain found within Sir2-like proteins. Sirtuins in yeast and higher eukaryotes have large amino- and carboxy-terminal extensions that are likely to regulate their enzymatic activity. In support of this model, studies have indicated that different modes of silencing are affected by various mutations outside the catalytic core (114). In addition, the structure of full-length yeast Hst2p indicates that the amino-terminal extension folds into the NAD⁺ binding pocket and that the carboxy-terminal extension may occlude the substrate binding cleft (114). The carboxy-terminal α 14 helix of yHst2p makes extensive interactions with residues within the large groove of the catalytic domain. It is proposed that apo-yHst2p exists in an auto-inhibited form in which the α 14 helix partially occludes the NAD⁺-binding site and the loop following β 1 is disordered (figure 1.3). NAD⁺ binding then promotes dissociation of the α 14 helix and ordering of the loop following β 1 to increase enzymatic activity (114). SIRT3, a human Hst2p homologue like SIRT2, is enzymatically inactive as a full-length protein and becomes catalytically active after proteolytic cleavage of its amino-terminus following import into the mitochondrial matrix (98). Of interest is the observation that SIRT3 might also be targeted to the nucleus, suggesting that either nuclear specific protease activity or posttranslational modifications might be involved in SIRT3 activation in the nucleus.

Although phosphorylation of SIRT2 by Cdk1 does not appear to regulate its enzymatic activity *in vitro* or *in vivo*, the amino acid modified by Cdk1 (serine-368) is required for the ability of SIRT2 to regulate cellular proliferation of glioma cells. Phosphorylation of SIRT2 may control its activity by regulating specific protein:protein

interactions, or may regulate its enzymatic activity on an unidentified substrate *in vivo*. Indeed, the peptide substrates used to assay for SIRT2 enzymatic activity might allow for promiscuous interactions that do not fully recapitulate the *in vivo* situation. In addition, phosphorylation might regulate the association of SIRT2 with an inhibitory protein. Our *in vivo* α -tubulin deacetylation studies in which substituting S368A or S368E has no effect on enzymatic activity might be a result of insufficient levels SIRT2-associated proteins that are integral in the regulation of SIRT2 activity.

A master regulator switch surrounding activation of the Cdk1 kinase controls mitotic entry at the G2 to M transition. Cdk1 activity regulates several cellular events associated with entrance into mitosis. These include, centrosome separation, golgi fragmentation, chromosome condensation, nuclear envelope breakdown, and spindle assembly (176). Our results suggest that regulation of SIRT2 by Cdk1-mediated phosphorylation might function to regulate any of these events. First, Cdk1 is active on the centrosome, where both SIRT2 and Cdk1 are localized during centrosome separation. Second, entering into the nucleus prior to nuclear envelope breakdown, SIRT2 and Cdk1-Cyclin B1 may together regulate proteins functioning in nuclear disassembly. Third, both proteins are found on the mitotic spindle, and potentially Cdk1 is regulating SIRT2 function towards α -tubulin acetylation on the spindle fiber. Interestingly, we have not observed any significant alterations in centrosome separation or spindle fiber assembly/function following overexpression or knockdown of SIRT2. However, redundancy with HDAC6, or lack of checkpoint control in tumor cells, might mask any effects on regulation of these processes. Our data suggest, but do not demonstrate, that phosphorylation of SIRT2 by Cdk1 functions to reduce proliferation rather than promote

mitotic progression. Although SIRT2 delays the rate of mitotic exit, we cannot exclude the possibility that expressing SIRT2 from an exogenous promoter might be forcing SIRT2 expression at stages of the cell cycle where it is normally not expressed. Aberrant expression of SIRT2 may negatively regulate cellular proliferation independent of any specific function during mitosis.

SIRT2 expression is increased during late G2, and the protein is reportedly degraded following mitosis in a CDC14B-dependent mechanism (218). However, our data have not been consistent with these observations. In contrast, we observe that SIRT2 is dephosphorylated by both CDC14A and CDC14B. However, cell-type specificity could account for these different observations since previous results were generated in an osteosarcoma cell line, while our studies were performed in an embryonic kidney cell line. The nucleolar targeted CDC14B protein was shown to regulate microtubule dynamics. When mutated to promote its relocalization from the nucleoli to the cytoplasm, CDC14B drove the formation of bundled microtubules (218). CDC14B is released from the nucleoli during mitosis, and this relocalization may allow CDC14B to carry out its function on microtubule bundling. During telophase and cytokinesis, microtubules form into a highly stable bundled structure known as the midbody. We speculate that, CDC14A or CDC14B regulation of SIRT2 may influence the formation of these bundles, or alter microtubule dynamics (figure 5.2). However, cells lacking SIRT2, or expressing SIRT2 mutants, have not shown any significant changes in microtubule structure during mitosis. This fact suggests that SIRT2 may be dispensable for regulating microtubule dynamics, or compensation by HDAC6 occurs in the absence of functional SIRT2. Determining the significance of the SIRT2 phosphorylation cycle in regulating mitotic

progression is of considerable interest to understand its role in regulating cellular proliferation.

Microtubules undergo dynamic instability during metaphase to promote the capture of kinetochores (219). Although the spindle fiber architecture is maintained during metaphase to allow for the occupancy of all kinetochores by microtubules, microtubules destined to bind to kinetochores are characterized by dynamic instability. This property facilitates active “searching” for kinetochores. Once complete occupancy of all kinetochores is achieved, a considerable alteration in microtubule dynamics takes place to facilitate the physical separation and segregation of chromosomes to the opposing spindle poles (219, 220). In yeast, the transition into anaphase is associated with a silencing of microtubule dynamic instability observed during metaphase, and is dependent on the phosphatase Cdc14p (220). The transition from metaphase into anaphase in mammalian cells might therefore involve regulation of tubulin modifying proteins, such as SIRT2, by mitotic exit regulators such as the human CDC14 proteins, to regulate the stability of microtubules (figure 5.2).

SIRT2, Aging and Human Disease

Sir2 proteins are involved in regulation of longevity in a wide variety of organisms (221). Hst2p, a yeast homologue of SIRT2 and SIRT3, can regulate yeast longevity in a *sir2* deletion strain by regulating *rDNA* stability (55). Like SIRT2, Hst2p is predominantly localized in the cytoplasm (54). The observation that Hst2p regulates nucleolar processes governing aging suggest that it might be targeted to the nucleus, and shuttle between the cytoplasm and nucleus similar to SIRT2. Understanding the role of nuclear SIRT2 during

interphase could reveal additional roles of SIRT2 in the nucleus, potentially connecting SIRT2 to the role of the yeast Sir2 proteins in regulating the aging process.

Here, we have characterized the human SIRT2 protein to be a α -tubulin deacetylase and regulated both by localization and posttranslational modification during the cell cycle. SIRT2 may be a tumor suppressor gene, and its function may be involved in the regulation of the rate of cell cycle progression. SIRT2 knockout-mice have no overt phenotype suggesting that SIRT2 is dispensable during development; however, there may be an age-associated phenotype (such as abnormal tumorigenesis) that has not been explored yet. The presence of two α -tubulin deacetylases, SIRT2 and HDAC6, suggests that there may be redundancy in the regulation of α -tubulin acetylation levels. However given that SIRT2 activity is sensitive to metabolism through the cofactor NAD^+ , significant phenotypes may be uncovered that are SIRT2-dependent as an organism ages and their metabolism adjusts, or in metabolically derived diseases. However, the intriguing finding that SIRT2 is a novel substrate for Cdk1, and that this phosphorylation of SIRT2 is necessary for SIRT2-mediated delay in cell cycle progression, suggests a potential role for SIRT2 in suppressing tumorigenesis. With the recent interest in identification of sirtuin activators, these results suggest that identification and utilization of activators that specifically target SIRT2 could be promising for cancer therapy.

References

1. Parekh RB, Rohlff C. (1997) Post-translational modification of proteins and the discovery of new medicine. *Curr Opin Biotechnol* 8:718-23.
2. Plevoda B, Sherman F. (2002) The diversity of acetylated proteins. *Genome Biol* 3:
3. Rice JC, Allis CD. (2001) Histone methylation versus histone acetylation: new insights into epigenetic regulation. *Curr Opin Cell Biol* 13:263-73.
4. Kuo MH, Allis CD. (1998) Roles of histone acetyltransferases and deacetylases in gene regulation. *Bioessays* 20:615-626.
5. Kouzarides T. (2000) Acetylation: a regulatory modification to rival phosphorylation? *Embo J* 19:1176-9.
6. de Ruijter AJ, van Gennip AH, Caron HN, Kemp S, van Kuilenburg AB. (2003) Histone deacetylases (HDACs): characterization of the classical HDAC family. *Biochem J* 370:737-49.
7. Verdin E, Dequiedt F, Kasler HG. (2003) Class II histone deacetylases: versatile regulators. *Trends Genet* 19:286-93.
8. Blander G, Guarente L. (2004) The Sir2 family of protein deacetylases. *Annu Rev Biochem* 73:417-35.
9. North BJ, Verdin E. (2004) Sirtuins: Sir2-related NAD-dependent protein deacetylases. *Genome Biol* 5:224.
10. Rine J, Strathern JN, Hicks JB, Herskowitz I. (1979) A suppressor of mating-type locus mutations in *Saccharomyces cerevisiae*: evidence for and identification of cryptic mating-type loci. *Genetics* 93:877-901.

11. Ivy JM, Hicks JB, Klar AJ. (1985) Map positions of yeast genes SIR1, SIR3 and SIR4. *Genetics* 111:735-44.
12. Ivy JM, Klar AJ, Hicks JB. (1986) Cloning and characterization of four SIR genes of *Saccharomyces cerevisiae*. *Mol Cell Biol* 6:688-702.
13. Rine J, Herskowitz I. (1987) Four genes responsible for a position effect on expression from HML and HMR in *Saccharomyces cerevisiae*. *Genetics* 116:9-22.
14. Landry J, Sutton A, Tafrov ST, Heller RC, Stebbins J, Pillus L, Sternglanz R. (2000) The silencing protein SIR2 and its homologs are NAD-dependent protein deacetylases. *Proc. Natl. Acad. Sci. USA* 97:5807-5811.
15. Smith JS, Brachmann CB, Celic I, Kenna MA, Muhammad S, Starai VJ, Avalos JL, Escalante-Semerena JC, Grubmeyer C, Wolberger C, Boeke JD. (2000) A phylogenetically conserved NAD⁺-dependent protein deacetylase activity in the Sir2 protein family. *Proc. Natl. Acad. Sci. USA* 97:6658-6663.
16. Imai S, Armstrong CM, Kaeberlein M, Guarente L. (2000) Transcriptional silencing and longevity protein Sir2 is an NAD-dependent histone deacetylase. *Nature* 403:795-800.
17. Frye RA. (2000) Phylogenetic classification of prokaryotic and eukaryotic Sir2-like proteins. *Biochem. Biophys. Res. Commun.* 273:793-798.
18. Frye RA. (1999) Characterization of five human cDNAs with homology to the yeast SIR2 gene: Sir2-like proteins (sirtuins) metabolize NAD and may have protein ADP-ribosyltransferase activity. *Biochem. Biophys. Res. Commun.* 260:273-279.

19. Starai VJ, Celic I, Cole RN, Boeke JD, Escalante-Semerena JC. (2002) Sir2-dependent activation of acetyl-CoA synthetase by deacetylation of active lysine. *Science* 298:2390-2.
20. Horswill AR, Escalante-Semerena JC. (2002) Characterization of the propionyl-CoA synthetase (PrpE) enzyme of *Salmonella enterica*: residue Lys592 is required for propionyl-AMP synthesis. *Biochemistry* 41:2379-87.
21. Bell SD, Botting CH, Wardleworth BN, Jackson SP, White MF. (2002) The interaction of Alba, a conserved archaeal chromatin protein, with Sir2 and its regulation by acetylation. *Science* 296:148-51.
22. Kupiec M, Byers B, Esposito RE, Mitchell AP. (1997) Meiosis and sporulation in *Saccharomyces cerevisiae*. In *The Molecular and cellular biology of the yeast Saccharomyces: Cell cycle and cell biology*. (Pringle JR, Broach JR, Jones EW, eds.) pp. 889-1036, Cold Spring Harbor Laboratory Press., Cold Spring Harbor, N.Y.
23. Boscheron C, Maillet L, Marcand S, Tsai-Pflugfelder M, Gasser SM, Gilson E. (1996) Cooperation at a distance between silencers and proto-silencers at the yeast HML locus. *Embo J* 15:2184-95.
24. Triolo T, Sternglanz R. (1996) Role of interactions between the origin recognition complex and SIR1 in transcriptional silencing. *Nature* 381:251-3.
25. Moretti P, Freeman K, Coodly L, Shore D. (1994) Evidence that a complex of SIR proteins interacts with the silencer and telomere-binding protein RAP1. *Genes Dev.* 8:2257-2269.

26. Gottschling DE, Aparicio OM, Billington BL, Zakian VA. (1990) Position effect at *S. cerevisiae* telomeres: reversible repression of Pol II transcription. *Cell* 63:751-62.
27. Bryan TM, Cech TR. (1999) Telomerase and the maintenance of chromosome ends. *Curr Opin Cell Biol* 11:318-24.
28. McEachern MJ, Krauskopf A, Blackburn EH. (2000) Telomeres and their control. *Annu Rev Genet* 34:331-358.
29. Wright JH, Gottschling DE, Zakian VA. (1992) *Saccharomyces* telomeres assume a non-nucleosomal chromatin structure. *Genes Dev* 6:197-210.
30. Bourns BD, Alexander MK, Smith AM, Zakian VA. (1998) Sir proteins, Rif proteins, and Cdc13p bind *Saccharomyces* telomeres in vivo. *Mol Cell Biol* 18:5600-8.
31. Liu C, Lustig AJ. (1996) Genetic analysis of Rap1p/Sir3p interactions in telomeric and HML silencing in *Saccharomyces cerevisiae*. *Genetics* 143:81-93.
32. Cockell M, Palladino F, Laroche T, Kyriou G, Liu C, Lustig AJ, Gasser SM. (1995) The carboxy termini of Sir4 and Rap1 affect Sir3 localization: evidence for a multicomponent complex required for yeast telomeric silencing. *J Cell Biol* 129:909-24.
33. Rusche LN, Kirchmaier AL, Rine J. (2002) Ordered nucleation and spreading of silenced chromatin in *Saccharomyces cerevisiae*. *Mol Biol Cell* 13:2207-22.
34. Hecht A, Laroche T, Strahl-Bolsinger S, Gasser SM, Grunstein M. (1995) Histone H3 and H4 N-termini interact with SIR3 and SIR4 proteins: a molecular model for the formation of heterochromatin in yeast. *Cell* 80:583-592.

35. Braunstein M, Sobel RE, Allis CD, Turner BM, Broach JR. (1996) Efficient transcriptional silencing in *Saccharomyces cerevisiae* requires a heterochromatin histone acetylation pattern. *Mol Cell Biol* 16:4349-56.
36. Braunstein M, Rose AB, Holmes SG, Allis CD, Broach JR. (1993) Transcriptional silencing in yeast is associated with reduced nucleosome acetylation. *Genes Dev* 7:592-604.
37. Hoppe GJ, Tanny JC, Rudner AD, Gerber SA, Danaie S, Gygi SP, Moazed D. (2002) Steps in assembly of silent chromatin in yeast: Sir3-independent binding of a Sir2/Sir4 complex to silencers and role for Sir2-dependent deacetylation. *Mol Cell Biol* 22:4167-80.
38. Moazed D, Rudner AD, Huang J, Hoppe GJ, Tanny JC. (2004) A model for step-wise assembly of heterochromatin in yeast. *Novartis Found Symp* 259:48-56; discussion 56-62, 163-9.
39. Rusche LN, Kirchmaier AL, Rine J. (2003) The establishment, inheritance, and function of silenced chromatin in *Saccharomyces cerevisiae*. *Annu Rev Biochem* 72:481-516.
40. Loo S, Rine J. (1994) Silencers and domains of generalized repression. *Science* 264:1768-71.
41. Bi X, Broach JR. (1997) DNA in transcriptionally silent chromatin assumes a distinct topology that is sensitive to cell cycle progression. *Mol Cell Biol* 17:7077-87.

42. Bryk M, Banerjee M, Murphy M, Knudsen KE, Garfinkel DJ, Curcio MJ. (1997) Transcriptional silencing of Ty1 elements in the RDN1 locus of yeast. *Genes Dev* 11:255-69.
43. Smith JS, Boeke JD. (1997) An unusual form of transcriptional silencing in yeast ribosomal DNA. *Genes Dev.* 11:241-254.
44. Fritze CE, Verschueren K, Strich R, Easton Esposito R. (1997) Direct evidence for SIR2 modulation of chromatin structure in yeast rDNA. *Embo J* 16:6495-509.
45. Gottlieb S, Esposito RE. (1989) A new role for a yeast transcriptional silencer gene, SIR2, in regulation of recombination in ribosomal DNA. *Cell* 56:771-6.
46. Straight AF, Shou W, Dowd GJ, Turck CW, Deshaies RJ, Johnson AD, Moazed D. (1999) Net1, a Sir2-associated nucleolar protein required for rDNA silencing and nucleolar integrity. *Cell* 97:245-56.
47. Shou W, Seol JH, Shevchenko A, Baskerville C, Moazed D, Chen ZW, Jang J, Charbonneau H, Deshaies RJ. (1999) Exit from mitosis is triggered by Tem1-dependent release of the protein phosphatase Cdc14 from nucleolar RENT complex. *Cell* 97:233-44.
48. Brachmann CB, Sherman JM, Devine SE, Cameron EE, Pillus L, Boeke JD. (1995) The SIR2 gene family, conserved from bacteria to humans, functions in silencing, cell cycle progression, and chromosome stability. *Genes Dev.* 9:2888-2902.
49. Martin SG, Laroche T, Suka N, Grunstein M, Gasser SM. (1999) Relocalization of telomeric Ku and SIR proteins in response to DNA strand breaks in yeast. *Cell* 97:621-633.

50. Mills KD, Sinclair DA, Guarente L. (1999) MEC1-dependent redistribution of the Sir3 silencing protein from telomeres to DNA double-strand breaks. *Cell* 97:609-620.
51. Laroche T, Martin SG, Gotta M, Gorham HC, Pryde FE, Louis EJ, Gasser SM. (1998) Mutation of yeast Ku genes disrupts the subnuclear organization of telomeres. *Curr Biol* 8:653-6.
52. Gravel S, Larrivee M, Labrecque P, Wellinger RJ. (1998) Yeast Ku as a regulator of chromosomal DNA end structure. *Science* 280:741-4.
53. Bedalov A, Hirao M, Posakony J, Nelson M, Simon JA. (2003) NAD⁺-dependent deacetylase Hst1p controls biosynthesis and cellular NAD⁺ levels in *Saccharomyces cerevisiae*. *Mol Cell Biol* 23:7044-54.
54. Perrod S, Cockell MM, Laroche T, Renauld H, Ducrest AL, Bonnard C, Gasser SM. (2001) A cytosolic NAD-dependent deacetylase, Hst2p, can modulate nucleolar and telomeric silencing in yeast. *EMBO J.* 20:197-209.
55. Lamming DW, Latorre-Esteves M, Medvedik O, Wong SN, Tsang FA, Wang C, Lin SJ, Sinclair DA. (2005) HST2 mediates SIR2-independent life-span extension by calorie restriction. *Science* 309:1861-4.
56. Freeman-Cook LL, Sherman JM, Brachmann CB, Allshire RC, Boeke JD, Pillus L. (1999) The *Schizosaccharomyces pombe* hst4(+) gene is a SIR2 homologue with silencing and centromeric functions. *Mol Biol Cell* 10:3171-86.
57. Tissenbaum HA, Guarente L. (2001) Increased dosage of a sir-2 gene extends lifespan in *Caenorhabditis elegans*. *Nature* 410:227-30.

58. Barlow AL, van Drunen CM, Johnson CA, Tweedie S, Bird A, Turner BM. (2001) dSIR2 and dHDAC6: two novel, inhibitor-resistant deacetylases in *Drosophila melanogaster*. *Exp Cell Res* 265:90-103.
59. Rosenberg MI, Parkhurst SM. (2002) *Drosophila* Sir2 is required for heterochromatic silencing and by euchromatic Hairy/E(Spl) bHLH repressors in segmentation and sex determination. *Cell* 109:447-58.
60. Furuyama T, Banerjee R, Breen TR, Harte PJ. (2004) SIR2 is required for polycomb silencing and is associated with an E(Z) histone methyltransferase complex. *Curr Biol* 14:1812-21.
61. Astrom SU, Cline TW, Rine J. (2003) The *Drosophila melanogaster* sir2+ gene is nonessential and has only minor effects on position-effect variegation. *Genetics* 163:931-7.
62. Newman BL, Lundblad JR, Chen Y, Smolik SM. (2002) A *Drosophila* homologue of Sir2 modifies position-effect variegation but does not affect life span. *Genetics* 162:1675-85.
63. Sakamoto J, Miura T, Shimamoto K, Horio Y. (2004) Predominant expression of Sir2alpha, an NAD-dependent histone deacetylase, in the embryonic mouse heart and brain. *FEBS Lett* 556:281-6.
64. Cheng HL, Mostoslavsky R, Saito S, Manis JP, Gu Y, Patel P, Bronson R, Appella E, Alt FW, Chua KF. (2003) Developmental defects and p53 hyperacetylation in Sir2 homolog (SIRT1)-deficient mice. *Proc Natl Acad Sci U S A* 100:10794-9.

65. McBurney MW, Yang X, Jardine K, Hixon M, Boekelheide K, Webb JR, Lansdorp PM, Lemieux M. (2003) The mammalian SIR2alpha protein has a role in embryogenesis and gametogenesis. *Mol Cell Biol* 23:38-54.
66. Shi T, Wang F, Stieren E, Tong Q. (2005) SIRT3, a mitochondrial sirtuin deacetylase, regulates mitochondrial function and thermogenesis in brown adipocytes. *J Biol Chem* 280:13560-7.
67. Michishita E, Park JY, Burneskis JM, Barrett JC, Horikawa I. (2005) Evolutionarily Conserved and Nonconserved Cellular Localizations and Functions of Human SIRT Proteins. *Mol Biol Cell*
68. Muth V, Nadaud S, Grummt I, Voit R. (2001) Acetylation of TAF(I)68, a subunit of TIF-IB/SL1, activates RNA polymerase I transcription. *Embo J* 20:1353-62.
69. Cohen HY, Miller C, Bitterman KJ, Wall NR, Hekking B, Kessler B, Howitz KT, Gorospe M, de Cabo R, Sinclair DA. (2004) Calorie restriction promotes mammalian cell survival by inducing the SIRT1 deacetylase. *Science* 305:390-2.
70. Cohen HY, Lavu S, Bitterman KJ, Hekking B, Imahiyerobo TA, Miller C, Frye R, Ploegh H, Kessler BM, Sinclair DA. (2004) Acetylation of the C terminus of Ku70 by CBP and PCAF controls Bax-mediated apoptosis. *Mol Cell* 13:627-38.
71. Luo J, Nikolaev AY, Imai S, Chen D, Su F, Shiloh A, Guarente L, Gu W. (2001) Negative control of p53 by Sir2alpha promotes cell survival under stress. *Cell* 107:137-148.
72. Vaziri H, Dessain SK, Ng Eaton E, Imai SI, Frye RA, Pandita TK, Guarente L, Weinberg RA. (2001) hSIR2(SIRT1) functions as an NAD-dependent p53 deacetylase. *Cell* 107:149-159.

73. Langley E, Pearson M, Faretta M, Bauer UM, Frye RA, Minucci S, Pelicci PG, Kouzarides T. (2002) Human SIR2 deacetylates p53 and antagonizes PML/p53-induced cellular senescence. *Embo J* 21:2383-96.
74. Motta MC, Divecha N, Lemieux M, Kamel C, Chen D, Gu W, Bultsma Y, McBurney M, Guarente L. (2004) Mammalian SIRT1 represses forkhead transcription factors. *Cell* 116:551-63.
75. Brunet A, Sweeney LB, Sturgill JF, Chua KF, Greer PL, Lin Y, Tran H, Ross SE, Mostoslavsky R, Cohen HY, Hu LS, Cheng HL, Jedrychowski MP, Gygi SP, Sinclair DA, Alt FW, Greenberg ME. (2004) Stress-dependent regulation of FOXO transcription factors by the SIRT1 deacetylase. *Science* 303:2011-5.
76. van der Horst A, Tertoolen LG, de Vries-Smits LM, Frye RA, Medema RH, Burgering BM. (2004) FOXO4 is acetylated upon peroxide stress and deacetylated by the longevity protein hSir2(SIRT1). *J Biol Chem* 279:28873-9.
77. Yeung F, Hoberg JE, Ramsey CS, Keller MD, Jones DR, Frye RA, Mayo MW. (2004) Modulation of NF-kappaB-dependent transcription and cell survival by the SIRT1 deacetylase. *Embo J* 23:2369-80.
78. Fulco M, Schiltz RL, Iezzi S, King MT, Zhao P, Kashiwaya Y, Hoffman E, Veech RL, Sartorelli V. (2003) Sir2 regulates skeletal muscle differentiation as a potential sensor of the redox state. *Mol Cell* 12:51-62.
79. Pagans S, Pedal A, North BJ, Kaehlcke K, Marshall BL, Dorr A, Hetzer-Egger C, Henklein P, Frye R, McBurney MW, Hruby H, Jung M, Verdin E, Ott M. (2005) SIRT1 regulates HIV transcription via Tat deacetylation. *PLoS Biol* 3:e41.

80. Bouras T, Fu M, Sauve AA, Wang F, Quong AA, Perkins ND, Hay RT, Gu W, Pestell RG. (2005) SIRT1 deacetylation and repression of p300 involves lysine residues 1020/1024 within the cell cycle regulatory domain 1. *J Biol Chem* 280:10264-76.
81. Rodgers JT, Lerin C, Haas W, Gygi SP, Spiegelman BM, Puigserver P. (2005) Nutrient control of glucose homeostasis through a complex of PGC-1alpha and SIRT1. *Nature* 434:113-8.
82. Zhao X, Sternsdorf T, Bolger TA, Evans RM, Yao TP. (2005) Regulation of MEF2 by Histone Deacetylase 4- and SIRT1 Deacetylase-Mediated Lysine Modifications. *Mol Cell Biol* 25:8456-64.
83. Senawong T, Peterson VJ, Avram D, Shepherd DM, Frye RA, Minucci S, Leid M. (2003) Involvement of the histone deacetylase SIRT1 in chicken ovalbumin upstream promoter transcription factor (COUP-TF)-interacting protein 2-mediated transcriptional repression. *J Biol Chem* 278:43041-50.
84. Picard F, Kurtev M, Chung N, Topark-Ngarm A, Senawong T, Machado De Oliveira R, Leid M, McBurney MW, Guarente L. (2004) Sirt1 promotes fat mobilization in white adipocytes by repressing PPAR-gamma. *Nature* 429:771-6.
85. Senawong T, Peterson VJ, Leid M. (2005) BCL11A-dependent recruitment of SIRT1 to a promoter template in mammalian cells results in histone deacetylation and transcriptional repression. *Arch Biochem Biophys* 434:316-25.
86. Afshar G, Murnane JP. (1999) Characterization of a human gene with sequence homology to *Saccharomyces cerevisiae* SIR2. *Gene* 234:161-168.

87. North BJ, Marshall BL, Borra MT, Denu JM, Verdin E. (2003) The human Sir2 ortholog, SIRT2, is an NAD⁺-dependent tubulin deacetylase. *Mol Cell* 11:437-44.
88. Yang YH, Chen YH, Zhang CY, Nimmakayalu MA, Ward DC, Weissman S. (2000) Cloning and characterization of two mouse genes with homology to the yeast Sir2 gene. *Genomics* 69:355-369.
89. Hiratsuka M, Inoue T, Toda T, Kimura N, Shirayoshi Y, Kamitani H, Watanabe T, Ohama E, Tahimic CG, Kurimasa A, Oshimura M. (2003) Proteomics-based identification of differentially expressed genes in human gliomas: down-regulation of SIRT2 gene. *Biochem Biophys Res Commun* 309:558-66.
90. Dryden SC, Nahhas FA, Nowak JE, Goustin AS, Tainsky MA. (2003) Role for human SIRT2 NAD-dependent deacetylase activity in control of mitotic exit in the cell cycle. *Mol Cell Biol* 23:3173-85.
91. Bae NS, Swanson MJ, Vassilev A, Howard BH. (2004) Human histone deacetylase SIRT2 interacts with the homeobox transcription factor HOXA10. *J Biochem (Tokyo)* 135:695-700.
92. Capecchi MR. (1997) Hox genes and mammalian development. *Cold Spring Harb Symp Quant Biol* 62:273-81.
93. McGinnis W, Krumlauf R. (1992) Homeobox genes and axial patterning. *Cell* 68:283-302.
94. Saleh M, Rambaldi I, Yang XJ, Featherstone MS. (2000) Cell signaling switches HOX-PBX complexes from repressors to activators of transcription mediated by histone deacetylases and histone acetyltransferases. *Mol Cell Biol* 20:8623-33.

95. Thorsteinsdottir U, Sauvageau G, Humphries RK. (1997) Hox homeobox genes as regulators of normal and leukemic hematopoiesis. *Hematol Oncol Clin North Am* 11:1221-37.
96. Satokata I, Benson G, Maas R. (1995) Sexually dimorphic sterility phenotypes in Hoxa10-deficient mice. *Nature* 374:460-3.
97. Onyango P, Celic I, McCaffery JM, Boeke JD, Feinberg AP. (2002) SIRT3, a human SIR2 homologue, is an NAD- dependent deacetylase localized to mitochondria. *Proc Natl Acad Sci U S A* 99:13653-13658.
98. Schwer B, North BJ, Frye RA, Ott M, Verdin E. (2002) The human silent information regulator (Sir)2 homologue hSIRT3 is a mitochondrial nicotinamide adenine dinucleotide-dependent deacetylase. *J Cell Biol* 158:647-57.
99. Liszt G, Ford E, Kurtev M, Guarente L. (2005) Mouse Sir2 homolog SIRT6 is a nuclear ADP-ribosyltransferase. *J Biol Chem* 280:21313-20.
100. Lin SJ, Defossez PA, Guarente L. (2000) Requirement of NAD and SIR2 for life-span extension by calorie restriction in *Saccharomyces cerevisiae*. *Science* 289:2126-8.
101. Wood JG, Rogina B, Lavu S, Howitz K, Helfand SL, Tatar M, Sinclair D. (2004) Sirtuin activators mimic caloric restriction and delay ageing in metazoans. *Nature* 430:686-9.
102. Rogina B, Helfand SL. (2004) Sir2 mediates longevity in the fly through a pathway related to calorie restriction. *Proc Natl Acad Sci U S A* 101:15998-6003.
103. Sinclair DA, Guarente L. (1997) Extrachromosomal rDNA circles--a cause of aging in yeast. *Cell* 91:1033-42.

104. Kaeberlein M, McVey M, Guarente L. (1999) The SIR2/3/4 complex and SIR2 alone promote longevity in *Saccharomyces cerevisiae* by two different mechanisms. *Genes Dev* 13:2570-80.
105. Kennedy BK, Gotta M, Sinclair DA, Mills K, McNabb DS, Murthy M, Pak SM, Laroche T, Gasser SM, Guarente L. (1997) Redistribution of silencing proteins from telomeres to the nucleolus is associated with extension of life span in *S. cerevisiae*. *Cell* 89:381-91.
106. Kenyon C, Chang J, Gensch E, Rudner A, Tabtiang R. (1993) A *C. elegans* mutant that lives twice as long as wild type. *Nature* 366:461-4.
107. Kimura KD, Tissenbaum HA, Liu Y, Ruvkun G. (1997) *daf-2*, an insulin receptor-like gene that regulates longevity and diapause in *Caenorhabditis elegans*. *Science* 277:942-6.
108. Guarente L. (2005) Calorie restriction and SIR2 genes--towards a mechanism. *Mech Ageing Dev* 126:923-8.
109. Guarente L, Picard F. (2005) Calorie restriction--the SIR2 connection. *Cell* 120:473-82.
110. Landry J, Slama JT, Sternglanz R. (2000) Role of NAD(+) in the deacetylase activity of the SIR2-like proteins. *Biochem Biophys Res Commun* 278:685-90.
111. Avalos JL, Celic I, Muhammad S, Cosgrove MS, Boeke JD, Wolberger C. (2002) Structure of a Sir2 enzyme bound to an acetylated p53 peptide. *Mol Cell* 10:523-35.
112. Finnin MS, Donigian JR, Pavletich NP. (2001) Structure of the histone deacetylase SIRT2. *Nat. Struct. Biol.* 8:621-625.

113. Min J, Landry J, Sternglanz R, Xu RM. (2001) Crystal structure of a SIR2 homolog-NAD complex. *Cell* 105:269-79.
114. Zhao K, Chai X, Clements A, Marmorstein R. (2003) Structure and autoregulation of the yeast Hst2 homolog of Sir2. *Nat Struct Biol* 10:864-71.
115. Sherman JM, Stone EM, Freeman-Cook LL, Brachmann CB, Boeke JD, Pillus L. (1999) The conserved core of a human SIR2 homologue functions in yeast silencing. *Mol Biol Cell* 10:3045-59.
116. Finnin MS, Donigian JR, Cohen A, Richon VM, Rifkind RA, Marks PA, Breslow R, Pavletich NP. (1999) Structures of a histone deacetylase homologue bound to the TSA and SAHA inhibitors. *Nature* 401:188-93.
117. DeLano WL. (2002) The PyMOL Molecular Graphics System.
118. Trzebiatowski JR, O'Toole GA, Escalante-Semerena JC. (1994) The cobT gene of *Salmonella typhimurium* encodes the NaMN: 5,6-dimethylbenzimidazole phosphoribosyltransferase responsible for the synthesis of N¹-(5-phospho- α -D-ribose)-5,6-dimethylbenzimidazole, an intermediate in the synthesis of the nucleotide loop of cobalamin. *J Bacteriol* 176:3568-75.
119. Trzebiatowski JR, Escalante-Semerena JC. (1997) Purification and characterization of CobT, the nicotinate-mononucleotide:5,6-dimethylbenzimidazole phosphoribosyltransferase enzyme from *Salmonella typhimurium* LT2. *J Biol Chem* 272:17662-7.
120. Tsang AW, Escalante-Semerena JC. (1996) cobB function is required for catabolism of propionate in *Salmonella typhimurium* LT2: evidence for existence of

- a substitute function for CobB within the 1,2-propanediol utilization (pdu) operon. *J Bacteriol* 178:7016-9.
121. Tanny JC, Dowd GJ, Huang J, Hilz H, Moazed D. (1999) An enzymatic activity in the yeast Sir2 protein that is essential for gene silencing. *Cell* 99:735-45.
 122. Denu JM. (2005) The Sir2 family of protein deacetylases. *Curr Opin Chem Biol* 9:431-40.
 123. Luo J, Su F, Chen D, Shiloh A, Gu W. (2000) Deacetylation of p53 modulates its effect on cell growth and apoptosis. *Nature* 408:377-81.
 124. Borra MT, O'Neill FJ, Jackson MD, Marshall B, Verdin E, Foltz KR, Denu JM. (2002) Conserved enzymatic production and biological effect of O-acetyl-ADP-ribose by silent information regulator 2-like NAD⁺-dependent deacetylases. *J Biol Chem* 277:12632-41.
 125. Tanner KG, Landry J, Sternglanz R, Denu JM. (2000) Silent information regulator 2 family of NAD- dependent histone/protein deacetylases generates a unique product, 1-O-acetyl-ADP-ribose. *Proc. Natl. Acad. Sci. USA* 97:14178-14182.
 126. Tanny JC, Moazed D. (2001) Coupling of histone deacetylation to NAD breakdown by the yeast silencing protein Sir2: Evidence for acetyl transfer from substrate to an NAD breakdown product. *Proc Natl Acad Sci U S A* 98:415-20.
 127. Denu JM. (2003) Linking chromatin function with metabolic networks: Sir2 family of NAD(+)-dependent deacetylases. *Trends Biochem Sci* 28:41-8.
 128. Garcia-Salcedo JA, Gijon P, Nolan DP, Tebabi P, Pays E. (2003) A chromosomal SIR2 homologue with both histone NAD-dependent ADP-ribosyltransferase and

- deacetylase activities is involved in DNA repair in *Trypanosoma brucei*. *EMBO J.* 22:5851-5862.
129. Nogales E. (2000) Structural insights into microtubule function. *Annu. Rev. Biochem.* 69:277-302.
130. MacRae TH. (1997) Tubulin post-translational modifications--enzymes and their mechanisms of action. *Eur. J. Biochem.* 244:265-278.
131. Piperno G, LeDizet M, Chang XJ. (1987) Microtubules containing acetylated alpha-tubulin in mammalian cells in culture. *J. Cell Biol.* 104:289-302.
132. Nogales E, Whittaker M, Milligan RA, Downing KH. (1999) High-resolution model of the microtubule. *Cell* 96:79-88.
133. Grozinger CM, Chao ED, Blackwell HE, Moazed D, Schreiber SL. (2001) Identification of a class of small molecule inhibitors of the sirtuin family of NAD-dependent deacetylases by phenotypic screening. *J. Biol. Chem.* 276:38837-38843.
134. Harrison RE, Turley EA. (2001) Active erk regulates microtubule stability in H-ras-transformed cells. *Neoplasia* 3:385-394.
135. Elliott G, O'Hare P. (1998) Herpes simplex virus type 1 tegument protein VP22 induces the stabilization and hyperacetylation of microtubules. *J. Virol.* 72:6448-6455.
136. Piperno G, Fuller MT. (1985) Monoclonal antibodies specific for an acetylated form of alpha-tubulin recognize the antigen in cilia and flagella from a variety of organisms. *J. Cell Biol.* 101:2085-2094.

137. Poole CA, Zhang ZJ, Ross JM. (2001) The differential distribution of acetylated and deetyrosinated alpha- tubulin in the microtubular cytoskeleton and primary cilia of hyaline cartilage chondrocytes. *J. Anat.* 199:393-405.
138. Pijnappel WW, Schaft D, Roguev A, Shevchenko A, Tekotte H, Wilm M, Rigaut G, Seraphin B, Aasland R, Stewart AF. (2001) The *S. cerevisiae* SET3 complex includes two histone deacetylases, Hos2 and Hst1, and is a meiotic-specific repressor of the sporulation gene program. *Genes Dev.* 15:2991-3004.
139. Furumai R, Komatsu Y, Nishino N, Khochbin S, Yoshida M, Horinouchi S. (2001) Potent histone deacetylase inhibitors built from trichostatin A and cyclic tetrapeptide antibiotics including trapoxin. *Proc. Natl. Acad. Sci. USA* 98:87-92.
140. Hubbert C, Guardiola A, Shao R, Kawaguchi Y, Ito A, Nixon A, Yoshida M, Wang XF, Yao TP. (2002) HDAC6 is a microtubule-associated deacetylase. *Nature* 417:455-8.
141. Matsuyama A, Shimazu T, Sumida Y, Saito A, Yoshimatsu Y, Seigneurin-Berny D, Osada H, Komatsu Y, Nishino N, Khochbin S, Horinouchi S, Yoshida M. (2002) In vivo destabilization of dynamic microtubules by HDAC6-mediated deacetylation. *Embo J* 21:6820-31.
142. Zhang Y, Li N, Caron C, Matthias G, Hess D, Khochbin S, Matthias P. (2003) HDAC-6 interacts with and deacetylates tubulin and microtubules in vivo. *Embo J* 22:1168-79.
143. Ziegelbauer J, Shan B, Yager D, Larabell C, Hoffmann B, Tjian R. (2001) Transcription factor MIZ-1 is regulated via microtubule association. *Mol. Cell* 8:339-349.

144. Sui D, Wilson JE. (2000) Interaction of insulin-like growth factor binding protein-4, Miz-1, leptin, lipocalin-type prostaglandin D synthase, and granulin precursor with the N-terminal half of type III hexokinase. *Arch. Biochem. Biophys.* 382:262-274.
145. Dignam JD, Lebovitz RM, Roeder RG. (1983) Accurate transcription initiation by RNA polymerase II in a soluble extract from isolated mammalian nuclei. *Nucleic Acids Res.* 11:1475-1489.
146. Emiliani S, Fischle W, Van Lint C, Al-Abed Y, Verdin E. (1998) Characterization of a human RPD3 ortholog, HDAC3. *Proc. Natl. Acad. Sci. USA* 95:2795-2800.
147. Bradbury CA, Khanim FL, Hayden R, Bunce CM, White DA, Drayson MT, Craddock C, Turner BM. (2005) Histone deacetylases in acute myeloid leukaemia show a distinctive pattern of expression that changes selectively in response to deacetylase inhibitors. *Leukemia* 19:1751-9.
148. van Vliet C, Thomas EC, Merino-Trigo A, Teasdale RD, Gleeson PA. (2003) Intracellular sorting and transport of proteins. *Prog Biophys Mol Biol* 83:1-45.
149. Pfanner N, Wiedemann N. (2002) Mitochondrial protein import: two membranes, three translocases. *Curr Opin Cell Biol* 14:400-11.
150. Pemberton LF, Paschal BM. (2005) Mechanisms of receptor-mediated nuclear import and nuclear export. *Traffic* 6:187-98.
151. Kutay U, Guttinger S. (2005) Leucine-rich nuclear-export signals: born to be weak. *Trends Cell Biol* 15:121-4.
152. Yoneda Y, Hieda M, Nagoshi E, Miyamoto Y. (1999) Nucleocytoplasmic protein transport and recycling of Ran. *Cell Struct Funct* 24:425-33.

153. Nishi K, Yoshida M, Fujiwara D, Nishikawa M, Horinouchi S, Beppu T. (1994) Leptomycin B targets a regulatory cascade of crm1, a fission yeast nuclear protein, involved in control of higher order chromosome structure and gene expression. *J Biol Chem* 269:6320-4.
154. Kudo N, Matsumori N, Taoka H, Fujiwara D, Schreiner EP, Wolff B, Yoshida M, Horinouchi S. (1999) Leptomycin B inactivates CRM1/exportin 1 by covalent modification at a cysteine residue in the central conserved region. *Proc Natl Acad Sci U S A* 96:9112-7.
155. Kudo N, Wolff B, Sekimoto T, Schreiner EP, Yoneda Y, Yanagida M, Horinouchi S, Yoshida M. (1998) Leptomycin B inhibition of signal-mediated nuclear export by direct binding to CRM1. *Exp Cell Res* 242:540-7.
156. Fukuda M, Asano S, Nakamura T, Adachi M, Yoshida M, Yanagida M, Nishida E. (1997) CRM1 is responsible for intracellular transport mediated by the nuclear export signal. *Nature* 390:308-11.
157. Fukuda M, Gotoh I, Gotoh Y, Nishida E. (1996) Cytoplasmic localization of mitogen-activated protein kinase kinase directed by its NH₂-terminal, leucine-rich short amino acid sequence, which acts as a nuclear export signal. *J Biol Chem* 271:20024-8.
158. Fischer U, Huber J, Boelens WC, Mattaj IW, Luhrmann R. (1995) The HIV-1 Rev activation domain is a nuclear export signal that accesses an export pathway used by specific cellular RNAs. *Cell* 82:475-83.

159. Yamaga M, Fujii M, Kamata H, Hirata H, Yagisawa H. (1999) Phospholipase C-delta1 contains a functional nuclear export signal sequence. *J Biol Chem* 274:28537-41.
160. Toyoshima F, Moriguchi T, Wada A, Fukuda M, Nishida E. (1998) Nuclear export of cyclin B1 and its possible role in the DNA damage-induced G2 checkpoint. *Embo J* 17:2728-35.
161. Dundr M, Misteli T, Olson MO. (2000) The dynamics of postmitotic reassembly of the nucleolus. *J Cell Biol* 150:433-46.
162. Phair RD, Misteli T. (2000) High mobility of proteins in the mammalian cell nucleus. *Nature* 404:604-9.
163. de Noronha CM, Sherman MP, Lin HW, Cavrois MV, Moir RD, Goldman RD, Greene WC. (2001) Dynamic disruptions in nuclear envelope architecture and integrity induced by HIV-1 Vpr. *Science* 294:1105-8.
164. Stenoi DL, Sen S, Mancini MA, Brinkley BR. (2003) Dynamic association of a tumor amplified kinase, Aurora-A, with the centrosome and mitotic spindle. *Cell Motil Cytoskeleton* 55:134-46.
165. Shindo M, Nakano H, Kuroyanagi H, Shirasawa T, Mihara M, Gilbert DJ, Jenkins NA, Copeland NG, Yagita H, Okumura K. (1998) cDNA cloning, expression, subcellular localization, and chromosomal assignment of mammalian aurora homologues, aurora-related kinase (ARK) 1 and 2. *Biochem Biophys Res Commun* 244:285-92.

166. Monzo P, Gauthier NC, Keslair F, Loubat A, Field CM, Le Marchand-Brustel Y, Cormont M. (2005) Clues to CD2-associated protein involvement in cytokinesis. *Mol Biol Cell* 16:2891-902.
167. Yang J, Bardes ES, Moore JD, Brennan J, Powers MA, Kornbluth S. (1998) Control of cyclin B1 localization through regulated binding of the nuclear export factor CRM1. *Genes Dev* 12:2131-43.
168. Hagting A, Karlsson C, Clute P, Jackman M, Pines J. (1998) MPF localization is controlled by nuclear export. *Embo J* 17:4127-38.
169. Tang Z, Shu H, Oncel D, Chen S, Yu H. (2004) Phosphorylation of Cdc20 by Bub1 provides a catalytic mechanism for APC/C inhibition by the spindle checkpoint. *Mol Cell* 16:387-97.
170. Shou W, Sakamoto KM, Keener J, Morimoto KW, Traverso EE, Azzam R, Hoppe GJ, Feldman RM, DeModena J, Moazed D, Charbonneau H, Nomura M, Deshaies RJ. (2001) Net1 stimulates RNA polymerase I transcription and regulates nucleolar structure independently of controlling mitotic exit. *Mol Cell* 8:45-55.
171. Li L, Ljungman M, Dixon JE. (2000) The human Cdc14 phosphatases interact with and dephosphorylate the tumor suppressor protein p53. *J Biol Chem* 275:2410-4.
172. Kaiser BK, Zimmerman ZA, Charbonneau H, Jackson PK. (2002) Disruption of centrosome structure, chromosome segregation, and cytokinesis by misexpression of human Cdc14A phosphatase. *Mol Biol Cell* 13:2289-300.
173. Mailand N, Lukas C, Kaiser BK, Jackson PK, Bartek J, Lukas J. (2002) Deregulated human Cdc14A phosphatase disrupts centrosome separation and chromosome segregation. *Nat Cell Biol* 4:317-22.

174. Bembenek J, Yu H. (2003) Regulation of CDC14: pathways and checkpoints of mitotic exit. *Front Biosci* 8:d1275-87.
175. Ohi R, Gould KL. (1999) Regulating the onset of mitosis. *Curr Opin Cell Biol* 11:267-73.
176. Nigg EA. (2001) Mitotic kinases as regulators of cell division and its checkpoints. *Nat Rev Mol Cell Biol* 2:21-32.
177. Knockaert M, Lenormand P, Gray N, Schultz P, Pouyssegur J, Meijer L. (2002) p42/p44 MAPKs are intracellular targets of the CDK inhibitor purvalanol. *Oncogene* 21:6413-24.
178. Poon RY, Yamashita K, Adamczewski JP, Hunt T, Shuttleworth J. (1993) The cdc2-related protein p40MO15 is the catalytic subunit of a protein kinase that can activate p33cdk2 and p34cdc2. *Embo J* 12:3123-32.
179. Solomon MJ, Harper JW, Shuttleworth J. (1993) CAK, the p34cdc2 activating kinase, contains a protein identical or closely related to p40MO15. *Embo J* 12:3133-42.
180. Fesquet D, Labbe JC, Derancourt J, Capony JP, Galas S, Girard F, Lorca T, Shuttleworth J, Doree M, Cavadore JC. (1993) The MO15 gene encodes the catalytic subunit of a protein kinase that activates cdc2 and other cyclin-dependent kinases (CDKs) through phosphorylation of Thr161 and its homologues. *Embo J* 12:3111-21.
181. Millar JB, McGowan CH, Lenaers G, Jones R, Russell P. (1991) p80cdc25 mitotic inducer is the tyrosine phosphatase that activates p34cdc2 kinase in fission yeast. *Embo J* 10:4301-9.

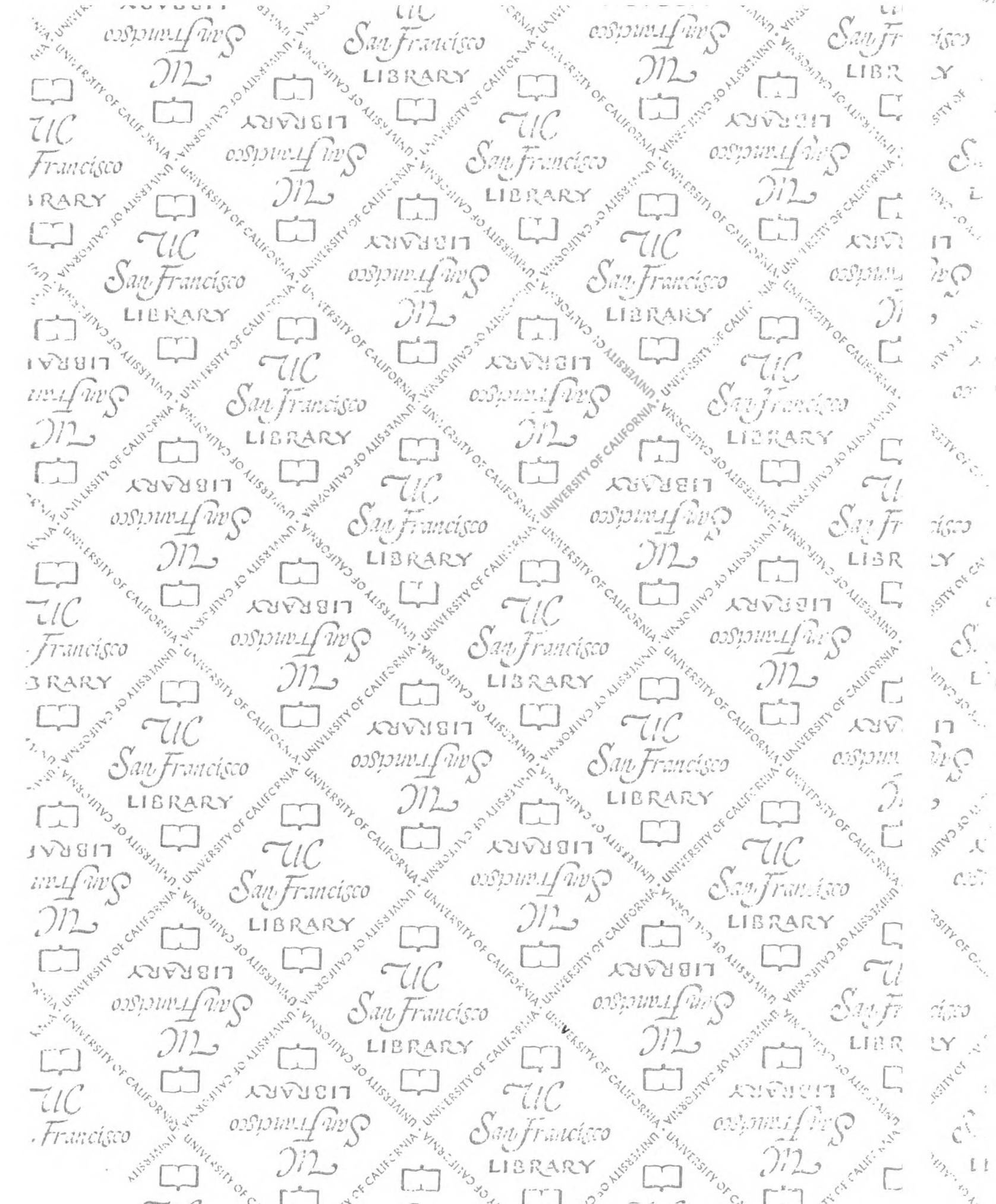
182. Russell P, Nurse P. (1986) *cdc25+* functions as an inducer in the mitotic control of fission yeast. *Cell* 45:145-53.
183. Moreno S, Nurse P, Russell P. (1990) Regulation of mitosis by cyclic accumulation of p80cdc25 mitotic inducer in fission yeast. *Nature* 344:549-52.
184. Parker LL, Piwnica-Worms H. (1992) Inactivation of the p34cdc2-cyclin B complex by the human WEE1 tyrosine kinase. *Science* 257:1955-7.
185. Borgne A, Meijer L. (1996) Sequential dephosphorylation of p34(cdc2) on Thr-14 and Tyr-15 at the prophase/metaphase transition. *J Biol Chem* 271:27847-54.
186. Krek W, Nigg EA. (1991) Mutations of p34cdc2 phosphorylation sites induce premature mitotic events in HeLa cells: evidence for a double block to p34cdc2 kinase activation in vertebrates. *Embo J* 10:3331-41.
187. Lyons AB. (2000) Analysing cell division in vivo and in vitro using flow cytometric measurement of CFSE dye dilution. *J Immunol Methods* 243:147-54.
188. North BJ, Schwer B, Ahuja N, Marshall B, Verdin E. (2005) Preparation of enzymatically active recombinant class III protein deacetylases. *Methods* 36:338-45.
189. L'Hernault SW, Rosenbaum JL. (1985) Chlamydomonas alpha-tubulin is posttranslationally modified by acetylation on the epsilon-amino group of a lysine. *Biochemistry* 24:473-8.
190. Greer K, Maruta H, L'Hernault SW, Rosenbaum JL. (1985) Alpha-tubulin acetylase activity in isolated Chlamydomonas flagella. *J Cell Biol* 101:2081-4.
191. Lloyd RA, Gentleman S, Chader GJ. (1994) Assay of tubulin acetyltransferase activity in subcellular tissue fractions. *Anal Biochem* 216:42-6.

192. Maruta H, Greer K, Rosenbaum JL. (1986) The acetylation of alpha-tubulin and its relationship to the assembly and disassembly of microtubules. *J Cell Biol* 103:571-9.
193. Kozminski KG, Diener DR, Rosenbaum JL. (1993) High level expression of nonacetylatable alpha-tubulin in *Chlamydomonas reinhardtii*. *Cell Motil Cytoskeleton* 25:158-70.
194. Gaertig J, Cruz MA, Bowen J, Gu L, Pennock DG, Gorovsky MA. (1995) Acetylation of lysine 40 in alpha-tubulin is not essential in *Tetrahymena thermophila*. *J Cell Biol* 129:1301-10.
195. Webster DR, Borisy GG. (1989) Microtubules are acetylated in domains that turn over slowly. *J Cell Sci* 92 (Pt 1):57-65.
196. Modig C, Stromberg E, Wallin M. (1994) Different stability of posttranslationally modified brain microtubules isolated from cold-temperate fish. *Mol Cell Biochem* 130:137-47.
197. Palazzo A, Ackerman B, Gundersen GG. (2003) Cell biology: Tubulin acetylation and cell motility. *Nature* 421:230.
198. Soltys BJ, Gupta RS. (1994) Immunoelectron microscopy of *Giardia lamblia* cytoskeleton using antibody to acetylated alpha-tubulin. *J Eukaryot Microbiol* 41:625-32.
199. Fouquet JP, Prigent Y, Kann ML. (1996) Comparative immunogold analysis of tubulin isoforms in the mouse sperm flagellum: unique distribution of glutamylated tubulin. *Mol Reprod Dev* 43:358-65.

200. Chen L, Fischle W, Verdin E, Greene WC. (2001) Duration of nuclear NF-kappaB action regulated by reversible acetylation. *Science* 293:1653-7.
201. Chen LF, Mu Y, Greene WC. (2002) Acetylation of RelA at discrete sites regulates distinct nuclear functions of NF-kappaB. *Embo J* 21:6539-48.
202. Vaquero A, Scher M, Lee D, Erdjument-Bromage H, Tempst P, Reinberg D. (2004) Human SirT1 interacts with histone H1 and promotes formation of facultative heterochromatin. *Mol Cell* 16:93-105.
203. Haggarty SJ, Koeller KM, Wong JC, Grozinger CM, Schreiber SL. (2003) Domain-selective small-molecule inhibitor of histone deacetylase 6 (HDAC6)-mediated tubulin deacetylation. *Proc Natl Acad Sci U S A* 100:4389-94.
204. Haller K, Rambaldi I, Daniels E, Featherstone M. (2004) Subcellular localization of multiple PREP2 isoforms is regulated by actin, tubulin, and nuclear export. *J Biol Chem* 279:49384-94.
205. Pockwinse SM, Rajgopal A, Young DW, Mujeeb KA, Nickerson J, Javed A, Redick S, Lian JB, van Wijnen AJ, Stein JL, Stein GS, Doxsey SJ. (2005) Microtubule-dependent nuclear-cytoplasmic shuttling of Runx2. *J Cell Physiol*
206. Qutob MS, Bhattacharjee RN, Pollari E, Yee SP, Torchia J. (2002) Microtubule-dependent subcellular redistribution of the transcriptional coactivator p/CIP. *Mol Cell Biol* 22:6611-26.
207. Strahl BD, Allis CD. (2000) The language of covalent histone modifications. *Nature* 403:41-45.
208. Fischle W, Wang Y, Allis CD. (2003) Histone and chromatin cross-talk. *Curr Opin Cell Biol* 15:172-83.

209. Wang Y, Fischle W, Cheung W, Jacobs S, Khorasanizadeh S, Allis CD. (2004) Beyond the double helix: writing and reading the histone code. *Novartis Found Symp* 259:3-17; discussion 17-21, 163-9.
210. Fischle W, Wang Y, Allis CD. (2003) Binary switches and modification cassettes in histone biology and beyond. *Nature* 425:475-9.
211. Peter M, Nakagawa J, Doree M, Labbe JC, Nigg EA. (1990) In vitro disassembly of the nuclear lamina and M phase-specific phosphorylation of lamins by cdc2 kinase. *Cell* 61:591-602.
212. Peter M, Heitlinger E, Haner M, Aebi U, Nigg EA. (1991) Disassembly of in vitro formed lamin head-to-tail polymers by CDC2 kinase. *Embo J* 10:1535-44.
213. Enoch T, Peter M, Nurse P, Nigg EA. (1991) p34cdc2 acts as a lamin kinase in fission yeast. *J Cell Biol* 112:797-807.
214. Dessev G, Iovcheva-Dessev C, Bischoff JR, Beach D, Goldman R. (1991) A complex containing p34cdc2 and cyclin B phosphorylates the nuclear lamin and disassembles nuclei of clam oocytes in vitro. *J Cell Biol* 112:523-33.
215. Toyoshima-Morimoto F, Taniguchi E, Shinya N, Iwamatsu A, Nishida E. (2001) Polo-like kinase 1 phosphorylates cyclin B1 and targets it to the nucleus during prophase. *Nature* 410:215-20.
216. Ferrell JE, Jr. (1998) How regulated protein translocation can produce switch-like responses. *Trends Biochem Sci* 23:461-5.
217. O'Farrell PH. (2001) Triggering the all-or-nothing switch into mitosis. *Trends Cell Biol* 11:512-9.

218. Cho HP, Liu Y, Gomez M, Dunlap J, Tyers M, Wang Y. (2005) The dual-specificity phosphatase CDC14B bundles and stabilizes microtubules. *Mol Cell Biol* 25:4541-51.
219. Mallavarapu A, Sawin K, Mitchison T. (1999) A switch in microtubule dynamics at the onset of anaphase B in the mitotic spindle of *Schizosaccharomyces pombe*. *Curr Biol* 9:1423-6.
220. Higuchi T, Uhlmann F. (2005) Stabilization of microtubule dynamics at anaphase onset promotes chromosome segregation. *Nature* 433:171-6.
221. Guarente L. (2000) Sir2 links chromatin silencing, metabolism, and aging. *Genes Dev* 14:1021-6.



LIBRARY

7486999



3 1378 00748 6999

For reference

Not to be taken from the room.

